

Shell imperfections

A study of the shape and magnitude
of geometrical imperfections in thin
concrete shell structures

Bart Elferink



Shell imperfections

A study of the shape and magnitude of
geometrical imperfections in thin concrete
shell structures

by

Bart Elferink

to obtain the degree of Master of Science
at the Delft University of Technology,
to be defended publicly on December 17th, 2015 at 15:00.

Student number: 1329502
Project duration: June 2014 – December, 2015
Thesis committee: Prof. dr. ir. J. G. Rots, TU Delft, chairman
Dr. P. C. J. Hoogenboom, TU Delft, weekly supervisor
Ir. P. Eigenraam, TU Delft

An electronic version of this thesis is available at <http://repository.tudelft.nl/>.

Preface

This report describes a thesis research for completing a Master in Structural Engineering at the department of Civil Engineering of the Technical University of Delft. The research will be done for the department of Structural Mechanics, under the supervision of Prof. dr. ir. J.G. Rots (structural mechanics Professor at CEG faculty, TU Delft) chairman of the thesis committee, Dr. ir. P.C.J. Hoogenboom (assistant structural mechanics professor at CEG faculty, TU Delft) as weekly supervisor and Ir. P. Eigenraam (assistant professor at the Department of Architecture, TU Delft). The assignment was created by Hoogenboom and was done in the field of shell structures.

This report is aimed at structural engineers, but can easily be read by civil engineers and fellow students of CEG faculty. Also anyone who is interested in the subject matter with a bachelor level of calculus and mechanics, should be able to understand the contents of this report.

The Report is built up in 5 chapters and 8 appendixes. The main matter of the report (Ch. 1 to 5) consists mostly research methodology and results, background information can be found in the appendixes. Along with those some references will be made to existing literature and websites. This report will also be posted on the TU Delft repository (title page for link), where web links to source material can be used. The main matter of the report consists of the following chapters:

- Chapter 1: Introduction. Here a short introduction is given on shell structures and theory of geometrical imperfections and their effects. The problem and goal of this thesis is described and the action plan is given.
- Chapter 2: Research methodology. In this chapter the used measurement method described and the measurement plans of the visited shell is given. Also containing a description of the data output of the measurements.
- Chapter 3: Data processing. This chapter describes the processes, which were used to create results from the data that was collected.
- Chapter 4: Results.
- Chapter 5: Conclusion and discussion.

I want to thank my entire committee for guiding me the last year and helping me complete my thesis. I want to thank Anneke Meijer for arranging the committee meetings and Deltares for lending out the needed equipment (Faro Focus 3D) for this research. Also Nicolas and his family for letting us stay at their home during the measurements in Switzerland. I want to thank Ilse Blokland for all of her support and advise on report technique. Lastly I specially want to thank my parents for supporting me throughout my bachelor and masters degree.

*Bart Elferink
Delft, Augustus 2015*

Abstract

Thin concrete shell structures are very efficient when it comes to material usage, but this comes at a price, because they can be susceptible to buckling. Studies have shown that initial geometrical imperfections can have a large effect on the ultimate strength of shell structures. For example in research a Finite Element (FE) model of a shell dome was made which showed a knock-down factor (in ultimate strength) of 0.66, when an imperfection of half the shell thickness was present. Although these imperfections have a great influence on the structural integrity of thin shells, little is known on the shape and size of these imperfections in current shell structures. On top of that, data is lacking on the dimensions of the shells made by Isler in Germany and Switzerland (which were used for measurements), which makes the process of finding imperfections harder.

The goal of this thesis was to develop a method which can accurately measure and represent the shape of spatial structures, to facilitate evaluating geometrical imperfections of shell structures and their consequences. The goal was subdivided into three parts: firstly the development of an accurate measuring method, secondly finding existing thin concrete shells that could be measured and thirdly developing a method for reliably finding imperfections using the collected data.

Finding a precise and fast measurement method was important for collecting accurate and sufficient data. Because of the lack of data on geometrical imperfections of shells it was not possible to predict the accuracy needed to successfully measure imperfections. Because all shells that would be measured were in use, the method had to be quick. Five options were investigated and the method chosen was the Faro Focus 3d laser scanner. It is a device that can measure millions of points with very high accuracy (± 0.5 mm) in a few minutes. The device was portable and created a digital point cloud, which made processing the data easier.

In total six concrete shells were measured. The Head office of the ANWB in the Hague and five shells made by Heinz Isler in Switzerland. These shells were selected on basis of their lack of surface finish on the bottom side of the shell. Most concrete shells are not visible from underneath and therefore were not suitable for measurement. Because the Swiss architect and engineer Heinz Isler is one of the few who designed numerous thin concrete shells in Switzerland, it was the ideal place to collect data for this research.

To calculate the shape and size of the imperfections of the shells, the data had to be compared to the original or intended shape of the shells. However, due to the lack of comparative data of the measured shells, the data itself was used to construct an intended shape. Several methods were tested and a solution was found using NURBS surfaces. This method was called the Double NURBS method. A bulge or a dent in a NURBS surface (or curve) is created by a control point. Therefore by minimizing the number of control points, a NURBS surface can be made of the measured data, which does not have enough control points to create waves with a wave length close to the buckling length. Using this method to create the comparative (or intended) shape, it is not possible to calculate the global imperfections of a shell. For instance if the curvature of the shell is too flat, this will not be taken into account in the size of the imperfection. But this method can show the imperfections which have a wavelength between approximately 0.5 to 6 meters. For all shells measured, the buckling length is within this interval. The buckling length is the theoretical wavelength for a shell when it buckles and imperfections of that length have the largest effect on the ultimate strength of a shell. The data processing method subtracted this self created intended surface from a NURBS surface approximating the measured data. The result of this subtraction was a surface of imperfections. This method produced reliable results in four out of six shells, the remaining two had too many gaps in the data due to obstacles hanging from the ceiling.

Alongside the Double NURBS method, a separate method was developed to extract the variance spectrum of wave lengths. It can be used to give an insight on the distribution of wave lengths in the imperfection field. The method was called the Single NURBS method, because it compares the point cloud to a series of single NURBS surfaces. The method also serves as a validation for the Double NURBS method and can be used as a fast estimation of the largest imperfection.

Maximum amplitude of shell imperfections ranged from 2 to 6 centimeters. The shape of the imperfections found was most similar to a summation of a small number of sine waves. The variance spectrum of wave lengths found was a fairly uniform distribution of waves between 1 and 6 meters. This study was the first to measure imperfections in shell structures and although more shells need to be measured, the developed method can be used for future research.

Contents

Abstract	v
1 Introduction	1
1.1 Shell structures in general	1
1.2 Buckling in shell structures	2
1.3 The impact of initial imperfections on shell buckling	2
1.4 Construction of thin concrete shells	3
1.5 Case study: Effect of initial imperfections on ultimate strength of a spherical shell	4
1.5.1 Setup	4
1.5.2 Results	5
1.6 Problem and Goal	6
1.6.1 Problem	6
1.6.2 Goal of the thesis	6
2 Research methodology	7
2.1 Measurement method	7
2.1.1 Requirements	7
2.1.2 Available methods	8
2.1.3 Chosen method	8
2.1.4 Specifications of the Faro Focus 3D X130	9
2.1.5 Data output	12
2.1.6 Plotting a 3D surface through the points	12
2.2 Measured shells	14
2.2.1 Deitingen	14
2.2.2 Heimberg Schimmbad	15
2.2.3 Heimberg Tennis	16
2.2.4 Grötzingen	17
2.2.5 Wyss Garten centre	18
2.2.6 ANWB head office	19
3 Data Processing	21
3.1 NURBS	21
3.1.1 Creation of NURBS	21
3.1.2 Determination of NURBS parameters	22
3.1.3 Purpose of NURBS in this research	25
3.2 Double NURBS method	26
3.2.1 Steps of the method	26
3.2.2 Requirements for the methods	32
3.3 Single NURBS Method	33
3.3.1 Assumptions	33
3.3.2 Using the Single NURBS method	36
3.3.3 Step 4: Estimation of peak amplitude of imperfection	38
3.3.4 Step 5 (optional): Estimation of the expected largest peak found in similar shells	38
3.3.5 Step 6: Verification using Double NURBS Method	38
4 Results	39
4.1 Contour plots	39
4.1.1 Shell 1: Deitingen	39
4.1.2 Shell 2: Heimberg Schwimmbad	40
4.1.3 Shell 3: Heimberg Tennis	41

4.2	Histograms	42
4.2.1	Shell 1: Deitingen	42
4.2.2	Shell 2: Heimberg Schwimmbad.	43
4.2.3	Shell 3: Heimberg Tennis	44
4.3	Single NURBS method	45
4.3.1	Verification using Double NURBS method	46
5	Conclusion and Discussion	47
5.1	Conclusion	47
5.2	Discussion	47
5.3	Recommendations	48
A	Measurement methods	49
A.1	Theodolite.	49
A.2	Total station.	51
A.3	Faro Focus 3d scanner.	52
A.4	Manual laser distance measurement	53
A.5	Manual measurement	54
B	Grasshopper scripts	55
C	NURBS	59
C.1	Origin of NURBS and splines	59
C.2	B-Spline.	59
C.3	NURBS specifications	60
C.4	Significance for this research	60
D	Fast Fourier transform	61
D.1	Using Fast Fourier transform	61
D.1.1	Fast Fourier transform	61
D.1.2	Example using Deitingen.	61
D.1.3	Turning Bins to wave lengths	61
D.1.4	Comparison collection methods of data for FFt	62
D.1.5	Conclusion	67
E	Swiss trip	69
E.1	Preparation	69
E.2	Visited shells	71
E.2.1	Naturtheater in Grötzingen	71
E.2.2	Swimming pool in Heimberg	72
E.2.3	Tennis hall in Heimberg	73
E.2.4	Garten centre in Zuchwill.	74
E.2.5	Service station in Deitingen	75
E.3	Collected data	76
E.4	Conclusion	76
F	Case study: Effect of initial imperfections on ultimate strength of a spherical shell	77
F.1	Geometry	77
F.1.1	Adding imperfection to geometry	78
F.2	Material properties	79
F.3	Mesh	79
F.4	Load.	82
F.5	Boundary conditions	82
F.6	Analyses	83
F.6.1	Linear	83
F.6.2	Geometrically non-linear	83

F.7	Results	84
F.8	Conclusion	85
F.9	Displacement and mean stress plots of all analyses	86
F.9.1	linear analysis of imperfect shell results	86
F.9.2	Non-linear analysis of perfect shell results	87
F.9.3	Non-linear analysis of imperfect shell (amplitude 5 cm) results	91
F.9.4	Non-linear analysis of imperfect shell (amplitude 1 cm) results	95
G	ANWB head office results and method	99
G.1	Method	99
G.1.1	Input.	99
G.1.2	How to compare surfaces	99
G.1.3	ANWB: From measured points to rectangular point cloud	99
G.1.4	Projecting the rectangular grid	100
G.1.5	Averaging and comparing	100
G.2	Results	102
G.2.1	Point deviation	102
G.2.2	Histogram	102
H	Bibliography	103

Introduction

1.1. Shell structures in general

Shell structures have been around since the Roman era. The Pantheon in Rome is a still standing concrete shell, which was finished in 125 AD (figure 1.1). It is a relatively thick dome with a diameter of 43 meter and it has an oculus (a hole at the top). Today shells can have larger spans and can be made thinner than their historical counterparts. Shell structures are so efficient, because of their shape; it allows the load to be transferred through membrane forces (thereby minimizing moment and shear forces).

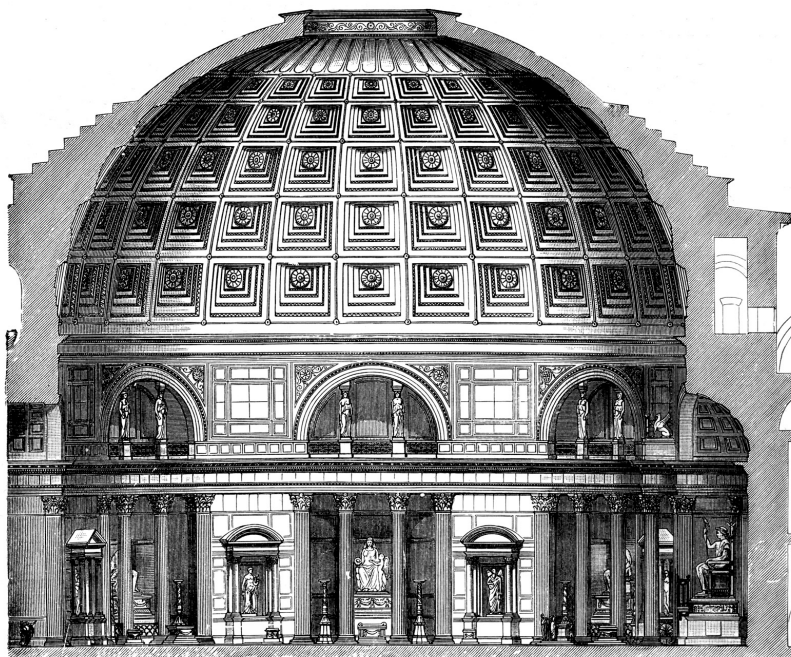


Figure 1.1: A drawing of the pantheon made in 1908

The relative thickness of a shell is determined by the ratio of radius/thickness or a/t . A shell is considered thin when $a/t > 30$.¹ For instance the pantheon in Rome has a $a/t = 18$ so it is considered a thick shell. Most modern shell structures are considered thin, like the Jena planetarium in Germany which has a $a/t = 470$. This thesis will focus on thin concrete shells, because they are more susceptible to buckling caused by imperfection.

¹Handout 1 CIE4143 shell analysis, theory and application, Dr.ir. P.C.J. Hoogenboom

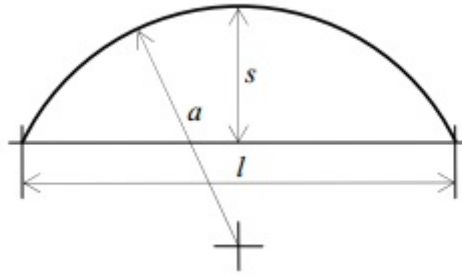


Figure 1.2: Shell variables where a is the radius, l the span and s the sagitta

1.2. Buckling in shell structures

Because buckling is a physically non-linear effect it is very hard to predict at which stress a structure will start to buckle. With thin shell structures this is especially true, because little imperfections can have a large effect on the ultimate strength. Some studies show that imperfections that are approximately as large as the buckling length of a shell will have the highest impact on the structural integrity. The buckling length of a shell is dependent on the radius a and thickness t .

$$l_{buc} = 2.4\sqrt{at} \quad (1.1)$$

For shells it has never been proven that an imperfection shape equal to the buckling shape can withstand the smallest ultimate load. In figure 1.3 the ultimate strength of a shallow spherical dome are displayed. There is a clear difference between a perfect geometry and one with imperfections.

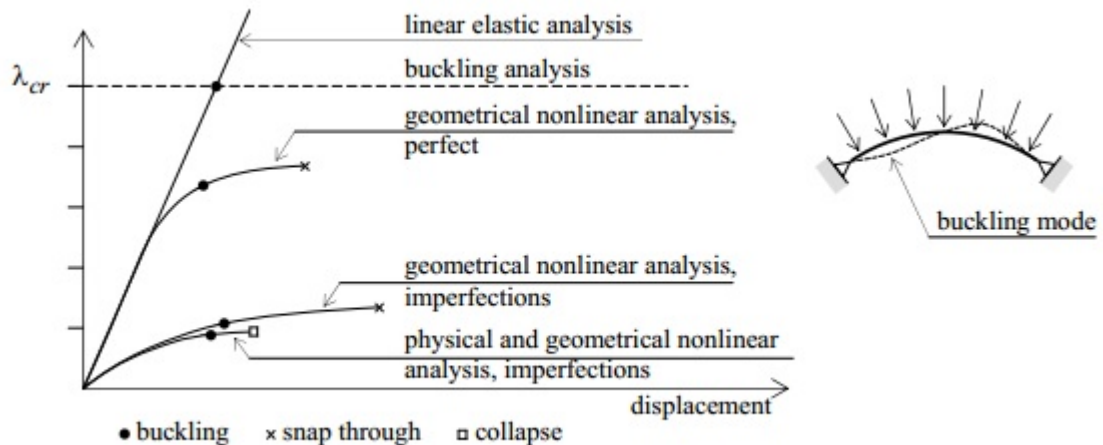


Figure 1.3: Ultimate strength of a shallow spherical dome in finite element method

1.3. The impact of initial imperfections on shell buckling

It is impossible to create a perfect smooth shape, where the stress in every point is parallel to the surface. This thesis will try to find out the typical imperfections which occur in shell structures. The causes for these mainly lie in the erection process of the shell. Evidence on how these imperfections are generated can be seen in some the results of the measurements.

As said in the previous paragraph a small imperfection can have a large effect on shell buckling. But not every shell structure is sensitive to imperfections. In table 1.1 the critical loading and imperfection sensitivity is shown.² For this research possible targets are shells that are sensitive to imperfections, so axially loaded open cylinders, closed cylinders, hyperboloids, spheres and domes.

²Handout 12, CIE4143 shell analysis, theory and application, Dr.ir. P.C.J. Hoogenboom

Type of shell	Critical loading p_{cr}	Critical membrane force n_{cr}	Imperfection sensitive
Open cylinder, radially loaded	$\frac{1}{4(1-\nu^2)} \frac{Et^3}{a^3}$	$\frac{-1}{4(1-\nu^2)} \frac{Et^3}{a^2}$	No
Open cylinder, axially loaded		$\frac{-1}{\sqrt{3(1-\nu^2)}} \frac{Et^2}{a}$	Yes
Open cylinder, torsionally loaded		$\frac{-1}{4(1-\nu^2)} \frac{Et^3}{a^2}$	No
Hyperboloid, axially loaded		$\frac{-1}{\sqrt{3(1-\nu^2)}} \frac{Et^2}{a}$	Yes
Closed cylinder, loaded in all directions	$\frac{2}{\sqrt{3(1-\nu^2)}} \frac{Et^2}{a^2}$	$\frac{-1}{\sqrt{3(1-\nu^2)}} \frac{Et^2}{a}$	Yes
Sphere	$\frac{2}{\sqrt{3(1-\nu^2)}} \frac{Et^2}{a^2}$	$\frac{-1}{\sqrt{3(1-\nu^2)}} \frac{Et^2}{a}$	Yes
Dome, base radius $> 3.8\sqrt{at}$	$\frac{2}{\sqrt{3(1-\nu^2)}} \frac{Et^2}{a^2}$	$\frac{-1}{\sqrt{3(1-\nu^2)}} \frac{Et^2}{a}$	Yes
Hypar	$\frac{2}{\sqrt{3(1-\nu^2)}} \frac{Et^2}{a^2}$	$\frac{-1}{\sqrt{3(1-\nu^2)}} \frac{Et^2}{a}$	No

Table 1.1: Critical loading and critical membrane forces of elementary shells

1.4. Construction of thin concrete shells

There several ways to construct a concrete shell. Heinz Bösiger constructed numerous thin concrete shells for the Swiss architect and engineer Heinz Isler from the 1954 to the end of the 20th century³. This research largely focuses on Isler shells in Switzerland, because there are numerous shells there, that can be measured easily. Isler and Bösiger used isolation panels (of rockwool and woodwool) as formwork for the concrete, which after erection stayed on the inner surface of the shell. These panels have a homogeneous thickness so will only give a small measuring error. The curvature of the shells was usually produced by shaped timber beams, which made a skeleton for the formwork. The concrete (with reinforcement) was laid on top of the formwork and was given an approximately uniform thickness.



Figure 1.4: Formwork of shell at Heimberg, Switzerland. On top the woodwool panels can be seen. Photo taken from the Journal of the international association for shell and spatial structures (IASS) Vol 52 (2011) No. 3

³Journal of the international association for shell and spatial structures (IASS) Vol 52 (2011) No. 3 page 161-169, Heinz Bösiger

1.5. Case study: Effect of initial imperfections on ultimate strength of a spherical shell

To clearly show the effect of geometrical imperfections on shell structures a finite element (FE) model was made. A spherical shallow dome with a perfect geometry was compared to two imperfect geometries (differing in amplitude of imperfection). The imperfections on the shell were created in Rhino 5.0, imported into FX+ for Diana and Diana was used for the analyses of these FE models. Appendix F contains a detailed description of the model, here a short summary of the setup will be given along with the results.

1.5.1. Setup

As stated before an spherical dome (20 m diameter, 3 m high and 10 cm thick) with a perfect geometry (figure 1.5) is compared to 2 imperfect shells, so the impact of the amplitude of the imperfection can also be shown. Both imperfect shells (figure 1.6) were given a sine imperfection with a wavelength of 4 meters and an amplitude of respectively 1 cm and 5 cm. The imperfection $I_{0.01}(x, y)$ and $I_{0.05}(x, y)$ can be expressed as:

$$I_{0.01}(x, y) = 0.01 \sin\left(\frac{2\pi}{4}x\right) \sin\left(\frac{2\pi}{4}y\right) \quad [m] \quad (1.2)$$

$$I_{0.05}(x, y) = 0.05 \sin\left(\frac{2\pi}{4}x\right) \sin\left(\frac{2\pi}{4}y\right) \quad [m] \quad (1.3)$$

All shells were loaded by an uniform face pressure in the z-direction (downwards) and were pinned along the edges. Then a linear elastic analysis of the perfect was done to indicate its stiffness. This analysis does not contain any second order effects, such as buckling. After this a geometrically non-linear analysis was done on all three shells. They were force controlled until they buckled. Force control is a method of increasing the load step by step until the structure fails at its ultimate strength. This method has the advantage that it is easier to produce than the arc-length method, but the method stops at ultimate strength and does not produce further results in the buckling phase. For this case study this was not a problem, because it focused on the ultimate strength of the shells. For more information on this topic search for the computational modeling of structures using the Finite Element Method.

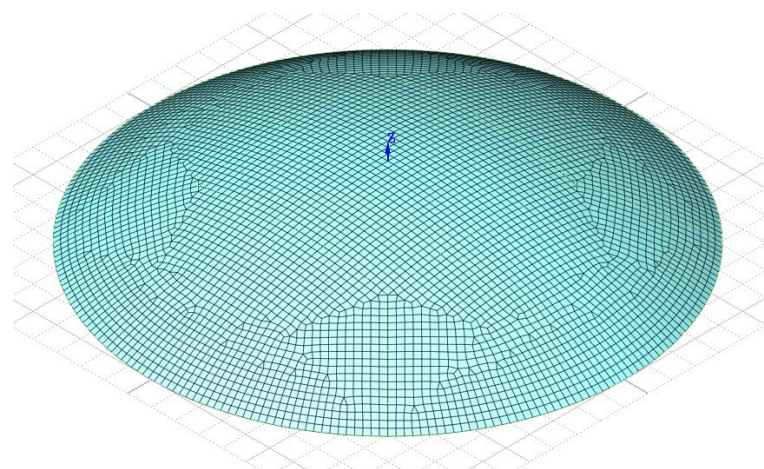


Figure 1.5: Visual representation of the mesh of the spherical shell in FX+, without imperfections

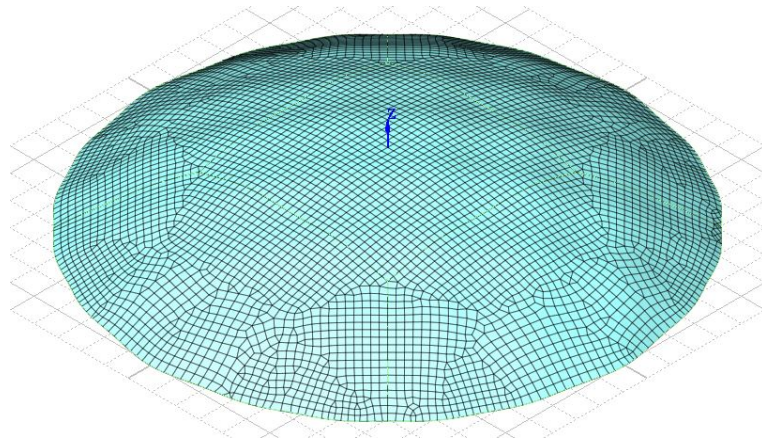


Figure 1.6: Visual representation of the mesh of the spherical shell in FX+, with imperfections

1.5.2. Results

From the data that was collected from the analyses, a load-displacement graph was made to indicate the ultimate strength. Figure 1.7 shows the displacement for an increasing load of the node at the side of the shells where buckling occurred (same position for all shells). In blue the linear elastic analysis can be seen, in red the geometrical non-linear analysis of the perfect shell and in yellow and purple the 2 non-linear analyses of the imperfect shells. The graph clearly shows a reduction in ultimate strength due to the imperfections. The ultimate strength of the shells is the load corresponding to the end of the load displacement line. It can clearly be seen that for an imperfection amplitude of 1 cm ($\frac{1}{10}$ the thickness) the structure loses $\pm 20\%$ of its strength and for an imperfection amplitude of 5 cm (half the thickness) it loses $\pm 33\%$ of its strength.

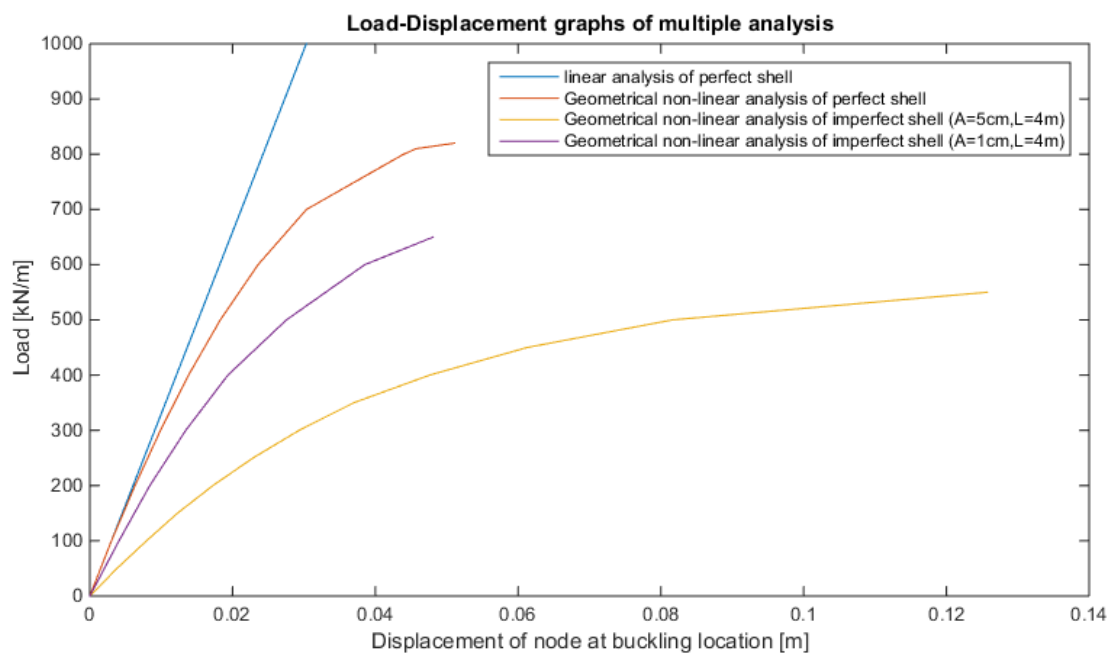


Figure 1.7: Load displacement graph of node at buckling location of multiple analyses

1.6. Problem and Goal

1.6.1. Problem

As the case study showed, imperfections in thin concrete shell structures have a significant effect on the ultimate strength. Imperfections can be taken into account for the design of shell structures in a number of ways. In most Finite Element programs a sinusoidal or another form of imperfection can be added to the geometry. But it is unknown if these forms of imperfections are representative. There is very little data on the actual geometrical imperfections of shell structures, therefore it is important to develop a method to measure these imperfections accurately. For if the characteristics of typical imperfections are known, the design process of shell structures will be significantly improved.

1.6.2. Goal of the thesis

The development of a method to accurately measure and represent the shape of spatial structures to facilitate evaluating geometrical imperfections of shell structures and their consequences.

2

Research methodology

This chapter focuses on methodology of this research in short. For more details and background of the decisions that were made see appendices. First an overview of the available measuring methods is given, resulting in the chosen method for this research. Then a short overview of the data output is discussed. And lastly the structures that were measured are listed.

2.1. Measurement method

2.1.1. Requirements

A method for measurement needed to be created for this research, at first it was thought that this had to be designed from scratch, luckily modern technology made this task easier. It was important to have a clear view on the requirements of the method. These were the most important ones:

- Accuracy: For buckling an accuracy of 1/10th of the thickness of the shell is needed (approximately 1 cm for the measured shells)
- Angle accuracy: The added error of the angle accuracy should be as little as the distance error. So if a shell is measured under a angle of 45 degrees at a distance of 10 m, total error of 1 mm is acceptable. Which gives a angle accuracy of approximately 30 arc seconds (120th of a degree)
- Speed of measuring: Because of the large number of points that need to be measured the total time it will take to measure a structure can become quite long. Therefore the speed of the method is an important factor. The aim was to measure a structure in a day or less. Taking into account the setup time, record time and breakdown time
- Output: Digital output is preferred, because it lowers the chance of errors and speeds up post-processing
- Weight and size: The method must be transportable by one person with a car and it is preferred the measuring can be done by one person
- Costs: Due to the limited budget of the TU Delft the components must not be too expensive

When comparing measuring methods it is easier to have a fixed example shell, therefore it is possible to make simple calculations. The example shell parameters are in tabel 2.1. Using the buckling length equation 1.1 the example shell has a buckling length of 3.4 meters, so in this range of wavelength of imperfections that should be searched for. Lets assume that for the detection of wave of that length you would need at least 6 points and a couple of buckling lengths are needed, then the example shell would need 400 measured points (20 by 20) to be mapped completely. Note that this was a rough approximation and that number of necessary points needed was much higher. It could be beneficial to measure a part of the shell with a higher concentration of points, so the entire measured surface could be interpreted better.

Parameter	Approximation
Thickness t	100mm
Radius a	20m
Relative thickness a/t	200
Width b	10m
Height h	10m
Buckling length l_{buc}	3.4m

Table 2.1: Example shell parameters

2.1.2. Available methods

There are a number of options which can be used to accurately measure a surface. In the table 2.2 are the parameters of 5 possible methods are given. In appendix A each method is described in detail. Because the Faro focus 3D scanner's speed (thousands of measurements a sec) is exponentially higher than the other methods, the measuring time of a single point is N.A. (non applicable) and total measuring time is an indication of the time it takes to measure 400 points (example shell).

Measuring methods	Accuracy	Angle accuracy*	Measuring time 1 point	Total time**	Output	Costs	Manpower
Theodolite	1mm	1'	2min	15h	analog	100 Euro/week	1
Total station	1mm	1"	20sec	4h	digital	200 Euro/week	1
Faro Focus 3D	2mm	1'	N.A.	1h	digital	20 Euro/week***	1
Manual Laser distance measurement	5mm	20'	30sec	5h	analog	80 Euro (buy)	1
Manual measurement	1cm	20'	1 min	8h	analog	free***	1

Table 2.2: Measurement method parameters.

* An arc second ["] is a 60th of an arc minute ['] which is a 60th of a degree, so if the accuracy is in the order of an arc minute it is precise enough.

** Total time was an approximation of measuring 400 points (example shell) with the setup and break off time included.

*** There was no company in the Netherlands which rents out Faro's scanners like theodolites are rented out. But via the department of Remote sensing contact was made with Deltares, which is a coastal engineering company, that had a Faro Focus 3D scanner. They were kind enough to lend out the device for 100 Euro for 1 month. Because of this the 3D scanner from Faro became one of the cheapest options as well.

2.1.3. Chosen method

Because of the accuracy and number of measurements that are needed on each surface, only two of the options were feasible. The first choice was the Faro Focus 3D scanner, because of its speed, high number of measured points, accuracy and the existence of post-processing programs. With this device a surface can be mapped within an hour, which makes it much easier to be granted access to a building. And with the post-processing programs it is easier to create a digital 3d surface. But most important is that a Faro focus 3D scanner can measure more than a thousand times more points compared to the other methods. This makes the result much more reliable

Second choice was the Total Station, because of its accuracy, digital output and relative short measuring time. If the device was not available at the TU Delft, but it could have been rented. The other three options were not accurate enough or the time it took to map 1 surface would be too long. Measurements need to be as short and unintrusive as possible, to have an higher chance of cooperation of the owners of the building or structure. The Faro Focus 3D laser scanner was therefore the preferred option.

2.1.4. Specifications of the Faro Focus 3D X130

In this paragraph the specifications of the Faro Focus 3D X130 scanner are listed, for a more information on the device see Faro's website.¹

Operation

For measurement a laser scanner by Faro technologies was used. Faro is an American company which specializes in mobile 3D measurement technologies². Via the remote sensing department of the CEG faculty, the delft based company Deltares was kind to lend out a new Faro focus 3D x130 scanner. The machine works by sending out laser pulses which reflect back from the measured surface to a light sensitive sensor of the machine. It can calculate the distance of the surface by measuring very precisely the time it takes for the pulse to return to the machine. Via the rotating mirror in the middle of the device (see figure 2.1) it can send out pulses at a very high rate. And by recording the position of the mirror and direction of the device itself, the x, y and z-coordinates of a measured point is calculated and stored in a simple matrix on the device. Using Scene (software from Faro itself) these points can be exported to most drawing or 3D modeling programs. For this research Rhinoceros 5.0 was used.

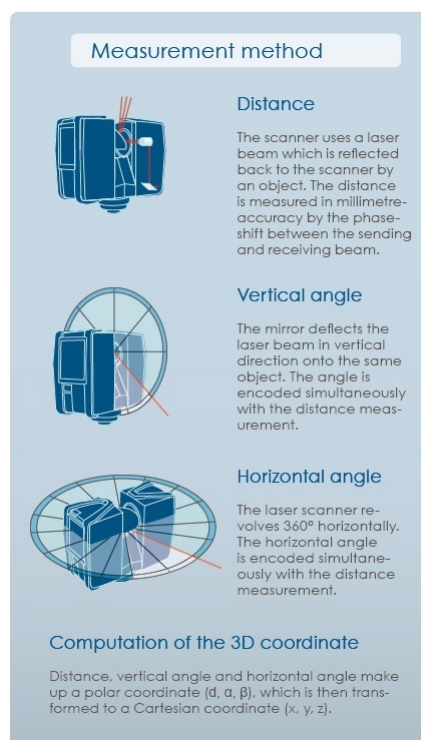


Figure 2.1: Workings of the laser scanner from Faro laser scanner Focus3D brochure

The workings of the Faro focus laser scanner are shown in 2.1. The device can be set to measure a certain part of its field of view only. This speeds up the measuring process, because the irrelevant area is not measured and stored.

Reference spheres

Multiple scans can be combined to make one large point cloud of measured data in post-processing. This can be done by manually placing several scans by mapping key features in the scans, but this is not very precise. The other option is to use so called reference spheres (figure 2.2). These are matte white balls with a very precise diameter at every point of the sphere. When enough points in a scan are measured on the surface of one of these spheres its exact location can be calculated. If 3 or more spheres are visible in 2 scans (for both and the same spheres without moving them), Faro's

¹<http://www.faro.com/en-us/products/3d-surveying/faro-focus3d/overview>

²<http://www.faro.com/nl-nl/producten/3d-landmeetkunde/laserscanner-faro-focus-3dlaserscanner-faro-focus-3d/overzicht>

software package Scene can connect scans with relative high precision. This precision depends on the number of spheres visible, the distance between the spheres and the number of measured points on their surface.

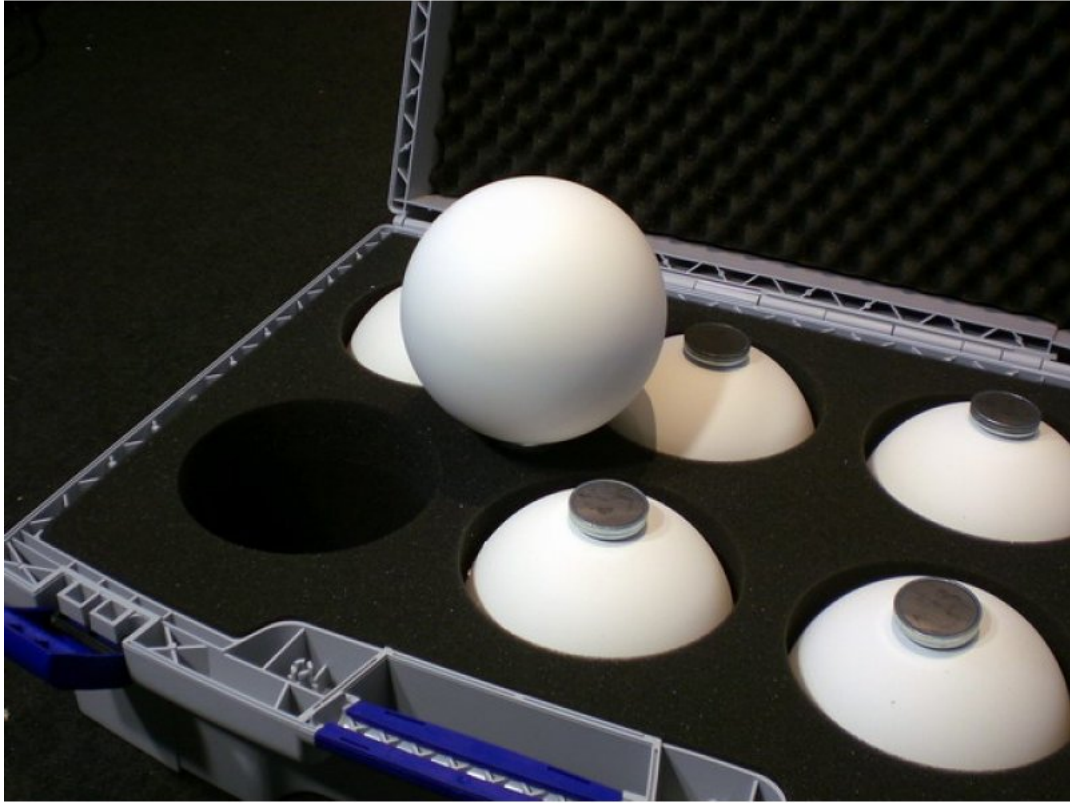


Figure 2.2: A couple of reference spheres in their protective suitcase

Specifications and certificate of accuracy

The specifications of the Faro Focus laser scanner X 130 are listed in table 2.3. For the calibration certificate see figure 2.3, which was the result of an accuracy test one month before the device was used.

Range	0.6-130m
Measurement speed	up to 976 000 points/second
Ranging error	±2mm
Ranging noise	@10m-raw data 0.3 mm @90 refl. @25m-raw data 0.3 mm @90 refl. @10m-raw data 0.4 mm @10 refl. @25m-raw data 0.5 mm @10 refl.
Laser class	laser class 1*
Weight	5.2kg
Multi-sensor	GPS, Compass, Height sensor, Dual Axis Compensator
Size	240 x 200 x 100mm
Scanner control	Via touchscreen and WLAN

Table 2.3: Specifications of the Faro Focus laser scanner X 130 * Laser class 1 cannot emit accessible laser radiation in excess of the applicable Class 1 AEL for any exposure times within the maximum duration inherent in the design or intended use of the laser. Class 1 lasers are exempt from all beam-hazard control measures.³

Calibration Certificate

Model: Focus 3D X 130 Serial Number: LLS071405971 Certificate Number: LLS05971-20141023-SM
Certification Date: 23-Oct-2014

Measurement Items Used, Traceable to National Standards

Laser Tracker Model: <u>Vantage</u>	Serial No.: <u>V01001304240</u>	Cert. No.: <u>V4240-1612014-PA</u>	Cert. Date: <u>16-Jan-2014</u>
Reflectance Targets Model: <u>SRS-90-020</u>	Serial No.: <u>TQ3342</u>	Cert. No.: <u>C13090912</u>	Cert. Date: <u>9-Oct-2013</u>
Model: <u>SRS-10-020</u>	Serial No.: <u>TQ3359</u>	Cert. No.: <u>C13090613</u>	Cert. Date: <u>9-Oct-2013</u>

Calibration Results

Ranging	Target	Distance [m]	Uncertainty, k=1 [mm]	Scanner [m]	Deviation [mm]	Specifications	Result
	CD6	10,5095	0,496	10,5098	-0,3	2,0	pass
	B07	22,6047	0,496	22,6057	-1,0	2,0	pass

Ranging Noise	Reflectance	Distance	Uncertainty, k=1 [mm]	Scanner	Specifications	Result
90%	10 m		0,067	0,17	0,30	pass
	25 m		0,067	0,20	0,30	pass
10%	10 m		0,067	0,23	0,40	pass
	25 m		0,067	0,42	0,50	pass

This certificate shall not be reproduced, except in full, without permission of FARO Technologies, Inc. It invalidates all other certificates generated before the certification date.
The results of this certificate relate only to the items calibrated or tested.
The calibration is done at FARO or FARO Scanner Production operations sites according to FARO test protocols integrating guidelines defined in the Joint Committee for Guides in Metrology guidance document JCGM 100:2008 - Evaluation of measurement data - Guide to the expression of uncertainty in measurement, and the requirements for traceability according to the International Vocabulary of Basic and General Terms in Metrology (VIM) and the National Institute of Standards and Technology (NIST).

Authorization: Simone Fackler Calibration Technician Date: 23-Oct-2014

FARO
FARO Swiss - Wiesengasse 20 - CH 8222 Beringen - Switzerland
Tel: +41 52 68719 00 - Fax: +41 52 68719 99 - Mail: support@faro-europe.com - www.FARO.com

Revised: 24 June 2014 © 2014 FARO | ELL-DE-01FRM208
Revised: 03 Sep. 2014 © 2014 FARO | FIJ-FN-07FRM010

Figure 2.3: Certificate of accuracy of the Faro Focus 3d x130 scanner used for this research

2.1.5. Data output

The Faro focus laser scanner produces a .fls file where all the measurement points are stored. Via Scene the entire scan or a part of it can be exported into a .pts file, which Rhinoceros can open. Figure 2.4 shows the workspace of Scene and the scale model Isler shell that has been selected. Only the points within the yellow rectangle will be exported into the .pts file.

The .pts file that is created contains a list of points (in this case 145824 points) with 4 point parameters. The parameters are X,Y,Z location of the point and a the gray scale of the measured point. When the camera is connected to the scanner the gray scale is changed into a red, blue and yellow scale for a color representation of each point, but this will not be used in this research.

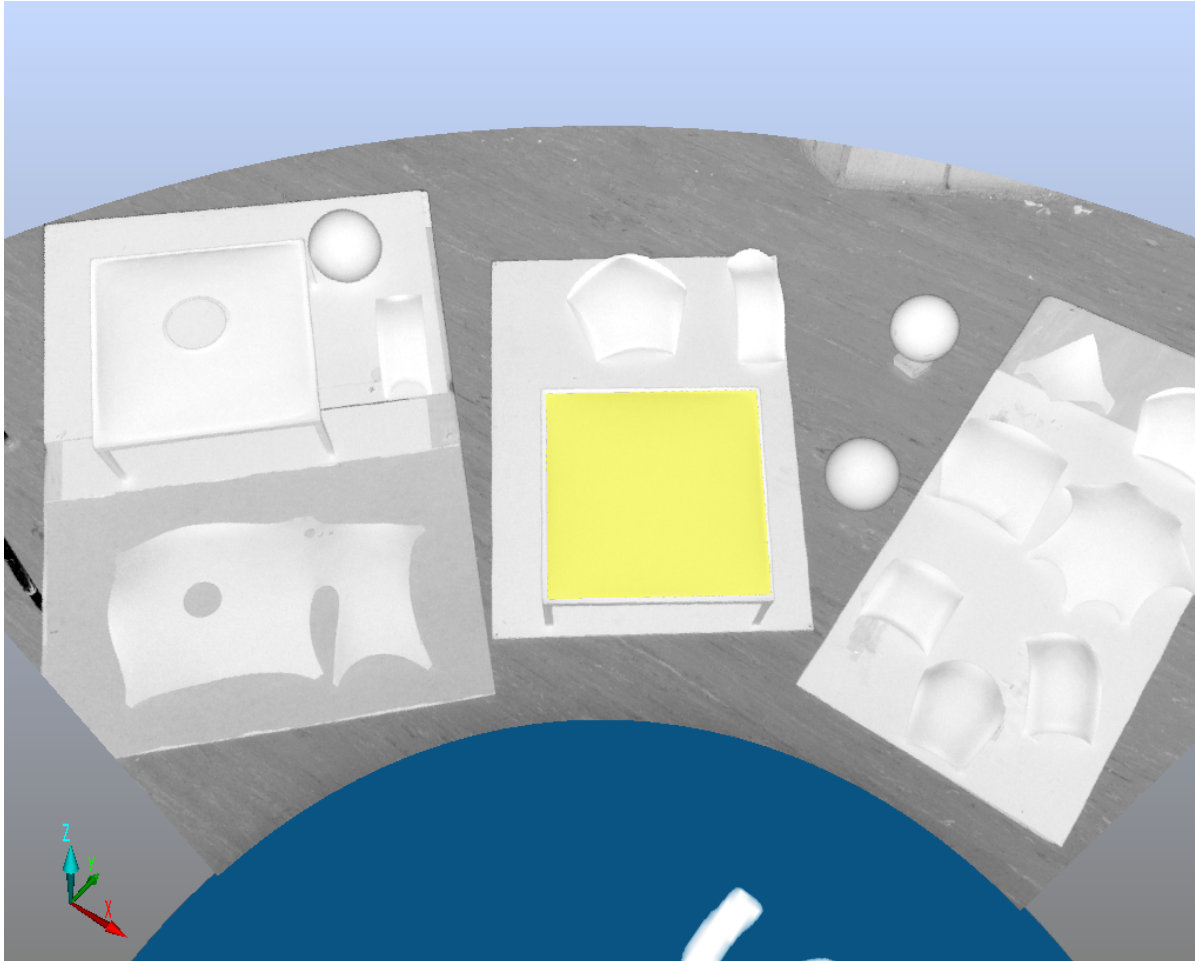


Figure 2.4: Scene workspace with scale model isler shells

2.1.6. Plotting a 3D surface through the points

When the .pts file is loaded into Rhinoceros a 3D representation of the points is shown (see figure 2.5). It is possible to fit a 3D NURBS surface through these points by using the command "patch". NURBS (Non-Uniform Rational B-Spline) curves and surfaces are a mathematically constructed and used in computer graphics. There are 3 variables which can influence the surface, namely: number of control points in u-direction, number of control points in v-direction and the stiffness. The surface can be seen as a canvas that is curved over the point cloud, so the stiffer the canvas is the smoother the surface will be. When it is less stiff the surface will follow the deviations of the points more closely. The number of control points influence the number and size of the waves the surface can make. u and v are used as the local coordinate system for the surface in the global x, y, z coordinate system. For more information on NURBS surfaces and their control points see appendix C.

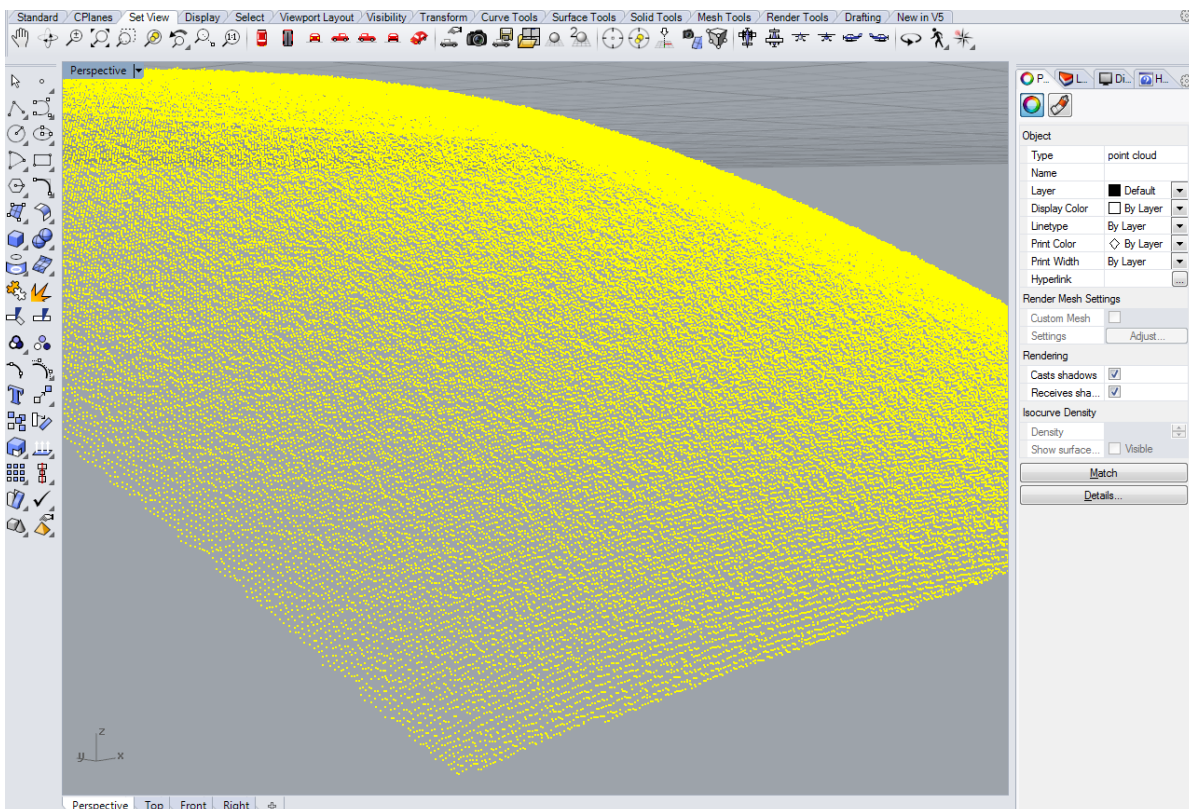


Figure 2.5: Point cloud in Rhinoceros zoomed in to show separate measured points

2.2. Measured shells

A short description of the measured shells is given, all shells were measured using the Faro Focus 3D x130 scanner. Five of the six shells are located outside the Netherlands (four in Switzerland and one in Germany), these structures were all measured during the first weekend of January 2015. A travel report was made and can be found in appendix E. The appendix describes the measurements of the target in detail and gives tips for anyone who is planning a similar trip.

2.2.1. Deitingen

Structure

Near Deitingen in Switzerland there is a service station which has two simplistic Isler shells (see figure 2.6). Because this shell is outside and has no surface finish it is an ideal candidate for measurement. Both shells are thin, made of concrete and dome shaped with tapered supports.

Measurement plan

The two shells at the service station in Deitingen were measured from the ground, without any problems (see figure 2.6). The top of the structure was also measured from a distance, but not the entire top could be measured. Furthermore the top and bottom scans were connected using the reference spheres, that Faro created for the focus 3d scanner. Because measurements at a high angle are not as precise as measurements where the surface is perpendicular to the laser, the thickness was only measured at the edges. This can easily be done with a ruler, so only the data bottom of the shell was collected.



Figure 2.6: Highway Service area Deitingen South, Switzerland

2.2.2. Heimberg Schimmbad

Structure

The swimming pool in Heimberg is a square shell with an oculus in the top. The structure is ideal for measurement, because it is quite large (span of 35 meter) and has relative low curvature. The surface of the shell has little finish and is accessible (see figure 2.7). Next to the swimming pool is a tennis hall which also is a shell by Isler. When visiting the Heimberg swimming pool the tennis hall could be measured without any extra travel time.

Measurement plan

The inside of the swimming pool was measured without any problems and by using the reference spheres a scan of the entire shell was made. There were also scans made of the outside of the structure, but it was not possible to connect the inside and outside in Scene.



Figure 2.7: Inside of the swimming pool in heimberg

2.2.3. Heimberg Tennis

Structure

Next to the swimming pool in Heimberg, there is a set of indoor tennis courts which has a couple of identical Isler shells as roofs (see figure 2.8). The finishing on the inside of the shell is the same material as in the swimming pool next to it. These insulation panels are of an uniform thickness, therefor only a small error is added to the measurements. This was taken into account when interpreting the results.

Measurement plan

Measurement was simple here, the entire roof could be captured in 1 scan. Only one shell of the 5 identical shell was measured, because at the moment of measurement the other courts were used.



Figure 2.8: A photo from the inside of the tennis hall in Heimberg

2.2.4. Grötzingen

Structure

There is an open air theater in Grötzingen (Germany) which has a Isler shell as a roof. A 3D representation is in figure 2.9 made by 3 students of Princeton university⁴ who visited the shell. The shell finishing is similar to the ones at Heimberg, but layers are also relatively thin and homogeneous.

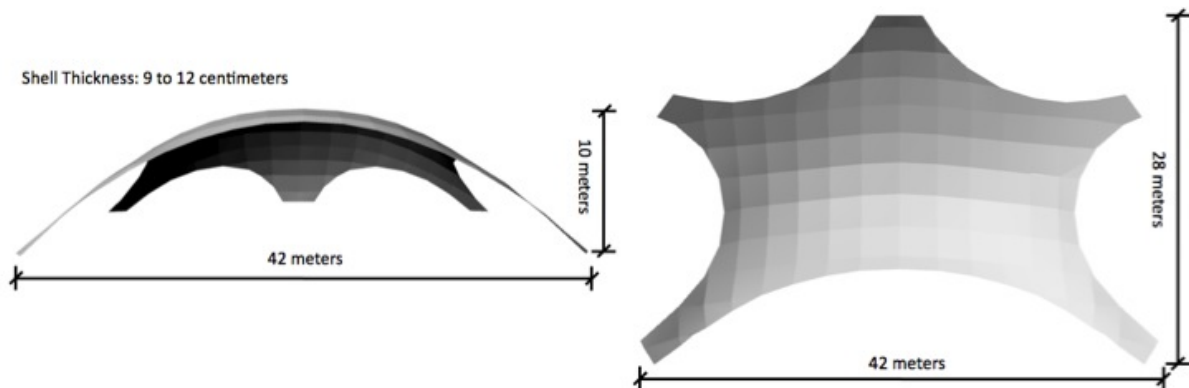


Figure 2.9: A 3D computer model of the Shell in Grötzingen with its parameters

Measurement plan

The open air theater in Grötzingen was measured from the ground without any problem, just like the service station in Deitingen. There are some lights and some rails hanging from the bottom of the shell (see figure 2.10). The top of the theater was hard to measure, because the theater was surrounded by vegetation and when the measurements were made the structure was covered by snow.



Figure 2.10: The open air theatre in Grötzingen

⁴Shells.princeton.edu/Grotz

2.2.5. Wyss Garten centre

Structure

The structure in Solothurn, Switzerland, is used as a garden center so it was a bit busy inside. Thankfully, the staff of the garden center let us measure the shell. It is a thin shell made of reinforced concrete (which can be seen in figure 2.11), with isolation panels as finishing on the ceiling (just like in Heimberg and in Grötzingen).

Measurement plan

Because of many obstacles inside the structure it was impossible to measure the entire shell from 1 point. Just like the measurement of the swimming pool in Heimberg the set of reference spheres was used to measure the entire ceiling of the shell.



Figure 2.11: Garden centre in Wyss, Switzerland

2.2.6. ANWB head office

Structure

The head office of the ANWB (Dutch national cyclist association) in The Hague has a dome for a roof in the main hall, see figure 2.12. It was possible to measure the surface of this dome, although there was a sort of chandelier hanging from the ceiling, which was between the scanner and part of the roof for all possible locations for the scanner. The shell had a rough cement finish, which will lead to a small measurement error (approximately 0.5 cm).

Measurement plan

Similar to the other structures a scan was made of the bottom of the shell. Due to the large chandelier it was only possible to measure half of the dome. Because there were many people present when the measurements were done, the reference spheres could not be used.



Figure 2.12: ANWB Headoffice The Hague

3

Data Processing

This chapter describes the methods used to create results from the collected data. A method was created that can calculate the geometrical imperfections in the measured shells, using only the point cloud that was created by the Faro Focus 3D. This was done by using NURBS surfaces, created in Rhinoceros 5.0. The first section of this chapter will go into detail on how these NURBS surfaces are created and what their properties are. Then in the second section a description of the data processing method is given. The last section describes another the method for calculating the largest imperfection in the data.

3.1. NURBS

3.1.1. Creation of NURBS

NURBS (Non-Uniform Rational B-Spline) curves and surfaces are mathematically constructed curves and surfaces, which are used in computer graphics. In appendix C the theoretical background of NURBS curves and surfaces is given. In this chapter the use of these computer generated surfaces will be discussed. For this research Rhinoceros 5.0 (or Rhino) with the plug-in Grasshopper was used. It is possible to create NURBS surfaces through point clouds with other programs, but Rhinoceros is a very versatile program with several available plug-ins, so it is recommended.

When a point cloud file is loaded into Rhino a 3D representation of the points is shown (see figure 3.1). It is possible to fit a 3D NURBS surface through these points by using the command "patch". There are 3 parameters which influence the surface geometry, namely: number of control points (cp's) in u-direction u , number of control points in v-direction v and the stiffness s . The surface can be seen as a canvas that is curved over the point cloud, so the stiffer the canvas is the smoother the surface will be. When it is less stiff the surface will follow the deviations of the points more closely. The number of control points influence the number and size of the waves the surface can make. u and v are used as the local coordinate system for the surface in the global x, y, z coordinate system.

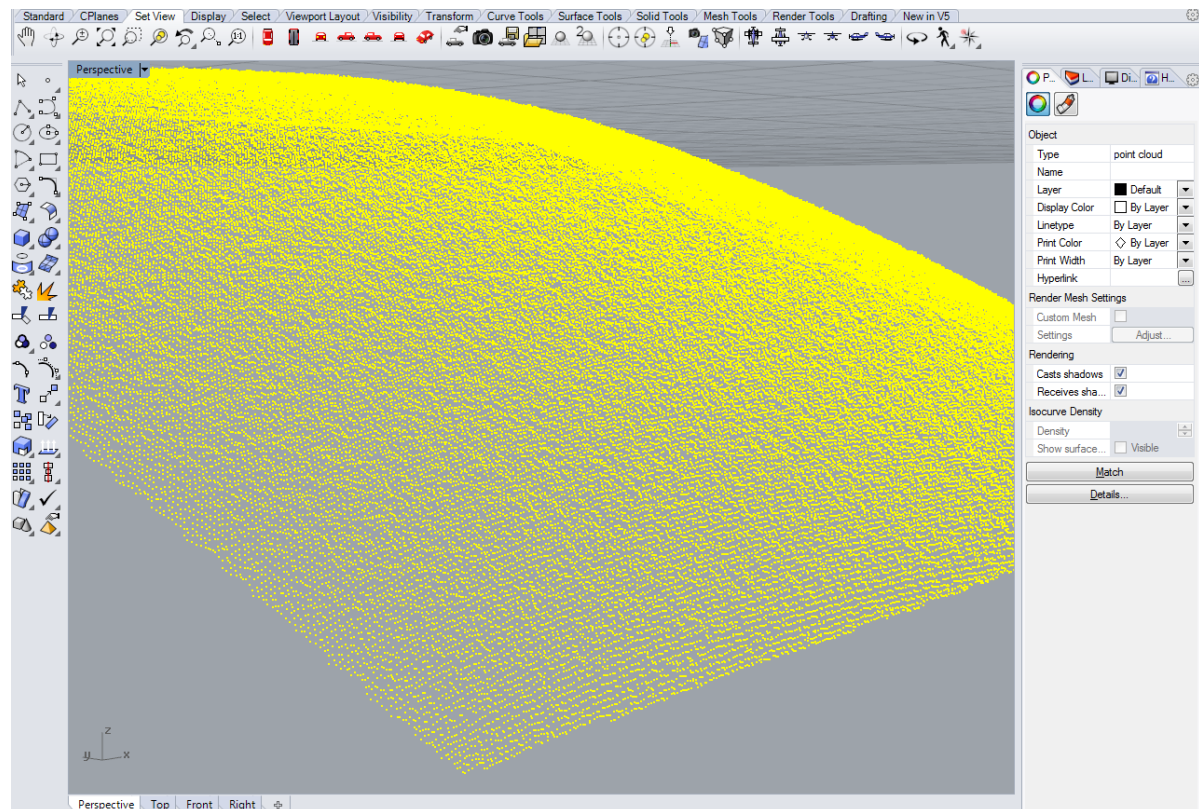


Figure 3.1: Point cloud in Rhinoceros zoomed in to show separate measured points

3.1.2. Determination of NURBS parameters

As stated all NURBS surfaces are created by defining 3 parameters (number of control points in u and v -direction and stiffness). For the purpose of this research it is important to understand how these parameters effect the NURBS surface. The aim of this research is to develop a method which can reliably find imperfections in shell structures. In the introduction the importance of imperfections in the size range of the shells buckling length was discussed. Analysis of the results has shown, that the method that was produced was not able to show wavelengths of imperfection near the length of the shell itself. This implies imperfections have wavelengths in the range of 10 meters or more were not taken into account. This is not a problem, because this research focusses on local imperfections and not global. The buckling length's for the measured shells are significantly smaller (2 to 5 meters of wavelength). Due to the effect imperfections within this wavelength range have on shells, only wavelengths smaller than the largest buckling length were searched for.

Influence of parameters

The patch function in Rhino creates a NURBS surface using three parameters; u , v and s . To check the influence each of these parameters, four graphs were made using Matlab (see figure 3.2). For two different number of control points, the stiffness was varied and the mean and standard deviation is for each setting is shown in the upper two graphs. And for two different stiffnesses, the number of control points was varied and the mean and standard deviation is for each setting is shown in the lower two graphs.

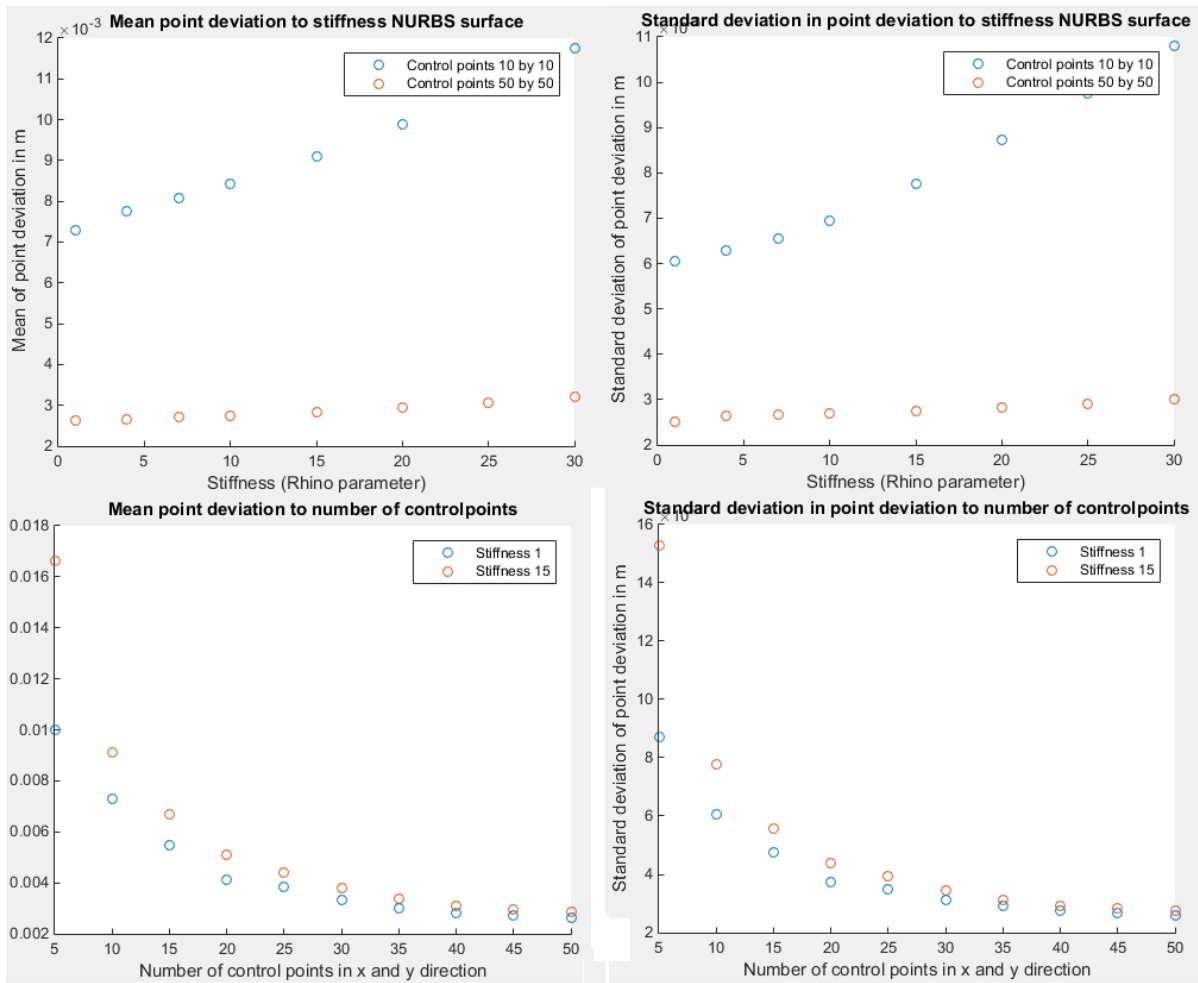


Figure 3.2: Graphs of the influence of NURBS parameters. Upper two graphs show the influence stiffness has on the mean and standard deviation of the point deviation. Lower two graphs show the influence the number of control points have on the mean and standard deviation of the point deviation.

In the upper two graphs it can clearly be seen, that stiffness of the NURBS has no influence for a large number of control points (50 by 50). With a lower number of control points (10 by 10), the influence of the stiffness parameter becomes more apparent. Although it can clearly be seen that the number of cp's has more effect. In the lower two graphs the relation between number of cp's and the point deviation between the NURBS and the measured points, becomes more clear. The higher the number of cp's the closer the NURBS approaches the point cloud. And with lower number of cp's the deviation grows exponentially.

Control points per wavelength

To indicate how the number of control points influences the geometry of NURBS surfaces, a point cloud with a sinus imperfection of 5 cm amplitude and wavelength of 2 m is created (see figure 3.3). The point cloud is a rectangular array of 1 million points (10 by 10 m) which is projected on a surface with a sinus imperfection in both directions. The scripts which were used can be seen in appendix B (rhino/grasshopper scripts).

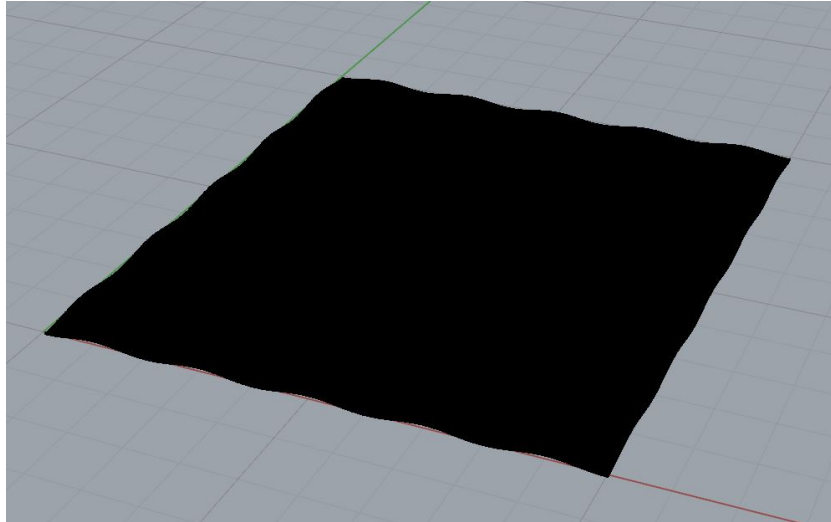


Figure 3.3: Generated 10 by 10 meter sinus field with grid of 1 million points, with an amplitude of 5 centimeters and a wave length of 2 meters

In figure 3.4 and 3.5 the point deviation of both a 11 by 11 patch and a 10 by 10 patch is shown (both with stiffness 1). It is clearly visible that distance between the control points needs to be the half of the full sinus wave as is in figure 3.4. When the distance between control points is less than half the sinus wave (as is in figure 3.5) the patch has trouble following the points (mean deviation is 1.95 cm instead of 0.04 cm) of the cloud and at every bulge or valley the geometry is not precise.

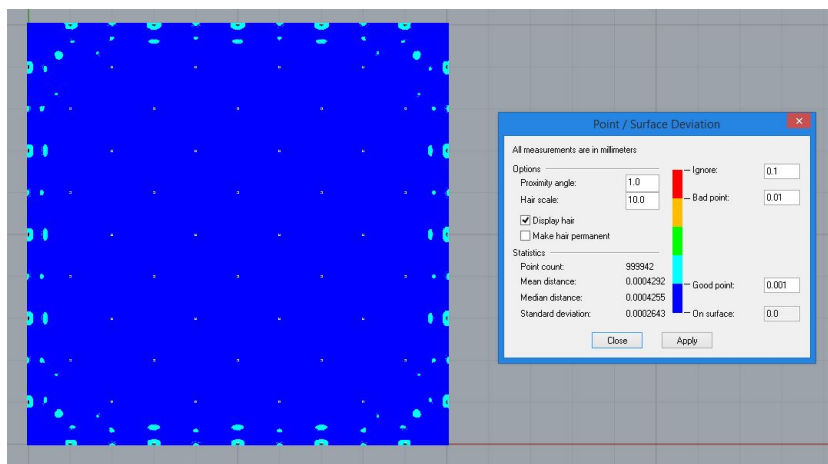


Figure 3.4: Point deviation of a NURBS surface with 2 control points per full sinus wave, mean deviation is equal to 0.04 cm

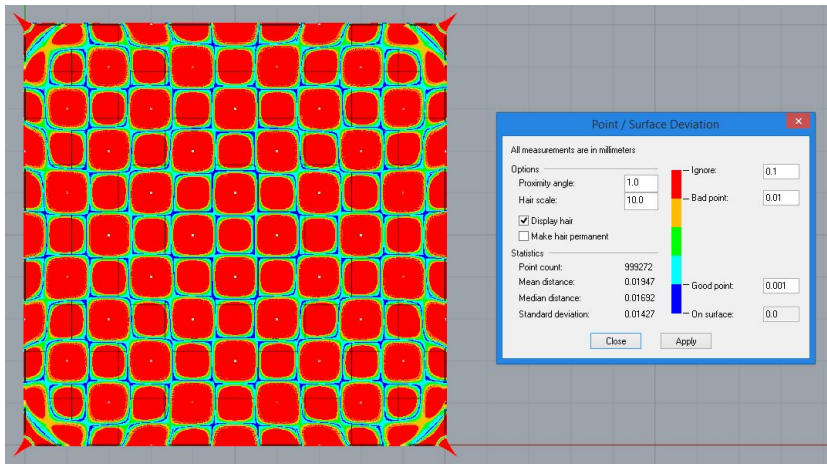


Figure 3.5: Point deviation of a NURBS surface with just less than 2 control points per full sinus wave, mean deviation is equal to 19.47 mm

Every wavelength of imperfection in a surface will show the same results. It can be concluded that for creating a complete sine (or cosine) wave in a NURBS surface 2 control points per wave length are needed. Therefore the following statement holds:

$$n_{cp} \approx 2L/l \tag{3.1}$$

Where n_{cp} is the number of control points needed to create wavelengths l (and smaller) and L is the length of the sample. Figure 3.6 shows that for less than 2 control points per wave length the NURBS does not follow the bulges and dents of the sinus field.

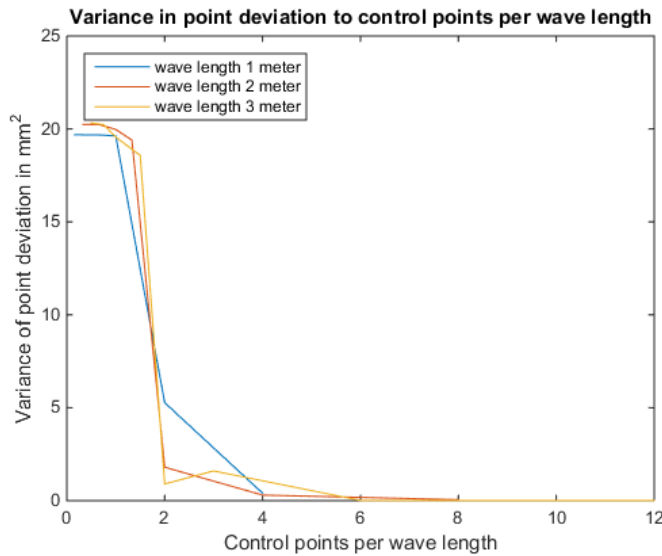


Figure 3.6: Graph which shows the relation of the standard deviation in deviation per number of control points per wave length l . For three different wave lengths the jump in standard deviation appears at 2 control points per wave length

3.1.3. Purpose of NURBS in this research

Although the stiffness of the NURBS does not significantly affect it, but by controlling the number of cp's, it can be assured that an intended shape can be created where no wavelengths can be present in the buckling length range. Therefore an intended shape can be made using the original data.

3.2. Double NURBS method

Multiple methods were tried in the course of the research. In this chapter only the method which can create reliable results is discussed. In appendix G a method is described, which makes use of symmetry in the measured shells. Appendix C describes the use of the Fast Fourier transform (FFT) on finding geometrical imperfections in the data. Both of these methods did not create reliable results, therefore the Double NURBS method is the only one used for creating results. This method uses the characteristics of NURBS described in the previous paragraph. As stated before no blueprints or other documents on the intended shapes of the shells was available, therefore an intended shape per shell had to be created, where the data can be compared to. This intended shape is made by using number of cp's per wavelength phenomena. A maximum number of control points can be calculated, which will make sure that the intended (or comparative) shape NURBS can not create waves within the buckling length range. These comparative NURBS surfaces can be compared to a approximated (or detailed) NURBS created from the data. This NURBS will have as much control points as possible and is thereby the closest approximation to the data.

3.2.1. Steps of the method

In this paragraph a step by step description of the NURBS compare method is given. For the explanation of the method the data from the tennis hall in Heimberg is used. The method uses the correlation of control points per wave length to create the original intended shape from the collected data itself.

Step 1: Create a continuous rectangular piece of data

To ensure that the method works reliably, a rectangular piece of measured data without too many gaps is needed. The dimensions of this piece of data can be chosen almost freely, but it is preferable to make sure it is as large as possible. This will minimize the loss of data that was collected. It is also preferable that the piece of data is entirely continuous, some small gaps (1 to 5 percent of data missing) are not a problem, but if large chunks are missing the method will not give reliable results. A example of this can be seen in figure 3.7. The point cloud of the shell at Zuchwill shows large gaps, due to objects on the ceiling and on the ground blocking the scanner. This problem can be solved by the use reference spheres, but these do add an error to the data. In the case of this shell that error was too large for the data to be usable.

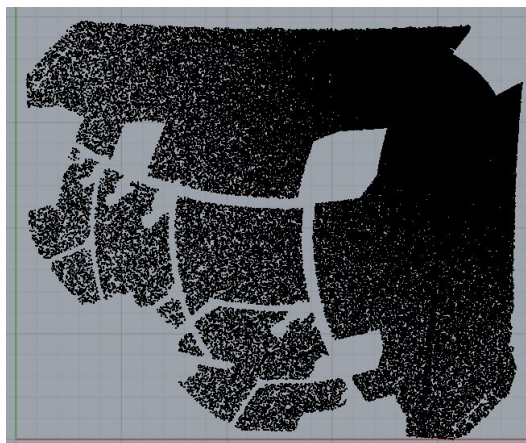


Figure 3.7: Top view of point cloud of one of the four scans made in Zuchwill. It show the gaps in the data due to obstacles present during measurements

An example of a usable piece of data is shown in figure 4.4. Here a continuous piece of data 12 by 12 meters could be cut out of the raw data. Figure 3.9 shows the piece of data in perspective. Because the shell was quite large two similar pieces of data were cut out of the raw data.

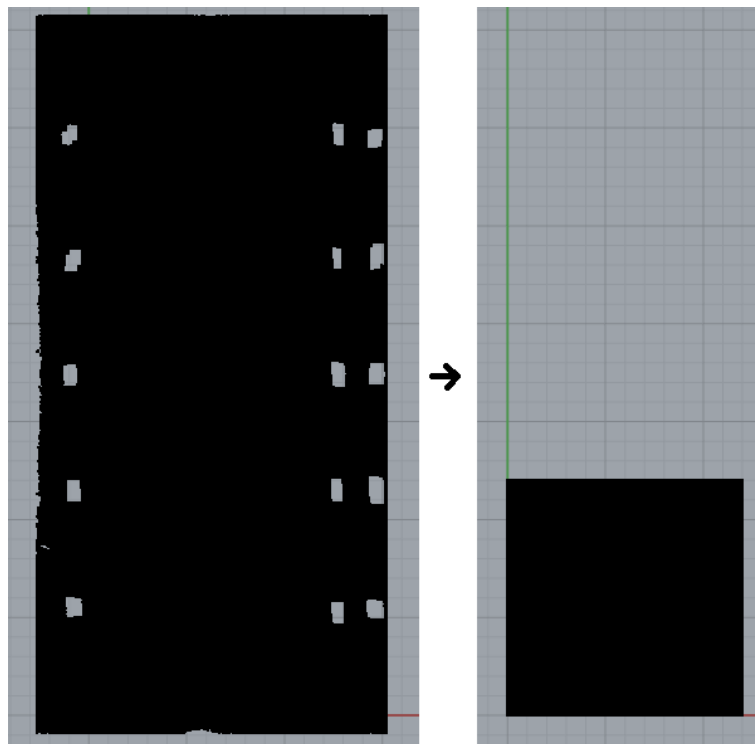


Figure 3.8: Top view of point cloud of entire tennis hall shell in Heimberg at the left, the right image shows a 12 by 12 m cutout piece of data. The gaps in the point cloud are lamps hanging from the ceiling, which blocks the laser pulses from reaching the shell.

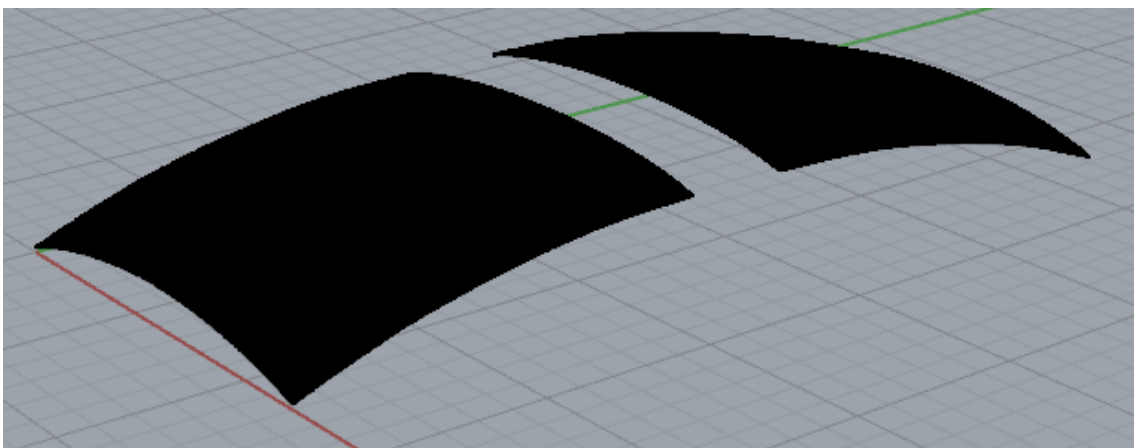


Figure 3.9: Perspective view of two (12 by 12 m) cutout pieces of data of tennis hall shell in Heimberg

Step 2: Calculate buckling length for shell, thereby determining number of control points for intended shape

Per individual shell an estimation for the buckling length can be created using the buckling length equation from chapter 1 (1.1). Using the relation shown in the last paragraph between the maximum number of control points to create a certain wavelength, a number of control points can be set for the intended shape. Because this is an estimation for the buckling length and the control points can only be set in integers, the number of control points is roughly half of that what is needed.

Step 3: Create intended and detailed NURBS surfaces

At this point the 2 NURBS surfaces are created. The approximated surface (sometimes called detailed) will be as close to the data as possible, therefore it will have the maximum number of control points the

computer can handle. The approximated surfaces can be seen in figure 3.10, where the high number of control points can be seen. The other surface (the intended or comparative shape) will have the set number of control points calculated in the last step to ensure this will surface will not contain wave lengths smaller than or equal to the buckling length. In this case the intended shape had 3 control points per direction. Figure 3.11 shows the intended or comparative shape.

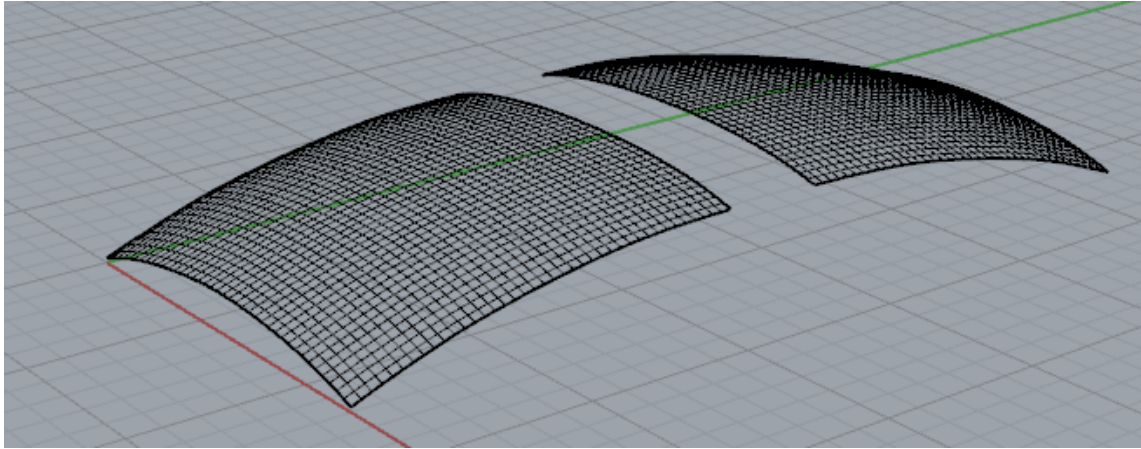


Figure 3.10: Perspective view of two approximated NURBS surfaces of tennis hall shell in Heimberg

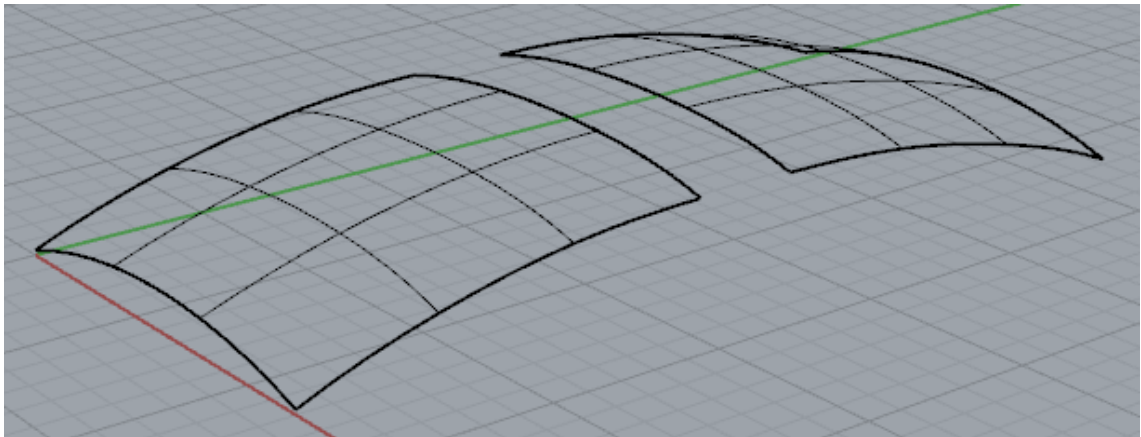


Figure 3.11: Perspective view of two comparative NURBS surfaces of tennis hall shell in Heimberg

Step 4: Project regular point grid on NURBS surfaces

It is not possible to subtract a surface from another surface in Rhinoceros or Grasshopper. When the mathematical expression of the surfaces was known this could be done analytically in Maple, but Rhinoceros does not have the option to export the expression of the NURBS surface created. Therefore the best option is to turn the surfaces into a rectangular grid of points. This way both surfaces have the exact same grid of point projected on them, with only a difference in z-coordinates. Figure 3.12 shows the rectangular grid of points (blue), which needs to be projected on the surfaces. Figure 3.13 shows the projected grid of points on both NURBS surfaces.

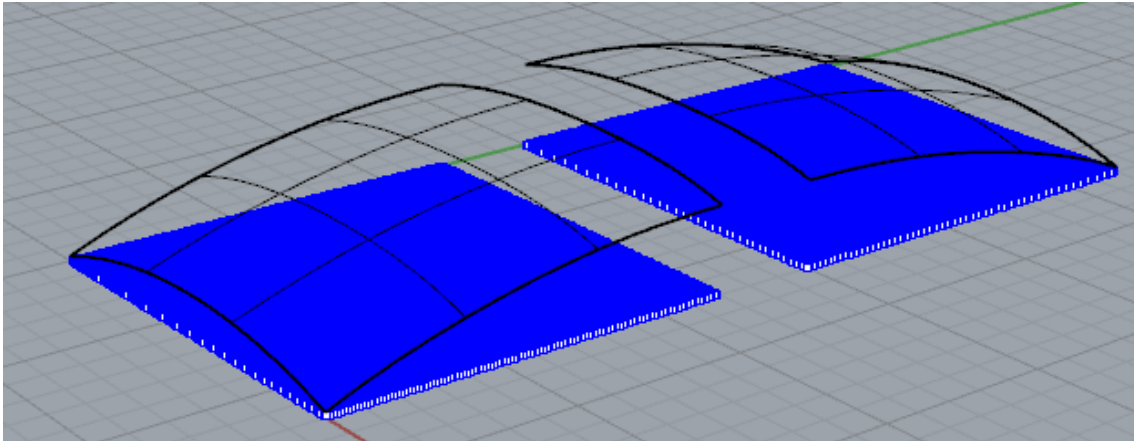


Figure 3.12: In blue the square grid of points is seen under the comparative shapes of the Heimberg tennis hall

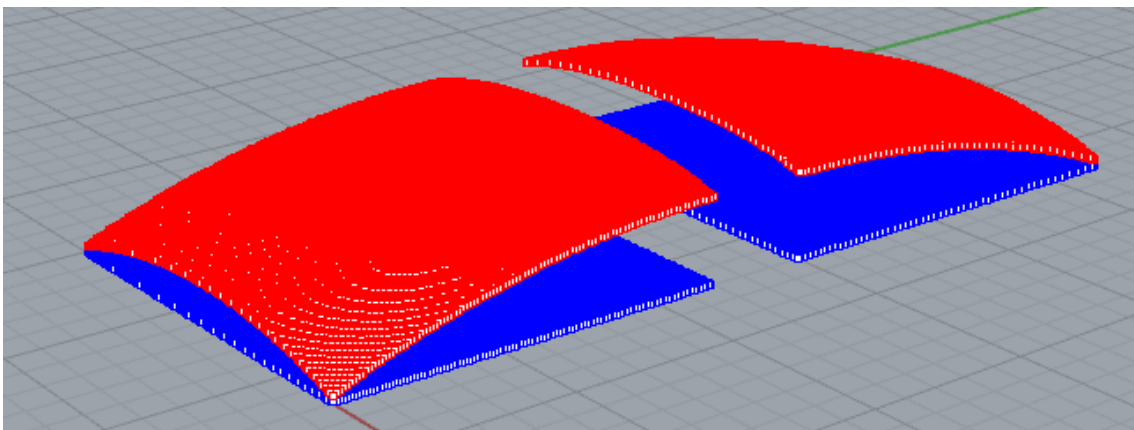


Figure 3.13: In blue the square grid of points is seen under the comparative shapes and in red the projected points of the grid on the NURBS surface can be seen

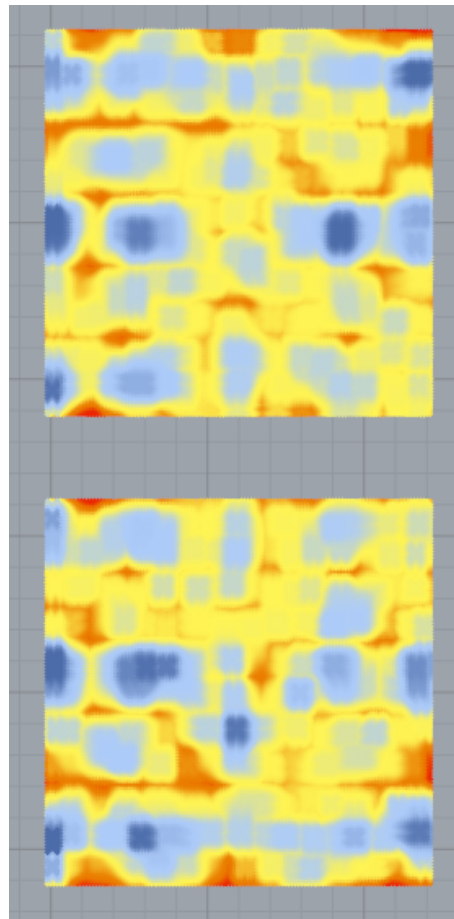


Figure 3.15: Contour plots of the imperfection of heimberg tennis hall (both 12 by 12 m). Red is -1.5 cm to blue is +1.5 cm of deviation

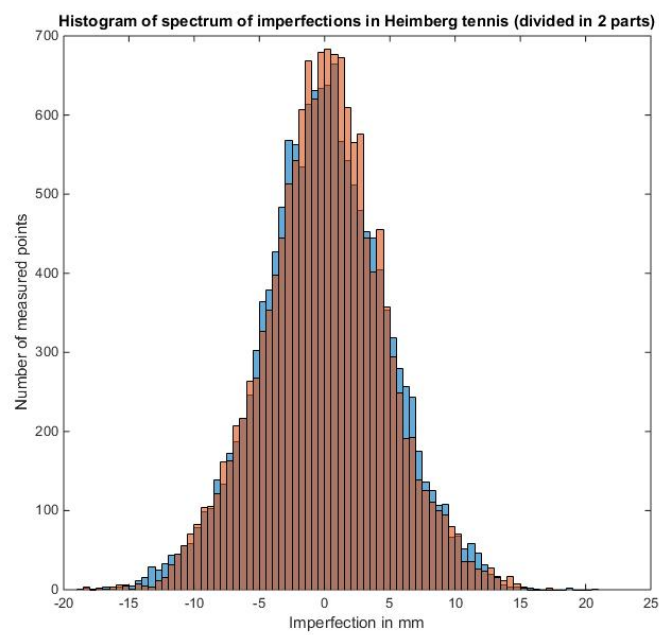


Figure 3.16: Heimberg tennis distribution of deviation

3.2.2. Requirements for the methods

There are some requirements for the method to ensure reliable results. These are:

- A rectangular and continuous piece of data must be available in the point cloud, that is a few times larger than the buckling length. If this is not the case, the data piece is too small to give good results
- The data piece must not be too curved, because the error on the edges of the data piece will be too large
- Enough measured points must be available at every place of the surface. Due to the way the Faro Focus 3d scanner measures surfaces some places of the scan contain less points. If the number of points becomes too low (less than ± 1000 points per meter squared) the method becomes unreliable.

3.3. Single NURBS Method

Alongside the Double NURBS method a different method was created, which could create reliable results. The method uses a single NURBS surface which is compared to the measured data, therefore it is called the Single NURBS method. The method can be used to quickly estimate the largest imperfection peak of a rectangular piece of data. Next to this it can calculate the distribution of wave lengths in the imperfection. The method uses the standard deviation and mean of the point deviation of the data to particular NURBS surface. This surface is created in the same manner as the Double NURBS method, such that due to control point spacing smaller wave lengths will not be present.

3.3.1. Assumptions

Assumptions were made when developing the Single NURBS method and this subparagraph describes all these assumptions. The assumptions were made on the results of the Double NURBS method. Although paragraph 3.3.1. is not needed for understanding the method, it clarifies the underlying theory.

The Single NURBS method uses the fact, that the results from the Double NURBS method show imperfections, which are very similar to a set of combined sine waves. The results also show that the imperfections are fairly continuous over all data, meaning that the imperfections are not one or two local bulges, but more of a wave pattern. This wave pattern can be recreated by a set sine (or cosine) waves.

Variance of sine and cosine waves

The Fourier transform is a mathematical tool to extract wavelengths (with their amplitudes) used to create a repeating curve of surface. This tool was tried but did not give workable results (for reasons see the appendix D). The Single NURBS method uses a characteristic found in sine (and cosine) curves and waves, for extraction individual wavelengths from the data. Namely that the sum of the variances of individual sine waves is equal to the variance of the sum of these waves. In practice this was not precisely identical ($\pm 10\%$ deviation found), it can be mathematically proven that this is true. To find a algebraic solution, Maple 18 was used

For 2D sine curves holds that:

$$\sum_i^n \text{Var}(A_i \cos(x_i)) = \text{Var}(f(x)) \quad (3.6)$$

With

$$f(x) = \sum_i^n A_i \cos(x_i) \quad (3.7)$$

And n being the number of sinus wave combined A_i is the amplitude and $f_i(x)$ being combined wave function.

For 3D sine curves holds that:

$$\sum_i^n \text{Var}(A_i \cos(x_i) \cos(y_i)) = \text{Var}(f(x, y)) \quad (3.8)$$

With

$$f(x, y) = \sum_i^n A_i \cos(x_i) \cos(y_i) \quad (3.9)$$

$$\text{Var}(f(x)) = \int_{-\infty}^{\infty} f(x)^2 dx \quad (3.10)$$

To help Maple with the calculations integrals will not be done from minus infinity to infinity, but from $-k * \pi$ to $k * \pi$ (which bounds of the reoccurring combined cosine wave which is created). This makes sure that the solution does not include insignificantly small parts, which are formed from numerical error

when the wave is cut of in the middle. Figure 3.17 shows the first part of the Maple script, which shows that:

$$\text{Var}(A\cos(x)) = \int_{-\infty}^{\infty} A\cos^2(x)dx = \frac{1}{2}A^2 \quad (3.11)$$

$$\text{Var}(A\cos(x)\cos(y)) = \int_{-\infty}^{\infty} \int_{-\infty}^{\infty} A\cos^2(x)\cos^2(y)dxdy = \frac{1}{4}A^2 \quad (3.12)$$

Figure 3.17 shows the Maple script. With A , B and C being the individual amplitudes for functions f_1 , f_2 and f_3 . The frequency (or wave length) of the sine functions need to be pre-determined, or else the integral will give problems. The script shows that:

$$\sum_i^n \text{Var}(A_i\cos(x_i)\cos(y_i)) = \sum_i^n \frac{1}{4}A_i^2 \quad (3.13)$$

```

> restart; n := 3;
                                n:=3
                                (1)
> f := A*cos(x);
                                f:=A cos(x)
                                (2)
> Var := int(f^2, x = 0 .. n*Pi)/(n*Pi);
                                Var := 1/2 A^2
                                (3)
> simplify(Var, trig);
                                1/2 A^2
                                (4)
>
>
> restart; n := 3;
                                n:=3
                                (5)
> f := A*cos(x)*cos(y);
                                f:=A cos(x) cos(y)
                                (6)
> Var := int(f^2, x = -n*Pi .. n*Pi, y = -n*Pi .. n*Pi)/(4*n*Pi*n*Pi);
                                Var := 1/4 A^2
                                (7)
>
>
> restart; n := 1*7*9;
                                n:=63
                                (8)
> f1 := A*cos(x)*cos(y);
                                f1:=A cos(x) cos(y)
                                (9)
> f2 := B*cos(x/7)*cos(y/7);
                                f2:=B cos(1/7 x) cos(1/7 y)
                                (10)
> f3 := C*cos(x/9)*cos(y/9);
                                f3:=C cos(1/9 x) cos(1/9 y)
                                (11)
> Var := int((f1+f2+f3)^2, x = -n*Pi .. n*Pi, y = -n*Pi .. n*Pi)/(4*n*Pi*n*Pi);
                                Var := 1/15876 (3969 A^2 pi^2 + 3969 B^2 pi^2 + 3969 C^2 pi^2)
                                (12)
> simplify(Var);
                                1/4 A^2 + 1/4 B^2 + 1/4 C^2
                                (13)

```

Figure 3.17: Variance of a cosine wave and field Maple proof

Figure 3.18 shows the variance of point deviation for 4 imperfection fields. Where the first three are simply flat 12 by 12 meter surface with a sinus imperfection, differing in wave length (1, 2 and 3 meters). The fourth imperfection field is a summation of the first three. Mathematically the imperfection fields can be described as:

$$I_1(x, y) = 0.05\sin\left(\frac{2\pi}{1}x\right)\sin\left(\frac{2\pi}{1}y\right) \quad [m] \tag{3.14}$$

$$I_2(x, y) = 0.05\sin\left(\frac{2\pi}{2}x\right)\sin\left(\frac{2\pi}{2}y\right) \quad [m] \tag{3.15}$$

$$I_3(x, y) = 0.05\sin\left(\frac{2\pi}{3}x\right)\sin\left(\frac{2\pi}{3}y\right) \quad [m] \tag{3.16}$$

$$I_{sum}(x, y) = I_1(x, y) + I_2(x, y) + I_3(x, y) \quad [m] \tag{3.17}$$

The graph shows that the variance of the combined imperfection field is practically equal to the sum of the variances of the individual imperfection fields.

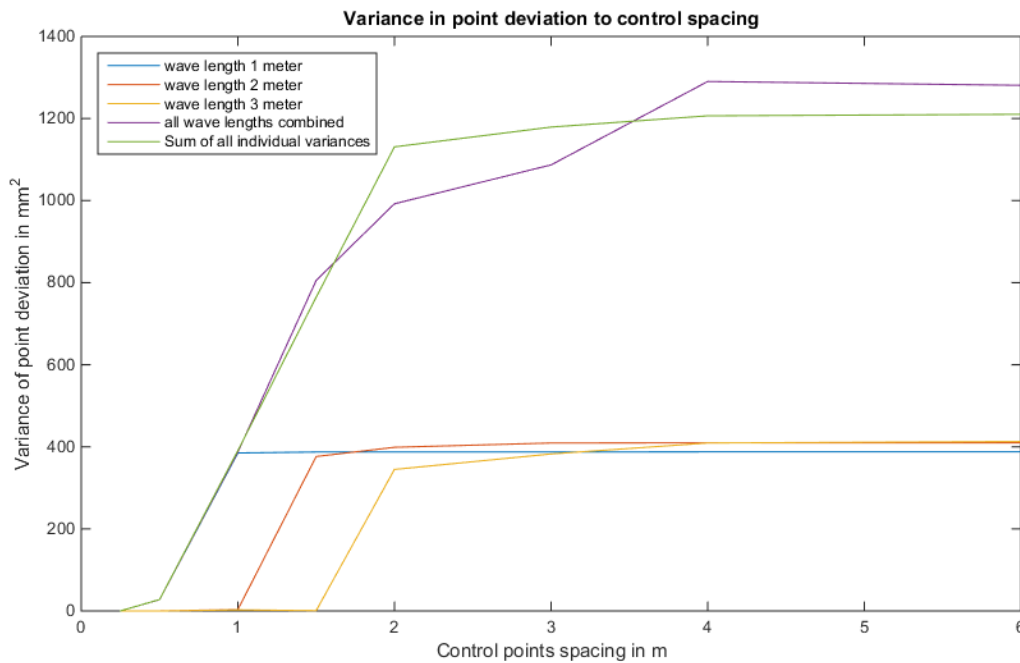


Figure 3.18: Graph shows the relation between the variance of the imperfection field to the NURBS surface and the control spacing of the NURBS surface. For 3 sinus imperfection fields and a combined imperfection field

This variance summation property of sine and cosine waves can be applied to the measurement results to find out which wavelengths are most present. It must be assumed that the imperfection waves found in the data are sine shaped. Fourier has taught us that any repeating curve or surface can be approximated by a sum of sine waves. Using Fast Fourier transform to find the spectrum of wavelengths was tried, but this did not give usable results. More information can be found in appendix D. This property can be used to find a rough estimate on which wave length are most present in the data, this is described in the next paragraph.

3.3.2. Using the Single NURBS method

This paragraph gives a step by step description of the Single NURBS method. For the explanation of the method the data from the first shell at the service station in Deitingen is used.

Step 1: Create a square piece of data

This method works best if a square piece of data is created from the point cloud of the measurements of the shell. The size of this piece has to be at least 2 full wave length of the largest wave length you want to find. In this case the largest wave length that was searched for is 6 meters, therefore a square piece of 12 by 12 meters was used. The larger the piece of data is the more accurate the results are, but throughout this research it has become clear that square continuous pieces of data larger than 15 meters across are hard to find. This comes from the dimensions of the shells that were measured. Cutting out this square piece of points can be done in Rhino, by deleting points outside of the square.

Step 2: Calculate standard deviation of imperfection using Rhino for steps of control points

When a NURBS is created in Rhino, it is possible to calculate the point deviation on the NURBS. This also gives the mean, median and standard deviation of the point deviation (see figure 3.19). The last can be used to calculate the variance of the point deviation. A NURBS is created through the piece of data for a set of steps in control point spacing. Ranging from 0.5 meters between control points to 6 meters between them. For each of these sets the standard deviation is calculated by Rhino (function: PointDeviation).

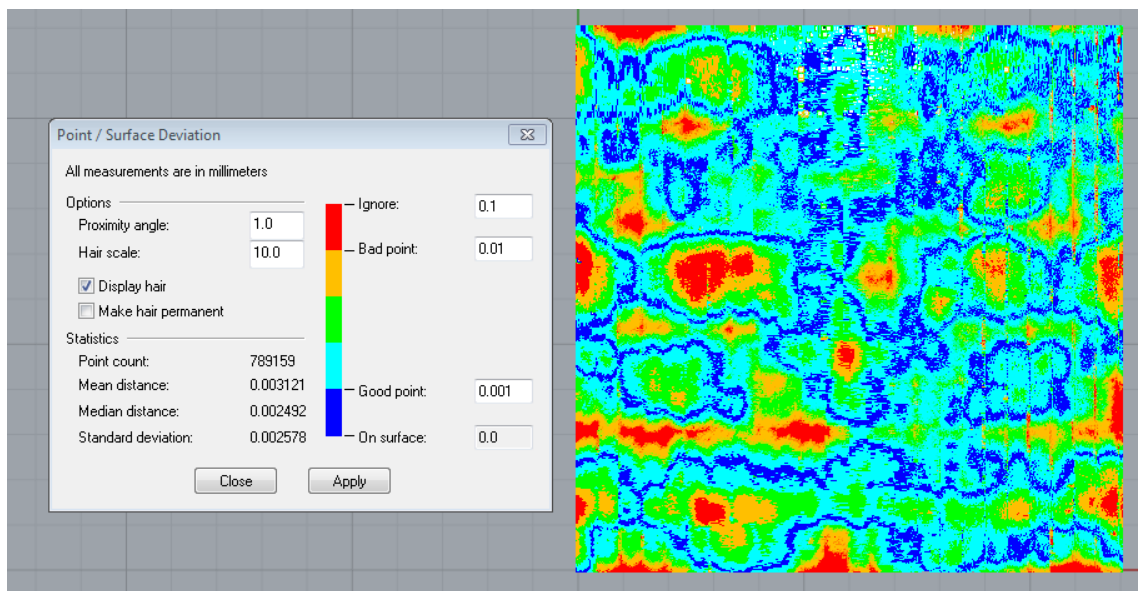


Figure 3.19: Point deviation of a NURBS surface for a piece of data from the tennis hall in Heimberg. At the left side of the figure the mean, median and standard deviation can be seen.

Step 3: Make graph of standard deviation and variance to control spacing

Variance is equal to the standard deviation squared, so this is also known for all steps of number of control points. A graph can be made to show the relation of control point spacing and the standard deviation of point deviation (see figure 3.20) and variance to control point spacing (Figure 3.21).

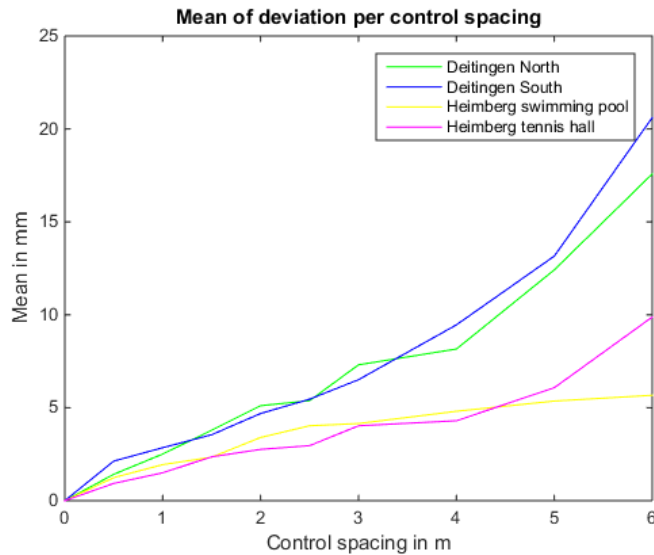


Figure 3.20: Graph of variance in deviation to control point spacing

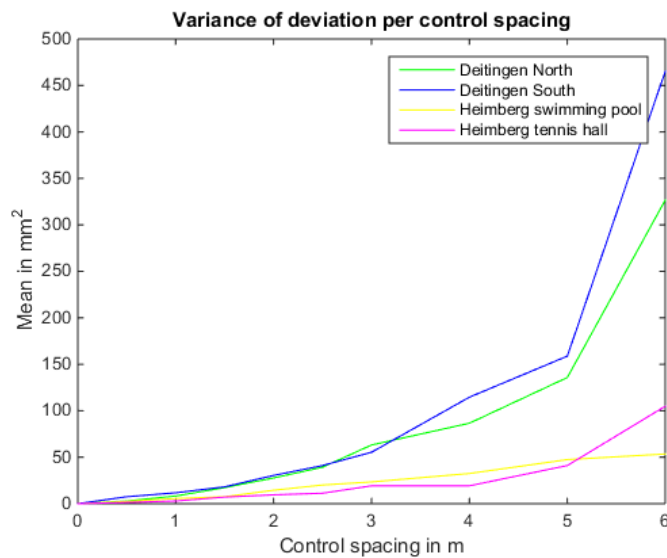


Figure 3.21: Graph of variance in deviation to control point spacing

The graph of the standard deviation per control spacing shows the distribution of wave lengths found in the data. If the wave lengths of the imperfection is evenly distributed, the relation between standard deviation and control spacing (therefore also wave length) will be linear. As graph 3.20 shows for all shells the relation is approximately linear up to 5 meters of control spacing. From 5 to 6 meters control spacing the relation does not behave linearly, this is because a 2 by 2 control point NURBS had to be used, which adds an error.

3.3.3. Step 4: Estimation of peak amplitude of imperfection

The imperfection is normally distributed for all measured shells. Therefore the standard deviation can be used to estimate the peak amplitude of imperfection. For every shell the theoretical buckling length l_{buc} is known, which has an equal control point spacing (because buckling length of shells are half a sine wave). The standard deviation of this control point spacing can be used to estimate the largest peak. In a normal distribution the 5 percent of the distribution is higher than 2 times the standard deviation (see figure 3.22). Because the distribution does not go to infinity, the maximum is equal to approximately 3 times the standard deviation. The standard deviation calculated by Rhino is for an absolute normal distribution and needs to be multiplied by $\sqrt{2}$. Therefore the estimation of the peak becomes:

$$A_{max,est} = 3\sqrt{2}\sigma_{abs} \quad (3.18)$$

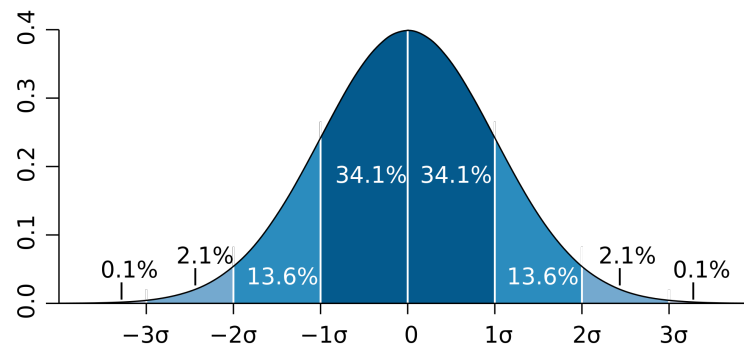


Figure 3.22: Normal distribution showing maximum at 3 times the standard deviation (source: Jeremy Kemp)

3.3.4. Step 5 (optional): Estimation of the expected largest peak found in similar shells

Although this research only produces results for 4 shells, a largest peak amplitude for all shells can be calculated. For this method to be reliable, more shells need to be measured. The expected largest peak can be represented by a Fréchet distribution, which is an extreme value distribution of type II maxima¹.

$$P(\hat{d} \leq \xi) = \exp\left(-\frac{u^k}{\xi^k}\right) \quad (3.19)$$

Where ξ is the 5% characteristic value of the largest imperfection, u is the mean of all peak amplitudes \hat{d} found in the results. The Fréchet distribution has the property, that the maximum of a number of maxima also has a Fréchet distribution. Therefore the expected peak amplitude in other shell, with a different surface area can be determined. The 5% characteristic value of the largest imperfection (or peak amplitude) for a shell n times larger is equal to:

$$1 - P = \exp\left(-\frac{nu^k}{\xi^k}\right) \rightarrow \xi = u\left(\frac{n}{-\ln(1 - P)}\right)^{\frac{1}{k}} \quad (3.20)$$

3.3.5. Step 6: Verification using Double NURBS Method

The Double NURBS method can be used to verify the results of the Single NURBS method and vice versa. The estimation of the peak amplitude of the single NURBS method should be equal to the largest amplitude found in the Double NURBS method (using the same piece of data). Next to this the mean and standard deviation calculated by Rhino should be equal to the mean and standard deviation found using the Double NURBS method. Given that the same control spacing is used for the intended shape in the Double NURBS method. In the results the results of the methods are compared.

¹Paper yet to be published: Shell Imperfections, B. Elferink, P.C.J. Hoogenboom, J.G. Rots, P. Eigenraam, HERON Vol 61 (2016) No 3.

4

Results

This chapter contains results for all shells, except the ANWB head office in the Hague, the open air theater in Grötzingen and the garden center in Zuchwill, because the data of these shells was not sufficient. Firstly the contour plots for all shells is presented. Here the pattern of the imperfections found can be seen and the size of the imperfection is shown in color. In the second section the histograms of all shells is shown. Here the maximum deviation and spectrum of the imperfections can be seen. The last part shows the representative imperfections for each shell. All imperfection field are created by taken 0.5 meters of control spacing (smallest computationally possible) NURBS surface and a ± 5 meters of control spacing NURBS surface, which is equal to the theoretical buckling length of the shells.

4.1. Contour plots

The contour plots for every shell are shown below. Dimensions of the shell and its imperfections can be found in the description of the figure. (A legend will be made for the final version of the report)

4.1.1. Shell 1: Deitingen

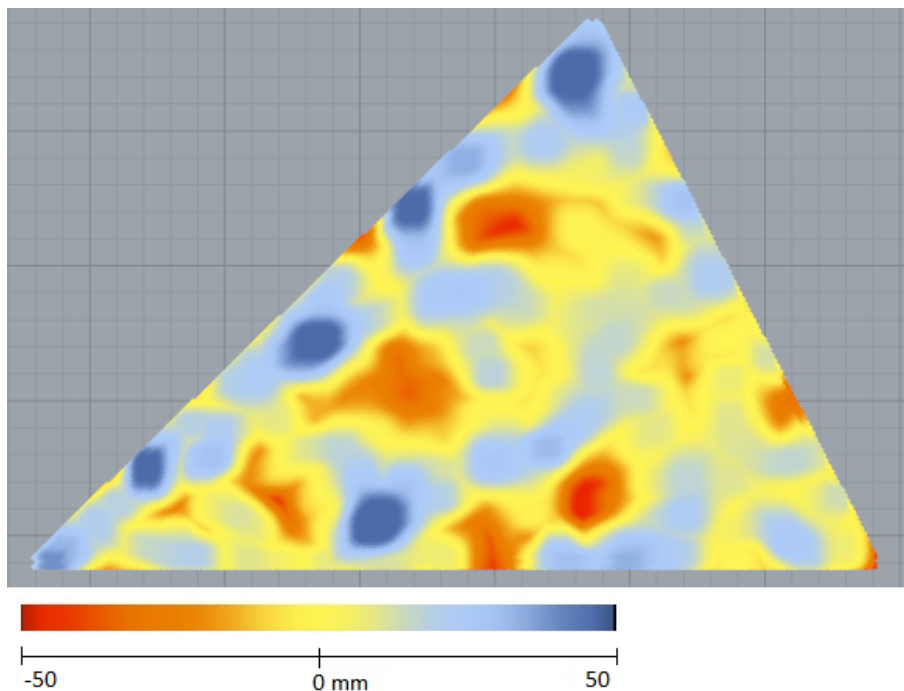


Figure 4.1: Imperfection field of Deitingen South shell. Red is -5 cm to blue is +5 cm of deviation. 1 grey square is 1 by 1 meter

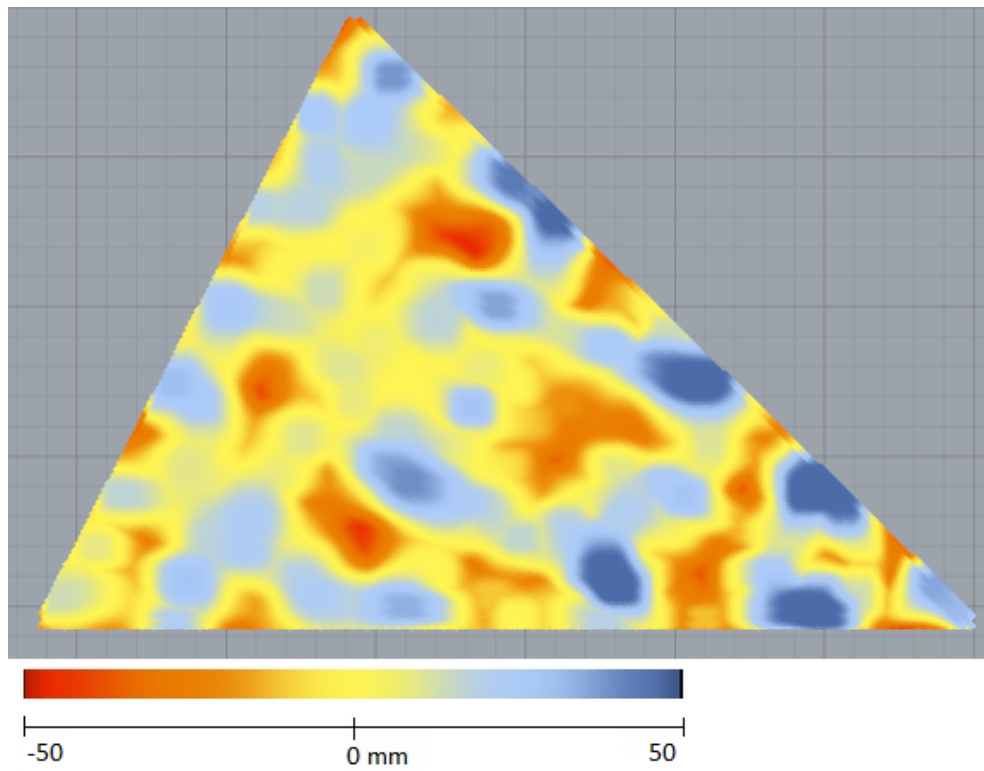


Figure 4.2: Imperfection field of Deitingen North shell. Red is -5 cm to blue is +5 cm of deviation. 1 grey square is 1 by 1 meter

4.1.2. Shell 2: Heimberg Schwimmbad

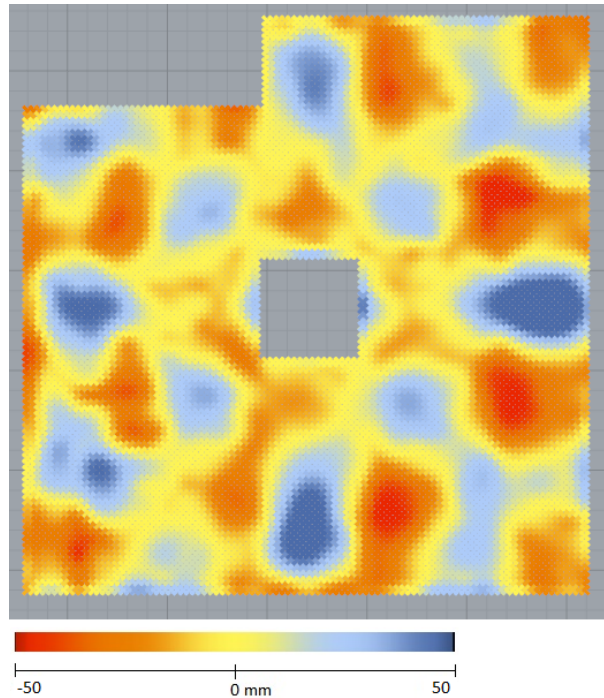


Figure 4.3: A visual representation of the imperfections in the entire Heimberg shell (24 by 24 meters). Red is -5 cm to blue is +5 cm of deviation. 1 grey square is 1 by 1 meter

4.1.3. Shell 3: Heimberg Tennis

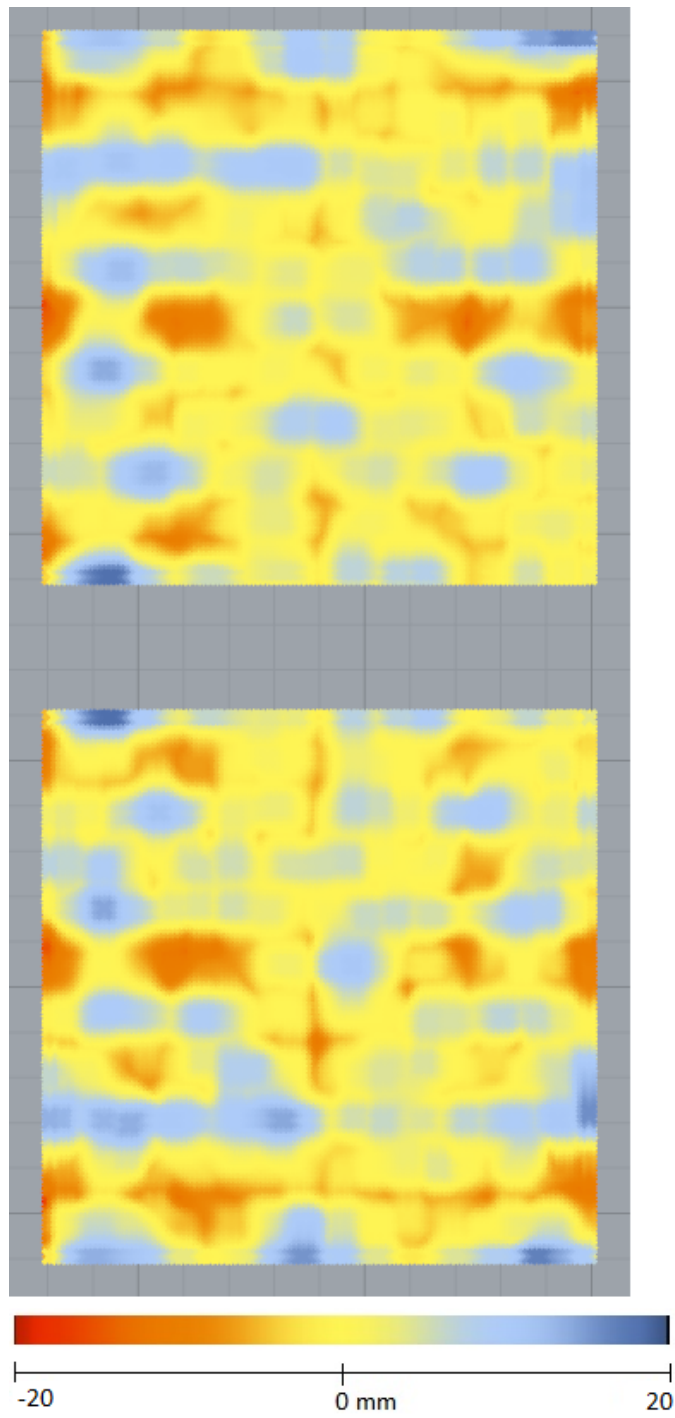


Figure 4.4: Imperfection in first part Heimberg tennis shell, 12 m by 12 m. Red is -20 mm to blue is +20 mm of deviation. 1 grey square is 1 by 1 meter

4.2. Histograms

For all shells the distribution of the deviation is shown below.

4.2.1. Shell 1: Deitingen

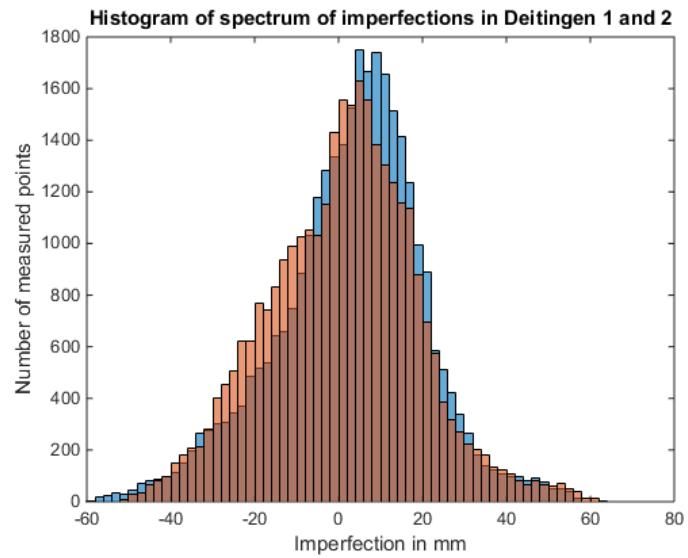


Figure 4.5: Histograms of shells in Deitingen

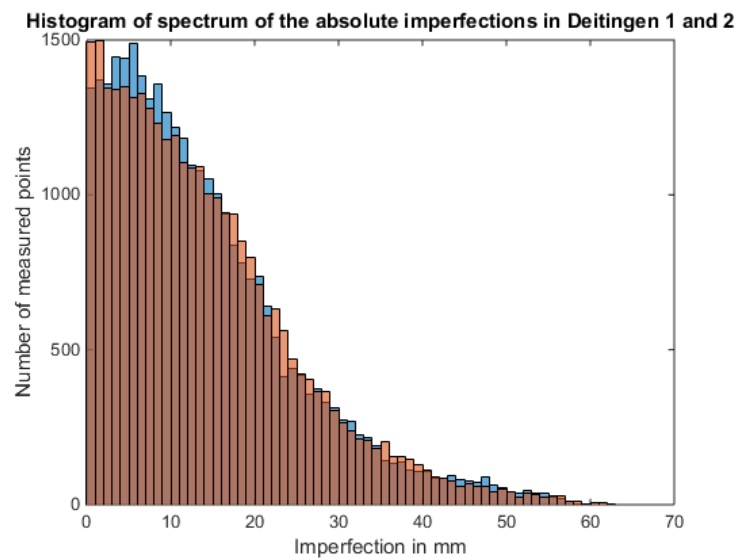


Figure 4.6: Absolute histograms of shells in Deitingen

4.2.2. Shell 2: Heimberg Schwimmbad

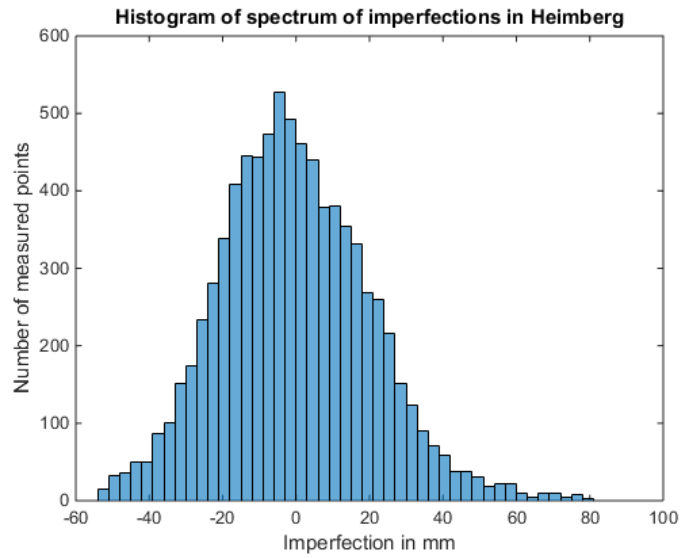


Figure 4.7: Heimberg Schwimmbad histogram

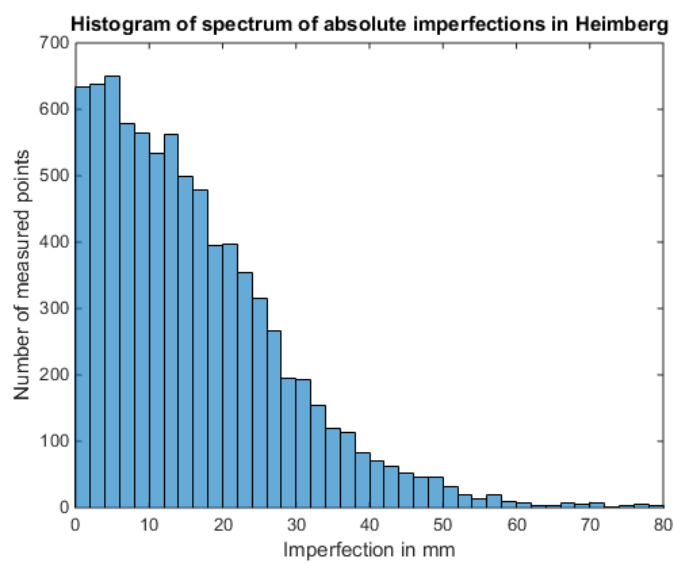


Figure 4.8: Heimberg Schwimmbad absolute histogram

4.2.3. Shell 3: Heimberg Tennis

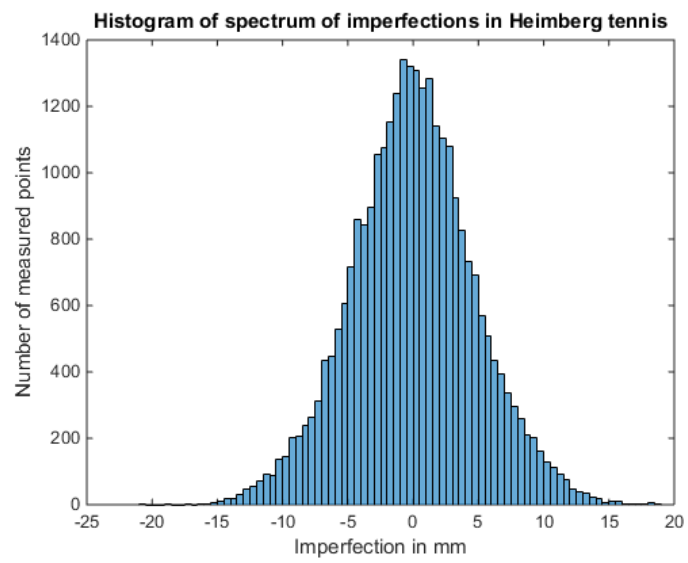


Figure 4.9: Heimberg tennis histogram

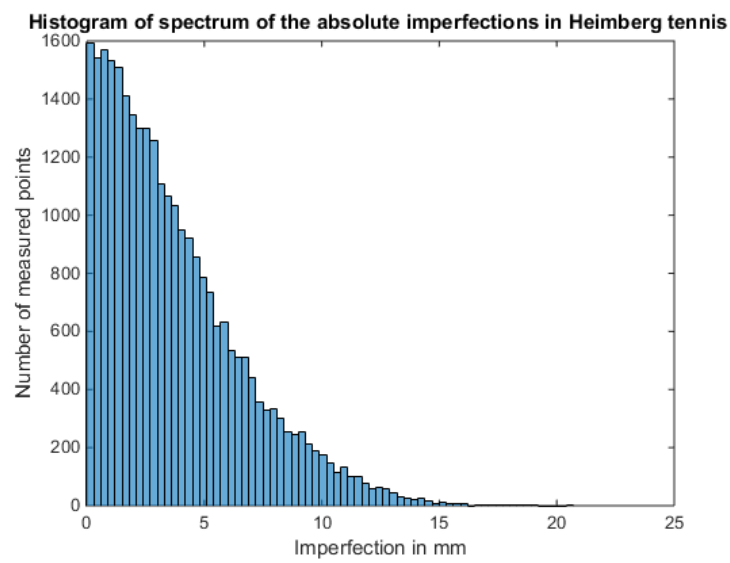


Figure 4.10: Heimberg tennis absolute histogram

4.3. Single NURBS method

Table 4.1 shows the statistical parameters determined by the Single NURBS method. Figure 4.11 shows the standard deviation per control spacing. For a control spacing of 5 meters or lower the relation is linear, therefor the wave lengths in the imperfection field is evenly distributed.

Control point spacing [m]	0.5	1	1.5	2	2.5	3	4	5	6
Deitingen North									
Mean [mm]	1.42	2.51	3.79	5.11	5.38	7.31	9.46	13.16	20.61
Standard deviation [mm]	1.20	2.03	2.94	3.72	4.43	5.62	7.57	8.91	15.25
Deitingen South									
Mean [mm]	2.13	2.85	3.55	4.69	5.46	6.51	8.16	12.43	17.58
Standard deviation [mm]	1.93	2.42	3.01	3.93	4.53	5.26	6.58	8.34	12.78
Heimberg swimming pool									
Mean [mm]	1.24	1.94	2.34	3.40	4.03	4.15	4.81	5.36	5.67
Standard deviation [mm]	1.11	1.66	1.93	2.69	3.17	3.42	4.03	4.87	5.17
Heimberg tennis hall									
Mean [mm]	0.93	1.50	2.36	2.76	2.96	4.03	4.30	6.08	9.88
Standard deviation [mm]	0.81	1.20	1.88	2.18	2.37	3.10	3.48	4.53	7.24

Table 4.1: Mean and standard deviation of imperfections for single NURBS method per control point spacing

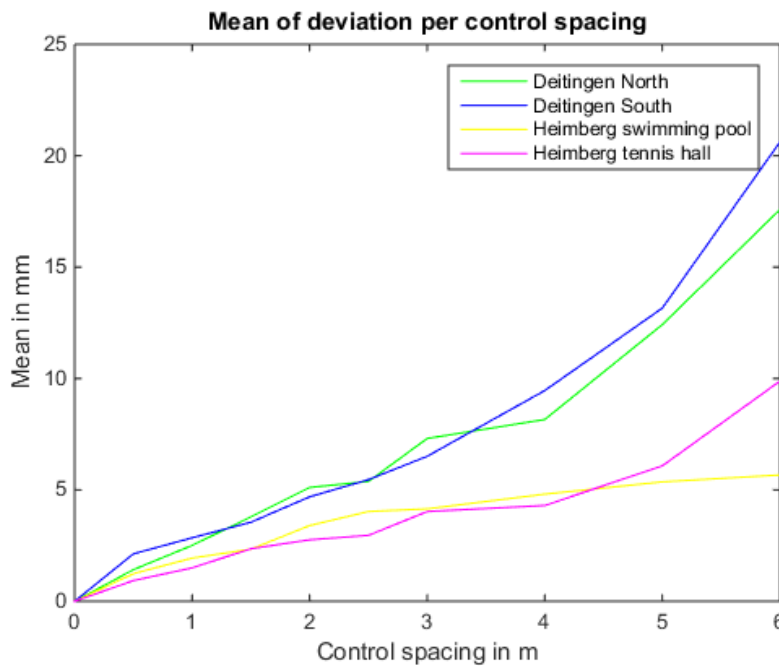


Figure 4.11: Graph of variance in deviation to control point spacing

4.3.1. Verification using Double NURBS method

To verify the Single NURBS method, the same piece of data was used in the Double NURBS method to calculate the statistical parameters and the peak amplitude of imperfection. Table 4.2 shows the mean and standard deviation using the Double NURBS method (4 meters of control spacing for comparative shape). Table 4.3 shows the comparison of the estimated peak amplitude of imperfection and the peak found in the double NURBS method.

Shells	Mean[mm]	Standard deviation[mm]	Mean absolute[mm]	Standard deviation absolute[mm]
Deitingen North	-0.028	9.690	7.615	5.993
Deitingen South	0.064	8.426	6.463	5.407
Heimberg swim- ming pool	0.077	6.443	5.039	4.016
Heimberg tennis hall	0.014	6.063	4.856	3.631

Table 4.2: Statistical parameters from double NURBS method, created using same data sample as single NURBS method. A control spacing of 4 meters was used as the comparative shape of the Double NURBS method

Shells	Peak Double NURBS method[mm]	Estimated peak Single NURBS method[mm]
Deitingen North	35	32.11
Deitingen South	35	27.91
Heimberg swimming pool	25	17.10
Heimberg tennis hall	23	14.76

Table 4.3: Largest observed imperfection double NURBS method using 4 meters of control spacing for comparative shape of Double NURBS method

As the verification shows the peaks and statistical parameters are not precisely equal. One reason is the different manner the methods calculate the standard deviation of of the surface. The Double NURBS method uses a homogeneous point raster, so therefor the standard deviation of the deviation of the points is equal to the standard deviation of the imperfection field. The Single NURBS method uses the measured points, which are not evenly spread. The Single NURBS method is still worked on and perfected for a paper in the Heron, therefore the report focuses on the Double NURBS method.

5

Conclusion and Discussion

5.1. Conclusion

At beginning of this research little was known on the size and shape of imperfections found in thin concrete shells. This study produced the first results on this topic. The Double NURBS method was developed to accurately measure geometrical imperfections of shell structures. Using this method, the point cloud collected by the Faro 3D laser scanner can be turned into a field of imperfections of the original shell shape. The Double NURBS method uses the characteristics of NURBS surfaces to create a reliable comparative surface from the original data. The Double NURBS method does not need the original geometry (in the form of blue prints or a mathematical expression) to find the geometrical imperfections of a shell. A prerequisite for using the Double NURBS method is a limited number of openings in the data (± 10 by 10 meters).

The results of the Double NURBS method show a largest imperfection amplitude of 6 cm (approximately half the shell thickness) with an average wave length of 4 meters. The results of the Single NURBS method show, that the wavelengths of the imperfections range between 1 and 6 meters, showing no trend towards a particular wavelength. The Single NURBS method show the same mean and standard deviation of the imperfection field as the Double NURBS method. Therefore the Single NURBS method can be used as a fast estimation of the largest imperfection in the measured data. Given that imperfections can be modeled by a summation of sine waves.

The FE model demonstrated the consequences of imperfections in shell structures. It showed a clear reduction of the ultimate strength of thin concrete shells when an imperfection was present and increasing the amplitude of the imperfection led to an even greater reduction. For an imperfection amplitude of half the shell thickness a reduction of the ultimate strength of 33% (knock down factor is 0.66) was found, whilst an imperfection amplitude $\frac{1}{10}$ of the full shell thickness led to a knock down factor of 0.8.

This project gives a better understanding on the size and shapes of geometrical imperfections which typically occur in thin concrete structures. The Double NURBS method, which was developed in this research, is a useful tool for easily calculating imperfection from raw data. It does not require any structural information on the measured shells to work. The representative imperfection can be used as a fast indication for a realistic imperfection in the design process of a shell and is easily applicable in FE modeling.

5.2. Discussion

As a measurement device the Faro Focus 3D surpassed all of the requirements. It took a relative short time to measure a shell, which helped to gain access to the structure. The large amount of measured points and the high accuracy of the laser scanner, made it possible to post process the data into results. The data that was collected by the device can be used for other research too, because this was the first time that these structures were measured in high detail. The scanner had an error of ± 0.5 mm which is small (only a hundredth of the maximum imperfection found). At some shells, reference spheres were used to combine multiple scans of a shell, to make a point cloud of the entire shell. This was successful for only one shell, the alignment was not accurate enough in two other shells and the scans

did not align properly. The practical use of the reference spheres was limited, it is therefore advised to measure the whole surface in one scan.

Successfully post processing the data was done by trial and error, because no similar research existed. Therefore the results could not be predicted and the data processing method could not be developed in advance. The data from ANWB in the Hague, the outdoor theatre in Grötzingen and the garden center in Zuchwill was not usable with the Double NURBS method. The shell in the Hague was finished with a mixture of small rocks and cement giving it an additional error of 1 cm, which was in the same range of the imperfections found. The other two shells had too many gaps in the data, because of obstacles between the scanner and the shell.

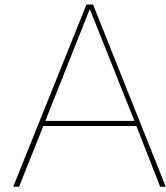
There is still some uncertainty in the precision of the results. The scanner adds a insignificantly small error, but due to the lack of additional data and the nature of Double NURBS method the exact error is hard to specify. The method compares a NURBS surface which approximates the raw data very close to an comparative NURBS surface created by the data. The first surface does not give a significant additional error. But in the making of the second surface some judgment needs to be made even though the set number of control points can be calculated through the buckling length. Some small shifting in the number of control points can produce a different ($\pm 20\%$) maximum imperfection. However, the shape of the imperfections does not change significantly.

The distribution of points in the measured data can affect the results of the Single NURBS method. The Faro Focus scanner measures significantly more points above it, then to the sides. So the points in the point cloud are not evenly spread. The calculated standard deviation, is depended on the points and not on the area. The Double NURBS method uses a homogeneous matrix of points, thereby eliminating the effect.

5.3. Recommendations

This study has led to the following recommendations for future research.

- More data is needed to reliably estimate imperfections. So more shells need to be measured, preferably directly after erection so the inner surface of the shell is still visible. This measurement can also serve as a validation of the assumed imperfections in the design process.
- The Double NURBS method needs further investigation in its accuracy and the process needs to be more refined. For example, the projection of the grid could be changed from an x, y, z coordinate system to a spherical projection system using 2 angles and a radius. Most shells are closer to a spherical shape than they are flat, for this type of shell an angular projection would increase the accuracy of the Double NURBS method.
- In this study only the inner surface of shells was measured. Ideally shells would also be measured from the top, most measured shells had no finish on top, but without a crane they could not be measured using the Faro Focus scanner. Due to the budget a crane was not an option, but it would be very useful to have data of both sides of the shell.
- When measuring shells, it would be advantageous to deviate the laser position from the horizontal reference plane. This would give a more homogeneous measured point spread. Unfortunately this is prevented by the device's safety features. The manufacturer is recommended to remove these safety features, if possible.



Measurement methods

A.1. Theodolite

The theodolite is an instrument for measuring angles in both the vertical and horizontal plane. The device consists of a mounted telescope connected two perpendicular axes. The angles can be measured with very high precision. With two measuring positions it is possible to accurately measure (x,y and z coordinates) any point on a surface. The x,y and z coordinates can be computed using simple trigonometry. The target for each measurement has to be marked with either a laser beam or with some sort of paint or ink, to make sure the measurement is precise.



Figure A.1: Theodolite

Positive:

- Because the instrument is analog no power is needed (or if it has a digital display only battery power is needed)
- The whole system can be operated and transported by 1 person
- Range is sufficient

Negative:

- The chance of measuring errors is high, because measuring is done by a human being.
- The measuring technique is very time consuming, because the instrument is not digital and every point has to be measured twice.
- The method is not as precise as a total station or a Faro laser scanner

This method seems to be too time consuming to be a viable option for surveying the shells.

A.2. Total station

The total station is a digital variant of the theodolite, which can measure distance via microwave, infrared or a laser beam. So with one measurement the x, y and z coordinates of a point on the surface are known. Although some total stations need a reflector on surface for distance measurements, there are total stations available which can measure distance without a reflector. The only conditions are that the surface is not too dark and the target is not directly in sunlight. The range of a total station which can measure without a reflector, is up to a kilometer, with a accuracy of about 1 mm and a angle accuracy of 0.5 to 2 arc seconds. Both the accuracy and the range are more than sufficient. A total station can be rented for about 150 Euro to 700 Euro's a week depending on the model. For this particular research very high angle precision is not needed so the price will be close to 150 Euro's a week.



Figure A.2: Total station

Positive:

- The instrument is very precise
- Measurements are fairly rapid so a large amount can be made in a day
- The output is digital which is good for post-processing and mitigates measuring errors
- The whole system can be operated and transported by 1 person
- Range is sufficient

Negative:

- The instrument is not cheap to rent
- The control of the instrument can be complex so time has to be invested to get used to the machine

The total station was a viable option.

A.3. Faro Focus 3d scanner

The Faro Focus 3D scanner is a digital device which maps a surface automatically with very high speed. The instrument has a spinning reflector which guide the targeting laser around the vertical plane taking 120,000 measurements every second and the machine rotates (slowly) horizontally to measure a surface¹. Which part of the total field of view of the instrument and the density of measurements can be controlled. All the data is stored automatically and a file is made containing measured points. With post-processing programs the data can be transferred into a surface. The range of a Faro Focus 3D scanner is up to 25 meters, and the accuracy is 2 mm (both are sufficient for this research). Just like the total station a Faro Focus 3D scanner is not cheap.



Figure A.3: Faro photon scanner (similar to the Faro Focus 3D scanner)

Positive:

- The method is very fast (a surface can be surveyed in less than an hour)
- The output is digital and there are programs especially designed for post-processing
- The number of measured points is much higher than with the other methods
- The whole system can be operated and transported by one person
- Accuracy and range are sufficient

Negative:

- The instrument is expensive, but it was lended out cheaply
- The control of the instrument was complex so time had to be invested to get used to the device

The Faro focus can be a viable option, if it is in budget of the TU Delft or lendable from the department of remote sensing.

¹http://www.dirdim.com/pdfs/DDI_FARO_Laser_Scanner_Photon.pdf

A.4. Manual laser distance measurement

A cheaper alternative (about 80 Euro's to buy) to map a surface was with a laser distance meter. This little device measure distances via a laser beam up to 60 meters with an accuracy of 1.5 mm. If this device was used, a system had to be created to log the horizontal and vertical angles. Also it had to be connected to a tripod or a similar stand so the device did not move in between measurements. Because of this further research had to go into this option. And because a part of the method still had to be developed, therefore accuracy could not be guaranteed.



Figure A.4: An example of a laser distance meter

Positive:

- The device itself is very cheap, but extra equipment is needed to make the method operational
- Distance precision is accurate enough, although angle precision is uncertain
- The whole system can be operated and transported by 1 person
- Range is sufficient

Negative:

- The post-processing will take longer than the digital alternatives, because output is not digital.
- Method has to be developed, made and tested before it is usable

This method could be usable, but needs further investigation on construction and final precision.

A.5. Manual measurement

It is possible to try and measure the surface without any electrical devices. A method can be created where a grid is laid out on the floor and on each point the height is measured with a measuring stick. This stick has to be leveled by two level meters (in both horizontal planes). The output of such a system has to be handwritten down. An important condition is that the ground surface on which the grid is laid out is flat and horizontal, otherwise the error is transferred to the data. It is very important that the measuring stick is perfectly vertical, because a small angle error over a few meters can have a large error (in the order of centimeters).

Positive:

- The method can be used without any power sources
- The whole system can be operated and transported by one person
- All the components of the system are not expensive and after the research the components can be separated and be used for other purposes

Negative:

- Because all the measurements are analog the chance for error is higher
- The precision of this system is fairly low
- The measuring rate is very low, so a fairly low number of points can be measured in a day
- The post-processing will take longer than the digital alternatives, because output is not digital.
- There is a limit on range, anything higher than the length of the measuring stick (max a few meters) is not reachable without constructing a platform which is also time consuming
- Method has to be developed, made and tested before it is usable

It is highly unlikely that this method is usable for this research, because of the amount of measurement points that will be needed for each surface. Because of that the time it will take to measure is too long. Also this is the least precise method of the 5. Maybe on a smaller scale in combination with a very low budget this method can be viable.

B

Grasshopper scripts

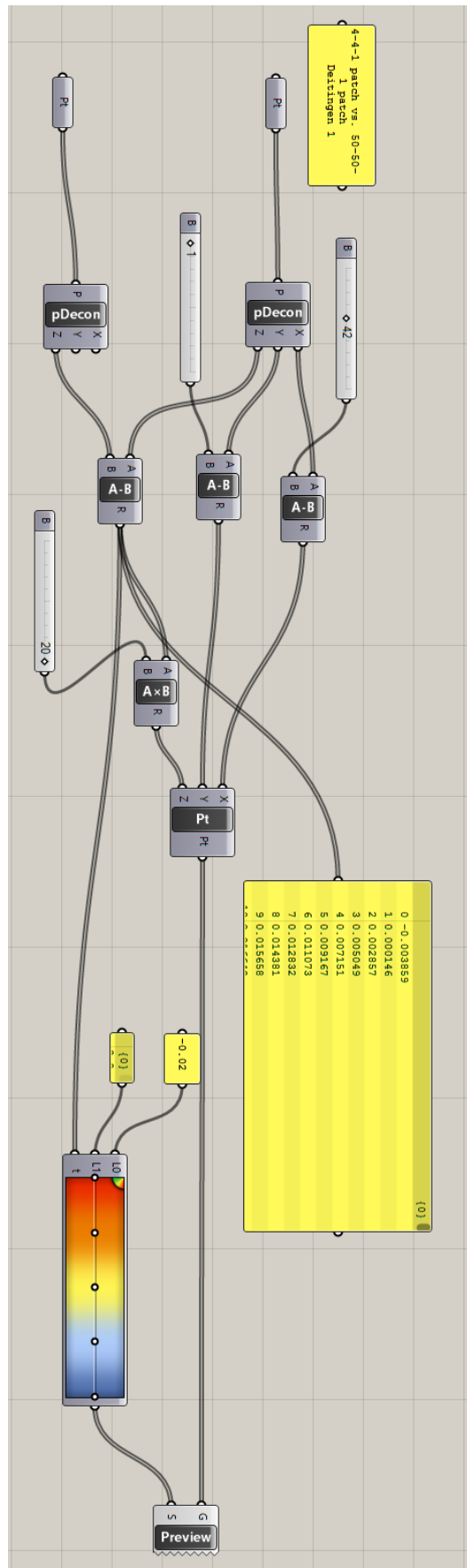


Figure B.1: Grasshopper script Double NURBS method

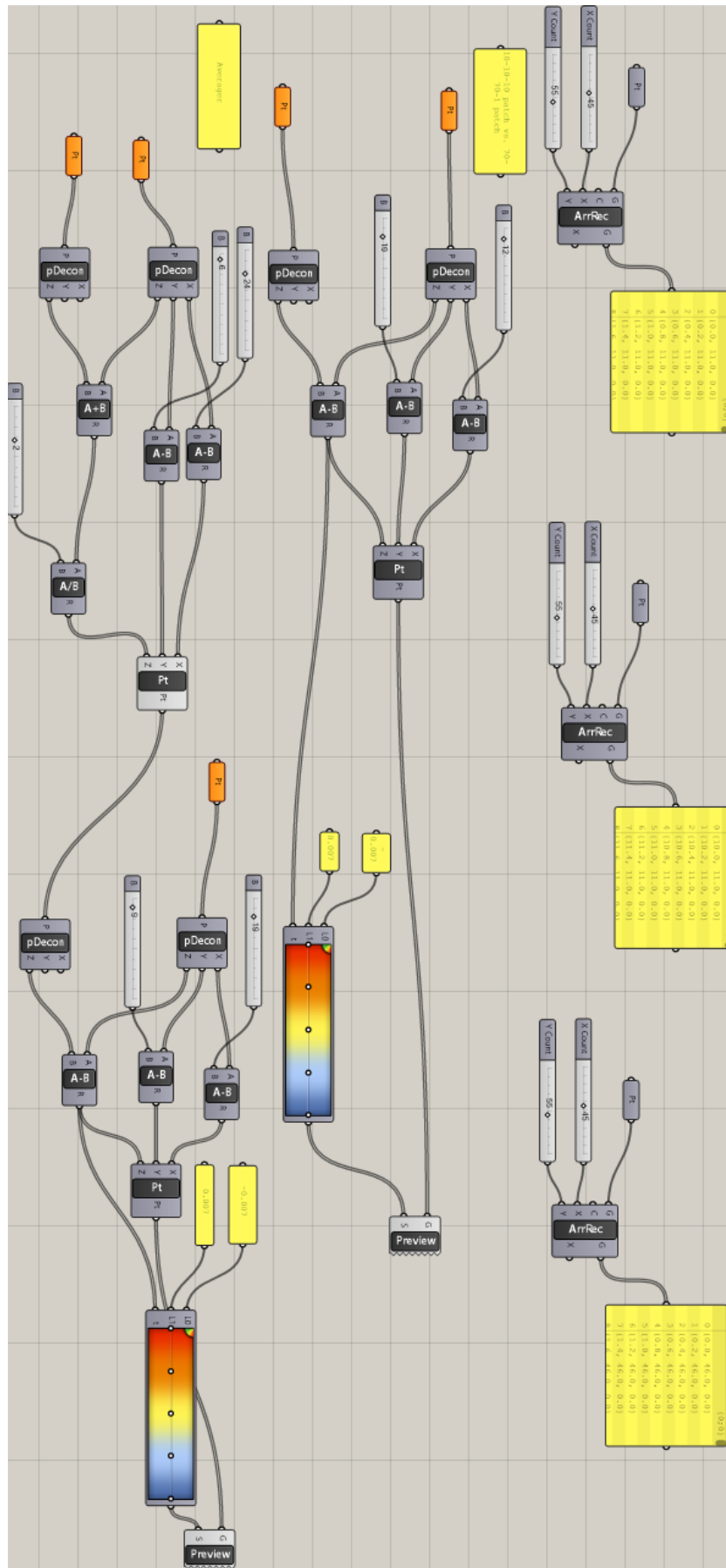
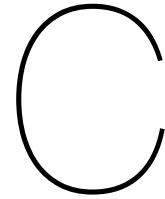


Figure B.3: Grasshopper script used for average segment method of the ANWB head office shell



NURBS

All fitted surfaces in this thesis are NURBS surfaces (or NURB surfaces as preferred by some). NURBS stands for Non-Uniform Rational B-Spline¹, where the “s” of spline in the abbreviation is being debated. NURBS curves and surfaces are a mathematically constructed and used in computer graphics for generating curves and surfaces². In this appendix the basics of NURBS curves and surfaces will be explained, but for more details on the matter, see links in footnote. For this appendix a basic understanding of mathematics is needed as some phenomena are presumed to be common knowledge.

C.1. Origin of NURBS and splines

Today NURBS curves and surfaces are implemented in most CAD and 3D graphics programmes and packages³, but it started out as a way to make free form curves for hand drawings. For example the shape of the bow of some ships can not be drawn by using rulers, compasses (for circles) and protractors (for angles). These shapes needed to be drawn freehand, and when larger shapes were needed this became a problem. The ship builders used flexible timber lattes for creating these shapes, and the lattes were called splines. The splines shape was determined by a number of predetermined points which held the timber latte in its place. Today these are replaced by control points or knots, which define the shape of the spline or NURBS curve.

C.2. B-Spline

A B-spline is comprised of a number of piecewise polynomial functions, where the points between the pieces are known as knots or break points.

A B-spline is defined as⁴

$$S_{n,t}(x) = \sum_i \alpha_i B_{i,n}(x) \tag{C.1}$$

This holds for every piece that is controlled by a control points between 2 knots. For a more detailed mathematical explanation of see wikipedia or the article of Schneider, who explain it in detail which is not needed for this research. Most important part is that it can be seen that every control point curves its part positive or negative and that between knots C_2 continuity is ensured (as can be seen in figure C.1). C_n continuity means that the n th derivative $\frac{d^n C(x)}{dx^n}$ are equal at that point. So C_0 is positional continuity, C_1 is tangential continuity and C_2 is curvature continuity, which can be seen figure C.1.

¹<http://whatis.techtarget.com/definition/nonuniform-rational-B-spline-NURBS>

²http://www.mactech.com/articles/develop/issue_25/schneider.html

³https://en.wikipedia.org/wiki/Non-uniform_rational_B-spline

⁴<https://en.wikipedia.org/wiki/B-spline>

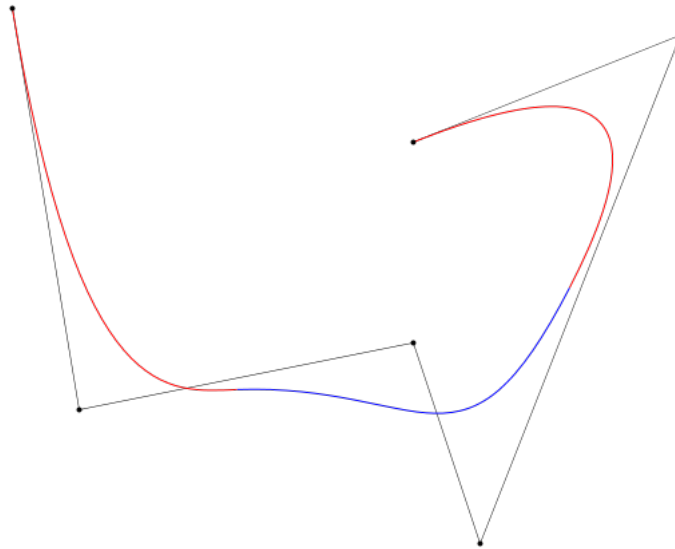


Figure C.1: B-spline with control points

C.3. NURBS specifications

A NURBS surface is comprised of a raster of NURBS curves, which are determined by their control points, see figure C.2. And the space between the B-splines is determined by the control polygon. Just as with NURBS curves or the B-splines each control point can only curve its domain in 1 direction (positive or negative curvature).

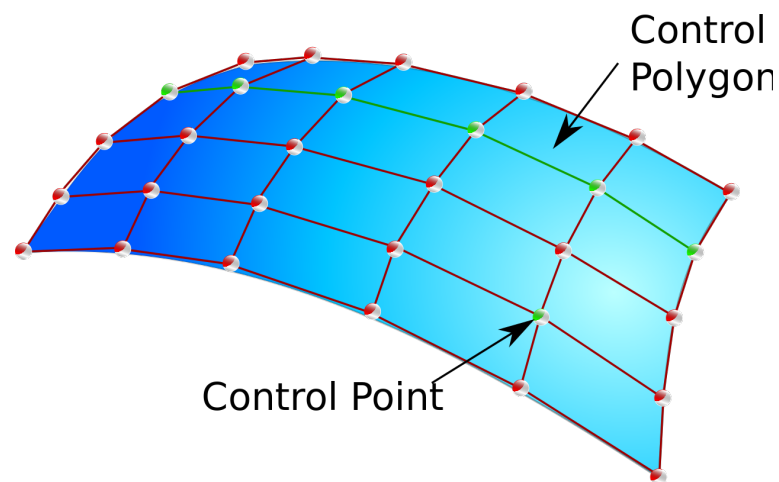
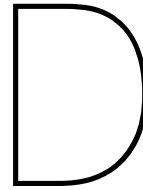


Figure C.2: Schematics of a NURBS surface

C.4. Significance for this research

In the process of defining the design imperfection the relation between control points per length and minimum wave length which can be created by the NURBS surface is critical. A minimum of 2 control points are needed per wave length to create a sinus wave. Which is logical because a control point can only have positive or negative curvature over its domain and a sine wave is comprised of a positive part and negative part of curvature.



Fast Fourier transform

D.1. Using Fast Fourier transform

D.1.1. Fast Fourier transform

Fast Fourier transform or in short FFT is an algorithm to compute the discrete Fourier transform (or DFT) and its inverse¹. Fourier analysis converts a time signal to frequency spectrum and the FFT is the algorithm which does this rapidly. FFT is a function which is built into Matlab. For this research FFT is used to compute a spectrum of length frequencies (1/wave length) of the collected data.

D.1.2. Example using Deitingen

To demonstrate the FFT application for this research the collected data of the service station in Deitingen will be used. As is described in the next chapter, the imperfections of this shell were the largest found. Therefore it is ideal when trying out post-process methods, because if it does not show results for Deitingen it can safely be said it will not produce better results with the other targets.

Just like the method used on the ANWB dome, a grid of points is projected on a smooth and detailed NURBS surface created by the measured points. And the z-coordinates of these points are subtracted from one another. Because the Deitingen shells are not symmetric in more than 2 ways, no averaging over parts of the structure will be done.

FFT is made for time depended waves, but with a little tweaking it could be used for a geometrical wave as well. The input for a fast Fourier transform can be a wave signal or list of amplitudes with a constant time interval (dt). When there is a constant horizontal length between points on the shell surface, a list of z-coordinates (the shell must be fairly horizontal) can be used as input for the FFT. The output consists of a spectrum with in the x-axis wave frequencies in bins and the y-axis is number of times a certain frequency is found.

D.1.3. Turning Bins to wave lengths

To find out what length corresponds to which bin number a sinus test wave is used. The exact same sample grid of points which is projected on the NURBS surfaces is also projected on a surface with a constant wave length (sinusoidal). When a FFT is done on these points only 1 spike will show in the spectrum (figure D.1), which is the frequency in bins corresponding to the wave length. So in this manner all other bin frequencies can be calculated and wave length which a predominant, can be determined.

¹http://en.wikipedia.org/wiki/FastFourier_transform

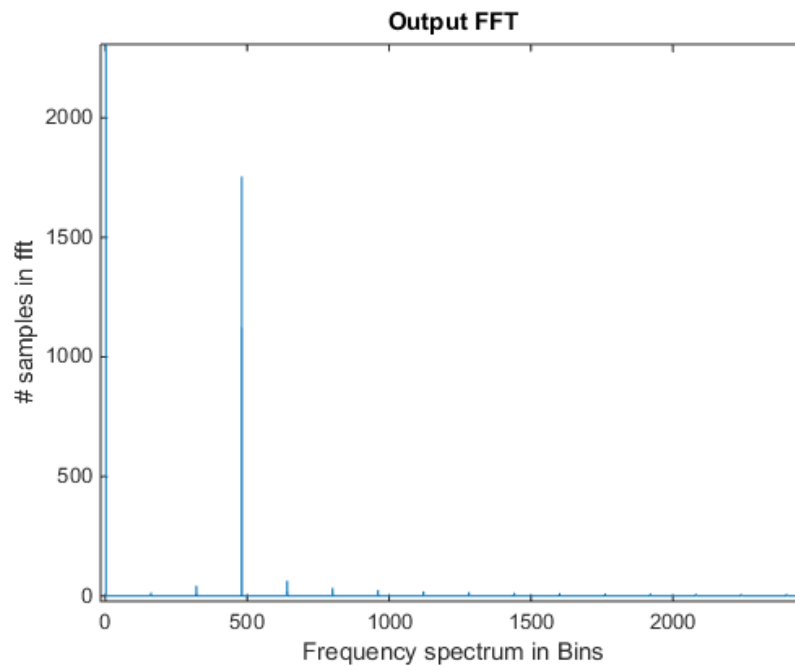


Figure D.1: Results of the FFT on a standard sinus wave with period length of 4.55 meter

D.1.4. Comparison collection methods of data for FFt

There are a few different sort of grids which can be projected on to the NURBS surfaces. The Surface of Deitingen is triangularly shaped (when viewed from above). The list of z-coordinates will be automatically sorted on first y then on x-coordinate. So the last point of the first row of points will be next to the first point of the second row. The z-coordinates of these points do not have to be equal. Therefore a jump in the sequence can happen, which disturbs the spectrum generated. Wave lengths which are a multiple of the row length are presented as more common as they really are. Therefore 3 types of sample grids are investigated; triangular, rectangular and spiral.

Triangular

The first type of sample grid is a triangular one, which follows the shape of the structure best. So most of the data is incorporated into the FFT. The row length of the sample grid differs per row, so its effect is not clearly visible in the results. And the top 2 meters of the triangle will not be in cooperation in the process, because the horizontal length is too short here. Making the input a trapezoid, which is not shown in figure D.2, because the data is filtered out in Grasshopper.

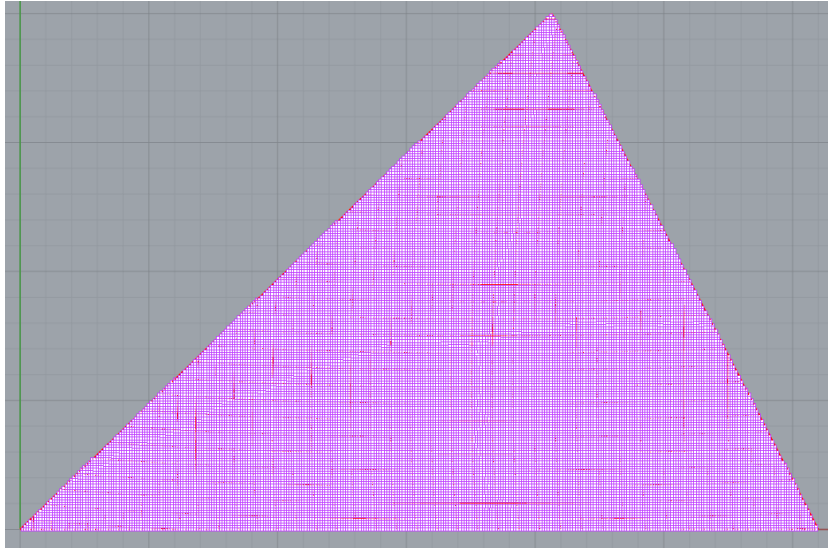


Figure D.2: Projected triangular grid on detailed NURBS surface

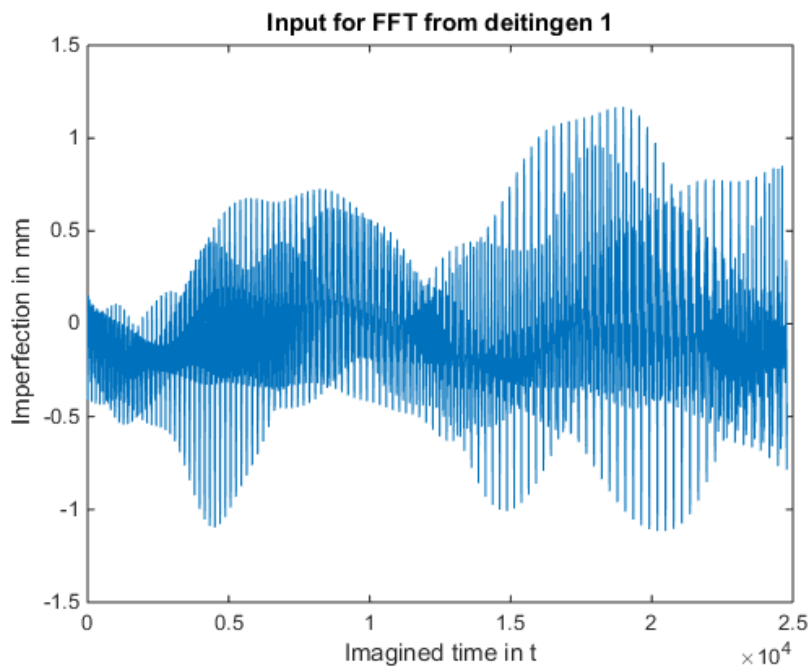


Figure D.3: Input triangular grid

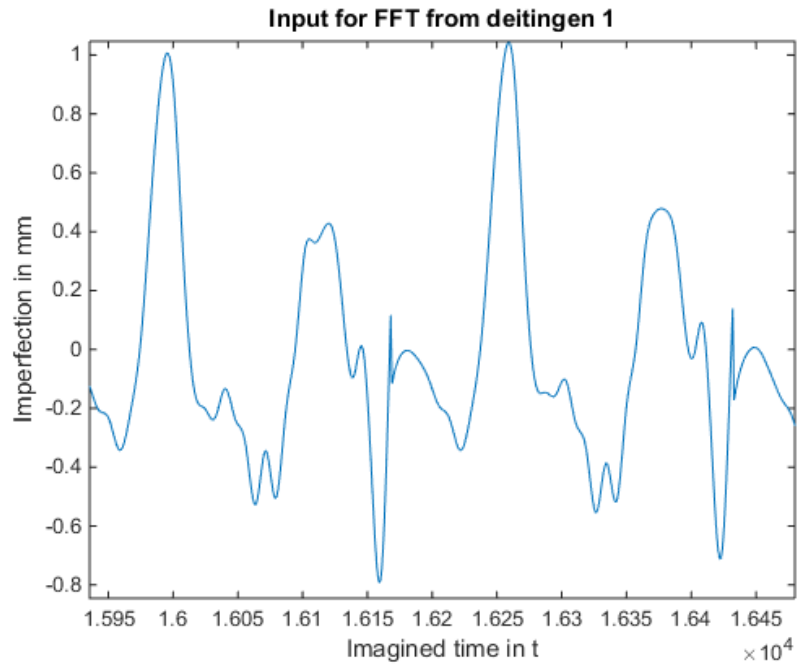


Figure D.4: Input triangular grid zoomed in to see the discontinuity created by the horizontal rows

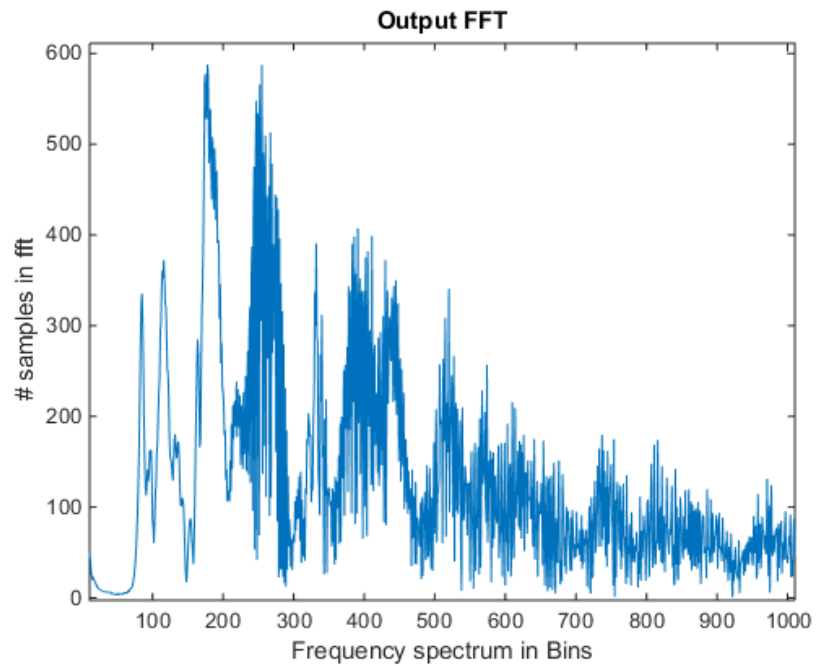


Figure D.5: Results of the FFT using a triangular grid

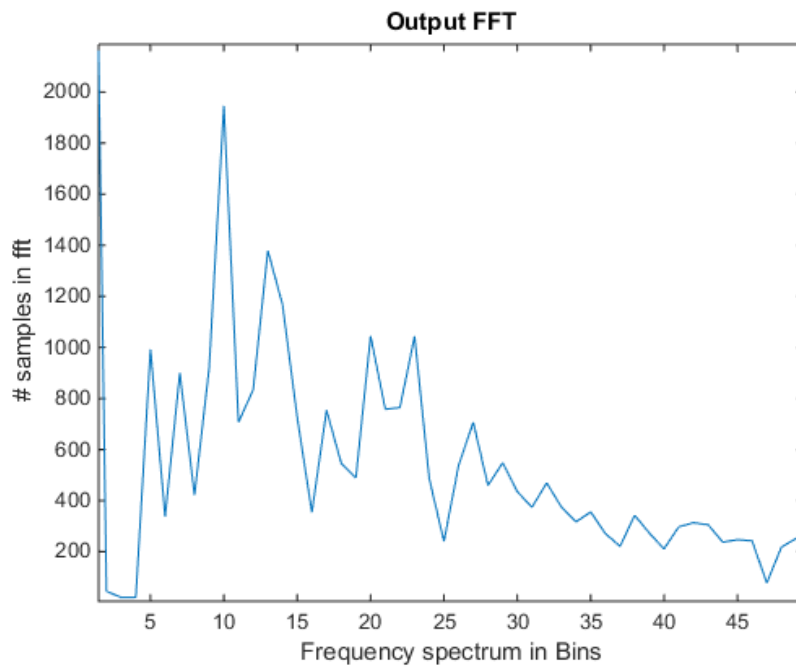


Figure D.6: Results of the FFT using a triangular grid, smoothed out by averaging over 20 terms

Rectangular

To make the effect of the row length more visible, a rectangular grid is projected onto both the shells at Deitingen. In the results it is clearly visible that every multiple of the row length creates a spike in the spectrum.

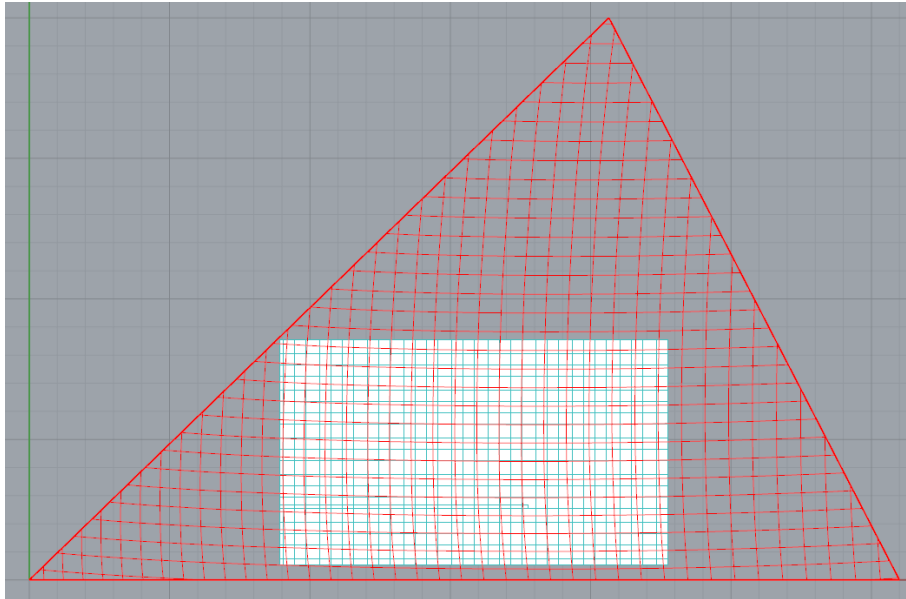


Figure D.7: Projected rectangular grid on detailed NURBS surface

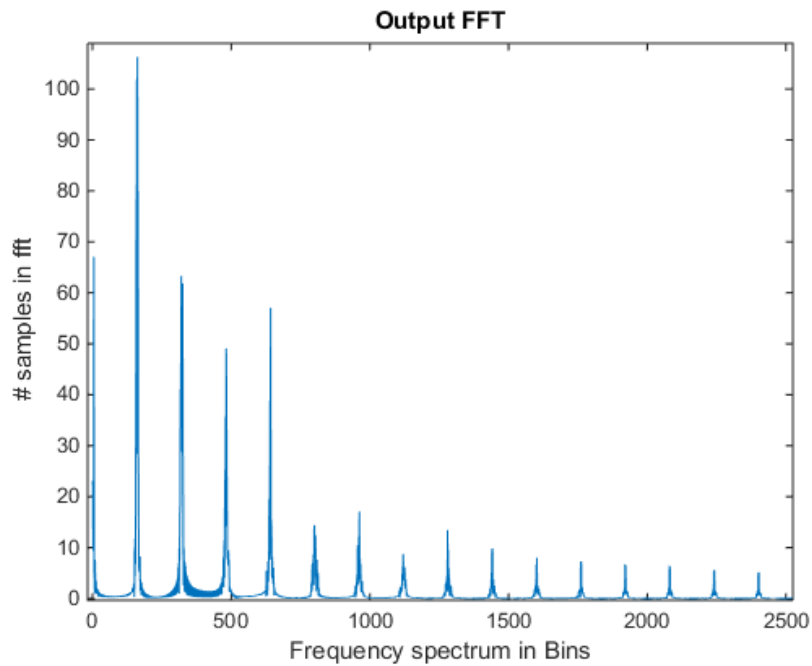


Figure D.8: Results of the FFT using a rectangular grid

Spiral

With a square shaped field of points projected on the surface the length of the sample interferes with the results. The repetitive length of the sample creates a spectrum which has spikes in every multiple of this length. Therefore a spiral shaped sampling method could be the answer to this problem. There are no jumps or repetitive lengths, when using this method to collected points along the surface.

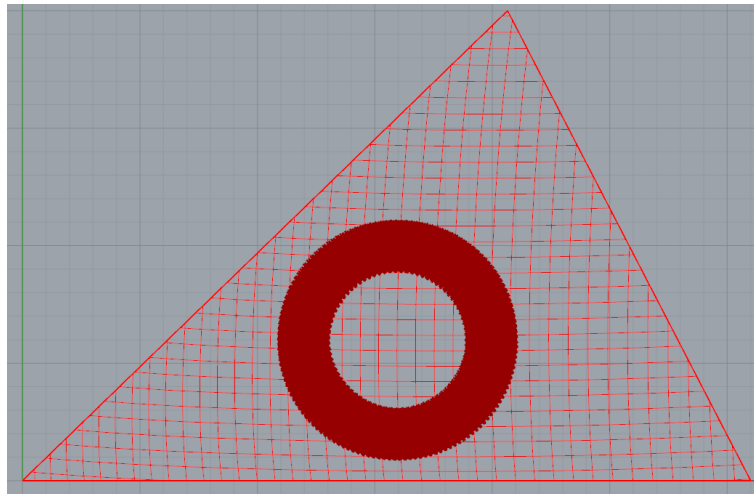


Figure D.9: Projected spiral grid on detailed NURBS surface

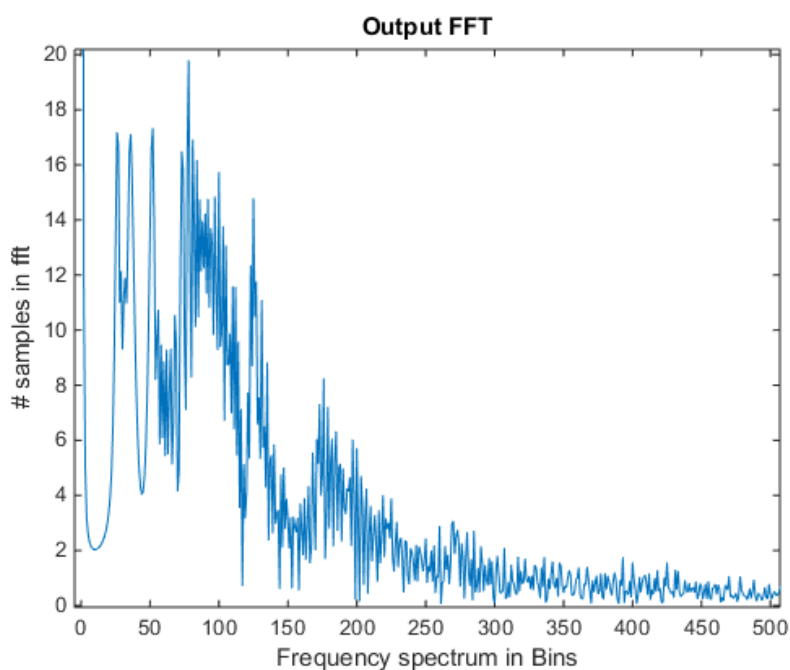
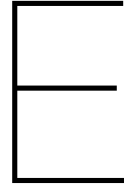


Figure D.10: Results of the FFT using a spiral grid

D.1.5. Conclusion

Using FFT for calculating the spectrum of imperfection wavelengths in shell structures is not without its faults. The method produces a spectrum of length frequencies, but due to the nature of the data it is questionable if this can be used.



Swiss trip

In this Appendix a short field report of the trip to Switzerland is given. The style of writing will be a bit more informal. This appendix can be useful for anyone who is interested in visiting (or measuring) the Isler Shell in Germany and Switzerland.

We arrived in Switzerland the day after new year's day of 2015. Peter Eigenraam went along with me for his own research on Isler shells for the faculty of architecture in Delft. Because I didn't have the luxury to wait for spring weather to go, we did the trip in the winter (which isn't ideal).

We used a Faro Focus 3d x130 laser scanner for measurement. This appendix will also describe the problems we faced using this device. For a detailed explanation on the workings of the laser scanner and reference spheres see chapter 2.

E.1. Preparation

Before we could go to Switzerland some preparation was needed aside from the equipment needed for measuring. In the months before the trip I've contacted all the building managers of every shell. I did this mostly via email, because my German isn't very good. I've found that all the people I've contacted, were very helpful. Only the service station was harder to contact, but we had the fortune that we knew a Swiss native, so he could call the service station. A former house mate of Peter (Nicolas) was visiting his family in Baden. He invited to stay with his family which was really nice and he help with contacting the sites we wanted to visit. If you don't know anyone who is German of Swiss it is also possible to make contact with the shell owners. If you make clear that your German is not very good most Swiss will talk very slow and clear.

Because we went in the winter our car needed to be prepared for winter conditions. In the winter it is illegal to ride on normal tires, when there is precipitation in Germany. So make sure that you have winter tires on your car if you are going through Germany. In Switzerland the law is a little less strict; you only get a fine when your car holds up traffic, because it is not suited for winter weather. We took snow chains with us just in case we needed them. If you want to plan a trip yourself I advise not to go in winter. Aside from the cold and the possibility of snowy roads, the snow on the shells made measuring the top geometry impossible.

For measurement of the shells we used a Faro Focus 3d x130 laser scanner. Although this is a expensive piece of equipment, it is the best way to measure concrete shells. Per structure we took scans containing millions of points and we were done in a few hours. The scanner has an incredible high accuracy for the speed that it measures points. A typical scan containing 2 million points takes a minute and each point is accurate to half a millimeter. It was hard to find Faro laser scanner to take to Switzerland, but it was worth it. Aside the quality of the data it collected, the speed of measurement made the process not very intrusive. For instance at the tennis hall in Heimberg almost all the fields where in use and the man at the front desk at first didn't want to let us in. But he changed his mind when we told him we only had to take 1 scan and that would take about 15 minutes (with setting up the device).

The scanner we used was 30 000 Euro's so buying one wasn't an option. At the time the department of remote sensing of the CEG faculty had an earlier version of the focus 3d in its collection, but it

broke before I could use it. They wanted to order a new one but that process would take a long time. Because this is my graduation project I didn't have the time to wait on that. Through the department of remote sensing I was informed that Deltares also had Faro laser scanner. Deltares is a company which focuses on coastal engineering, hydraulic structures and everything related to river delta's. Because the company has a good connection with the university, they were willing to help me with my project. Because my budget at the TU delft is limited, they offered to lend me a Faro focus 3d scanner for 100 Euro's for one month (which is very cheap considering its costs). The only problem was that the week 1 would pick up the device, they loaned it out to another company. Due to financial reasons the person that promised me the scanner was overruled and it was loaned out for half a year. Which was understandable from their point of view, but it cost a lot of time. Luckily they ordered a new one and I got priority to use it, so I could still go to Switzerland. The last problem in my preparations was the insurance of the laser scanner. Because of its costs i couldn't take it to Switzerland without having it insured and because I was not an employee of Deltares they couldn't help me either. Luckily the TU could handle the insurance for me, because it is hard to insure something that you loaned by private insurance companies.

The week before we went to Switzerland, I measured the dome at the head office of the ANWB in the Hague. This shell isn't one from Heinz Isler, but is interesting for my research and it was good practice with the device before we went to Switzerland. The scanner is very intuitive, it works like a smart phone, but if you want to use it, make sure you practice with it a lot. Especially the use of the reference balls can be tricky.

E.2. Visited shells

In total we visited 5 concrete shells designed by Heinz Isler, due to our schedules we did this in 3 days. It was a tight schedule, but we did everything we had planned.

E.2.1. Naturtheater in Grötzingen

On the first day we drove to Grötzingen near Stuttgart in Germany. In this town there is a open air theater and through their website¹ we got in contact with Barbera Koch and Herr Oppermann, the latter welcomed us at the theater. Because the total geometry of the shell could not be seen from one point, we had to take a total of 5 scans and with the help of the reference spheres combine them to 1 scan. For the reference spheres to work more than 50 measured points (more than 150 preferred) need to be on its surface. Because the spheres had to be quite far from the scanner the resolution of the scans in Grötzingen needed to be high (27 million points per scan). Because of this the first shell took 4 hours to measure. We had to be sure that the scans we took could be combined by using Scene (editing software made for the focus 3d). We could not measure the top surface, because it was covered with snow. When we were done we drove to Baden where the family of Nicolas (house mate of Peter) lived.



Figure E.1: Photos of the naturtheater in Grötzingen

¹www.naturtheater-groetzingen.de/

E.2.2. Swimming pool in Heimberg

The next day we went to Heimberg, a small town near Thun. In this town is a swimming pool and a tennis hall next to each other both designed by Heinz Isler. Through their website² we came in contact with bath superintendent, she was very helpful. Like the open air theater, multiple scans where needed for this structure. The measuring process was the same as in Germany. High humidity can be a problem when you use a laser scanner around a indoor pool. Because the machine was quite cold the mirror fogged up. This only can be solved by waiting, because the mirror must not be touched. When the machine was warmer and almost clear of fog, we did a test scan which heated up the scanner further and made it ready for measurements. In Heimberg portions of the roof were not covered in snow so we also did some measurements on the outside of the shell.



Figure E.2: Photos of the swimming pool in Heimberg

²<http://www.sportzentrum-heimberg.ch/hallenbad>

E.2.3. Tennis hall in Heimberg

The bath superintendent introduced us at the reception of the tennis hall next to the swimming pool. Because the entire roof could be seen from 1 point, 1 scan was sufficient and the reference balls weren't needed. Therefor we were done very quickly. At the tennis hall we also did a scan on the outside of the shell, to measure the variation in thickness of the shell edge. This is important for Peter's research.



Figure E.3: Photo of the tennis hall in Heimberg (with the author of this report)

E.2.4. Garten centre in Zuchwill

Via the website of the garten center³ we came in contact with the owner and with the floor manager (Herr Fassler). Because this shell is used as a garden store, there are a sorts of things blocking the view to the roof (see figure below). So we had to use the same method as we did with the swimming pool and the open air theater. Placement of the spheres was critical here, because there was not a simple scheme possible where all 5 of the spheres were visible from every scan. Scene needs 3 spheres to place 2 scans, but accuracy is increased when 4 spheres are visible in both scans. We took a scan from each of the 4 corners placing 1 sphere per corner. The last sphere we had was placed between scan 1 and 2, and then moved to the other side of the room when we did scan 3 and 4. This was the only way every scan had 4 spheres in it. After we did the inside of the shell, Peter took 1 scan of the outside arch for his research and we went back to Baden.



Figure E.4: Photos of the Wyss garten centre in Zuchwill

³<https://www.wyssgarten.ch/Standorte/Zuchwil>

E.2.5. Service station in Deitingen

On the last day we visited Deitingen and this was the first time the locals weren't very cooperative. Via Nicolas we had permission of the manager (Herr Ernie), but because it was Sunday morning he was not present. The man in charge didn't want us to measure without Ernie permission and didn't want to take our word. He told us we had to come back in the afternoon when the manager arrived. This was not an option because we had to drive back to Delft that day. But because the scanner is quick and it was quiet, we took the scans we needed and were done before they noticed it. We would not have done this if we didn't already had permission. This way the worst that could happen is that halfway our measurements we would have to stop. If I would visit the service station another time for measurements, I would plan a specific date and time with the manager or make sure to have written permission. The lack of a surface finish on the shells, made the service station essential for my research. The other shells all have insulation panels on the inside. Aside from this there are 2 exact replica's next to each other and with the reference spheres we were able to measure the thickness of the shell.



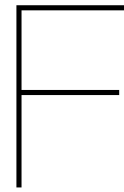
Figure E.5: Photos of the service station in Deitingen

E.3. Collected data

After we were back in Delft there were 2 slight problems. A few scans from Heimberg were corrupted, so Scene refused to open them. If this is the scanner fault or the a problem in Scene is not yet known. The second problem is a matter of file size. We weren't expecting that point clouds could get so large, that they would become a problem using a "normal" PC. With Matlab it is possible to randomly delete measured points, but if points clouds are 27 million points big, 8 Gb of RAM is not enough. (At this moment I've found some leads to overcome this problem.) Using a typical computer it is advised not to load much more than a million points into Rhino, otherwise some functions will not work. For my purposes a million points is easily sufficient.

E.4. Conclusion

The trip to Switzerland was a success. We did everything we set out to do, but the failed scans in Heimberg were a pity. I will advise anyone to double check if the scans open on location. We did this regularly, but it turns out not often enough. The contact we made with all the owners and managers of the shells was very helpful. Even if you are just visiting this is advised. If Anyone would ever like to measure other Isler shells or any sort of structure, I would highly recommend (if possible) using a laser scanner from Faro. The newer versions are very portable, just a normal size briefcase (1 extra for reference spheres) and a tripod. The speed of the device will make sure that people will cooperate and the accuracy is extraordinary.



Case study: Effect of initial imperfections on ultimate strength of a spherical shell

When trying to measure imperfections in shells it is important know where exactly to search for. An imperfection with a wave length equal to the buckling length as described in equation 1.1 may not lead to the lowest ultimate strength. Therefore a case study is done where the ultimate strength is calculated for a spherical dome using a finite element program. The FEM software package which was used is created by TNO, and is called Diana. There were a few other options like AnSys. But the licence for Diana and its modeling program Fx+ for Diana was available and Diana is most suited for non-linear shell modeling.

As stated in the introduction of the main matter; a case study was done to show the impact of initial geometrical imperfections on shell structures using finite element (FE) software. This case study will be described in detail in this appendix. For the FE calculations Midas FX+ for Diana 3.1.0 and Diana Finite Elements 9.6.0 were used.

F.1. Geometry

For this case study a simple geometry was chosen, because complex geometries are not needed to show the effect of imperfections in shells. Shell is a spherical dome which is 3 meters high, 20 meter wide and 10 centimeters thick (Figure F.1). The shell has a constant radius of 18.167 meter, which theoretically gives it a buckling length of approximately 1 meter (using 1.1).

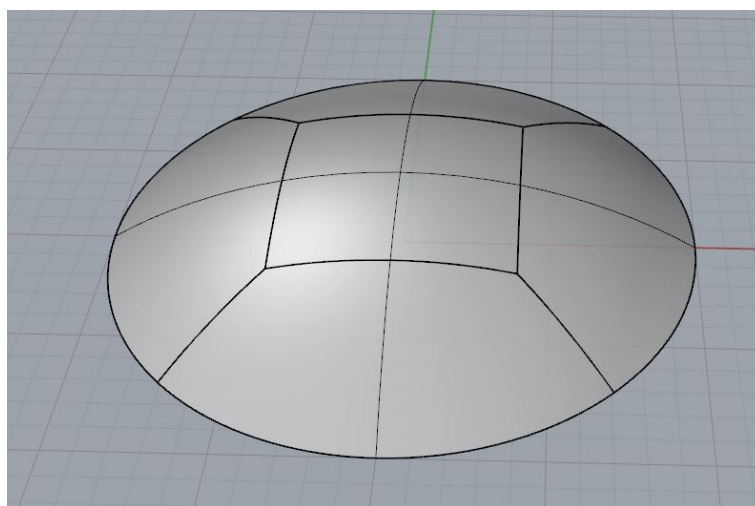


Figure F.1: Visual representation of the shell geometry in Rhino (height is 3 m, width is 20 m and thickness 10 cm)

The dome is cut into 5 pieces, because this helps with making a homogeneous mesh. The 5 pieces

of the shell were exported to FX+ as a "step" geometry.

F.1.1. Adding imperfection to geometry

There are several ways to add a imperfection to the geometry. In this case study the imperfection was created in Rhino. A surface with sine waves was created, using Grasshopper (figure F.2). To show the significance of the size of the imperfection, meaning the amplitude not the wave length, two separate sine imperfections were created and added to the original geometry. The imperfections in meters can be described as:

$$I_{0.05}(x, y) = 0.05 \sin\left(\frac{2\pi}{4}x\right) \sin\left(\frac{2\pi}{4}y\right) \quad (\text{F.1})$$

$$I_{0.01}(x, y) = 0.01 \sin\left(\frac{2\pi}{4}x\right) \sin\left(\frac{2\pi}{4}y\right) \quad (\text{F.2})$$

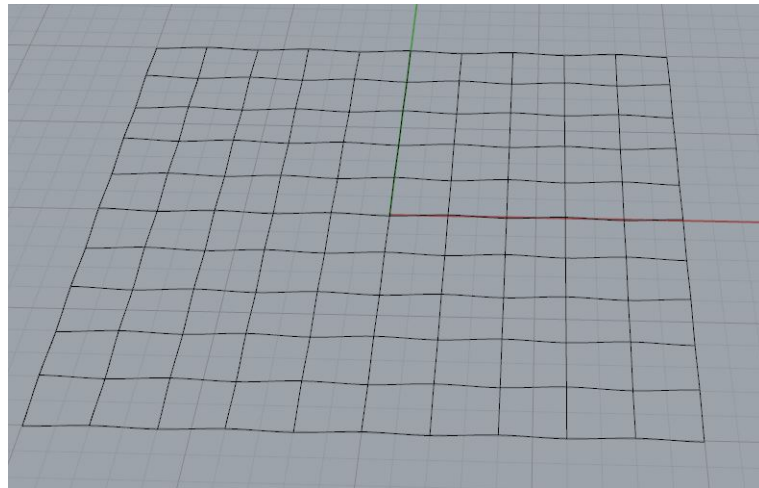


Figure F.2: Visual representation of the imperfection in Rhino, before it is added to the geometry

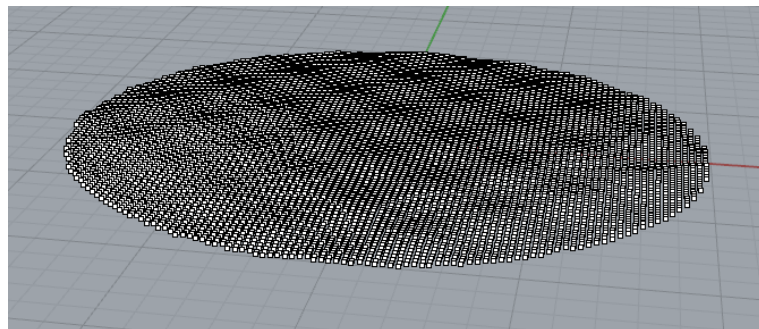


Figure F.3: Projected grid of points on sine field created in Grasshopper.

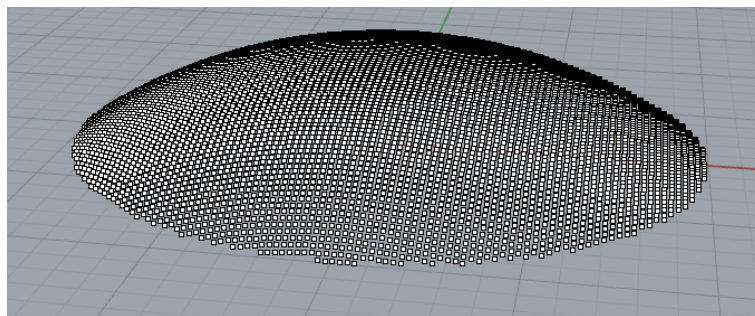


Figure F.4: Projected grid of points on perfect dome geometry

The imperfection surface was added to the geometry of the dome in the same way the combined sine field was created in chapter 3. A grid of points (100 by 100) was projected on the sine field (figure F.3) and the shell geometry (F.4), then the z-coordinates of these points grid were added to each other using Grasshopper. After this a new geometry can be created by fitting a NURBS surface through these points (see figure F.5).

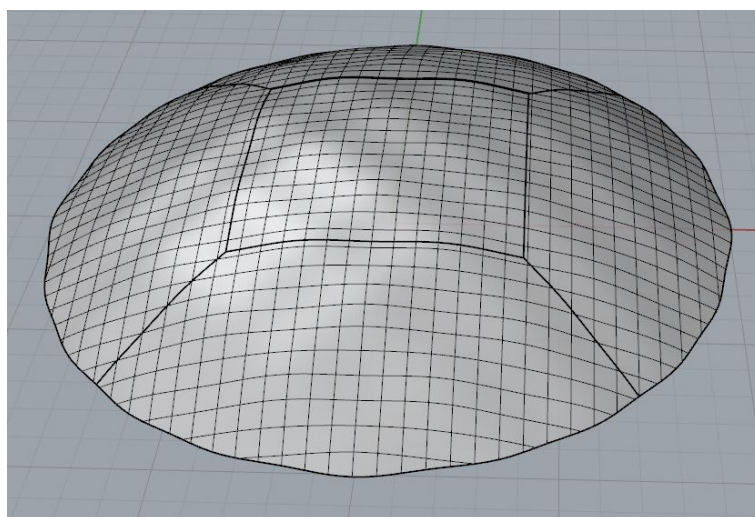


Figure F.5: Visual representation of the shell geometry in Rhino with imperfections (height is 3 m, width is 20 m and thickness 10 cm)

F.2. Material properties

Property	Value
Young's modulus E	28000 N/mm ²
Poison ratio ν	0.2
Shear modulus G	1167 N.mm ²
Mass density ρ	2400 N/m ³ / g

Table F.1: Material properties for thin concrete shell used in FE model

F.3. Mesh

For mesh creation the auto mesh (Delauney) function of FX+ was used. Element size was set on 0.125 meters and

Property	
Element size	0.125 m
Number of elements	5671
Element types	Quadrilateral and triangular
Elements	Q20SH And T15SH
Auto mesher	Delaunay

Table F.2: Mesh properties of FE model in Fx+ for Diana

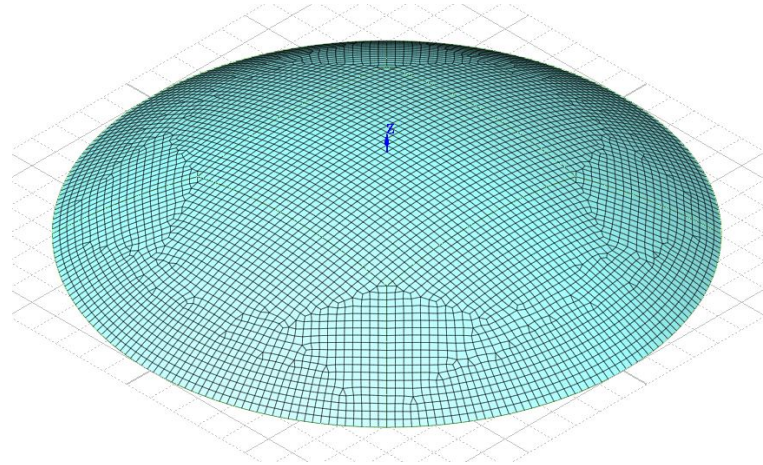


Figure F.6: Visual representation of the mesh of the spherical shell in FX+, without imperfections

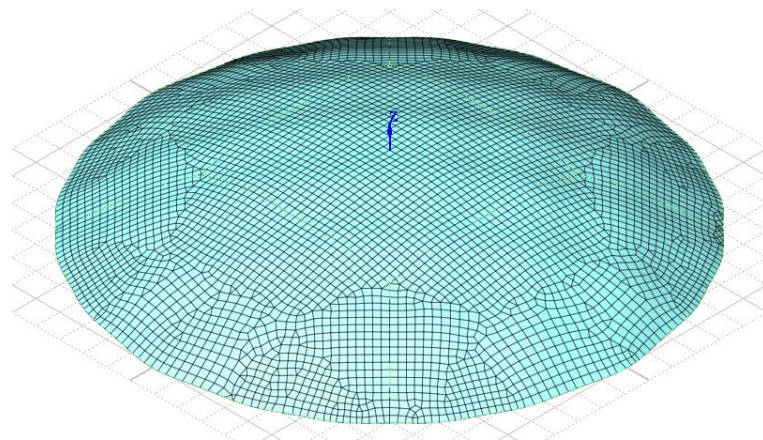


Figure F.7: Visual representation of the mesh of the spherical shell in FX+, with imperfections

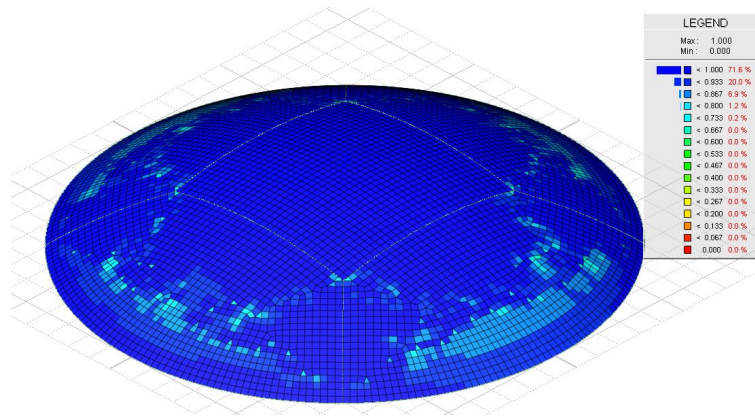


Figure F.8: Visual representation of the mesh quality in FX+, without imperfections. Figure shows the aspect ratio per element, where 1 is preferred

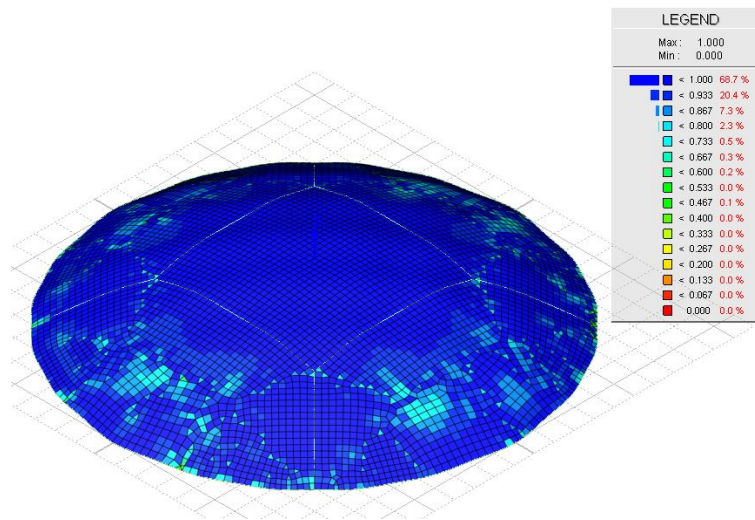


Figure F.9: Visual representation of the mesh quality in FX+, with imperfections. Figure shows the aspect ratio per element, where 1 is preferred

F.4. Load

For the load a face pressure of 1000 kN/m^2 was used. This pressure was in the global z direction (downwards), see figure F.10.

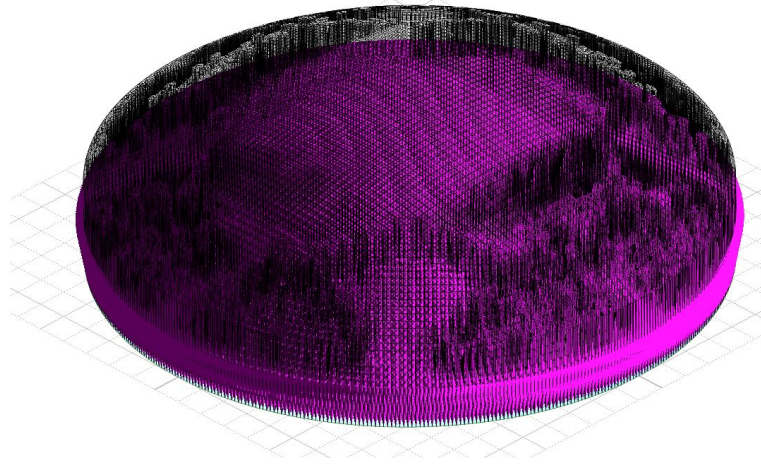


Figure F.10: Visual representation of the load on the spherical shell in FX+

F.5. Boundary conditions

All elements at the base of the dome were pinned, meaning no displacement in x,y and z direction were possible, see figure F.11.

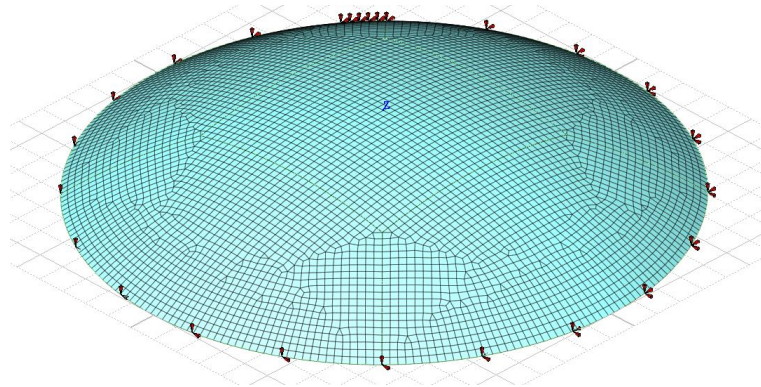


Figure F.11: Visual representation of the boundary conditions on the spherical shell in FX+

F.6. Analyses

In total three analyses were run: linear, geometrically non-linear and geometrically non-linear with imperfect geometry. The last two analyses are identical with different starting conditions, therefore these two are described as one.

F.6.1. Linear

In Diana a linear elastic analysis of the perfect dome was done using the mesh and properties described in the previous paragraphs. The command file can be seen in figure F.12

```
*LINSTA LABEL="Structural linear static"
SOLVE PARDIS
BEGIN OUTPUT
TEXT "Output linear static analysis"
FXPLUS
BINARY
SELECT LOADS ALL /
END OUTPUT
*END
```

Figure F.12: Command for for linear analysis in Diana which was used

F.6.2. Geometrically non-linear

For the geometrically non-linear analysis some alterations were made in the command file of Diana (see in figure F.13). The analysis was done on all three shells. They were force controlled until they buckled. Force control is a method of increasing the load step by step until the structure fails at its ultimate strength. This method has the advantage that it is easier to produce than the arc-length method, but the method stops at ultimate strength and does not produce further results in the buckling phase. For this case study this was not a problem, because it focused on the ultimate strength of the shells.

```
*NONLIN LABEL="Structural nonlinear"
BEGIN TYPE
PHYSIC OFF
BEGIN GEOMET
UPDATE
NLPREB ON
END GEOMET
LINSTR ON
END TYPE
BEGIN EXECUT
BEGIN LOAD
LOADNR 2
STEPS EXPLIC SIZES 0.500000 0.100000 0.100000 0.100000 0.0100000(10)
END LOAD
BEGIN ITERAT
MAXITE 20
METHOD NEWTON MODIFI
CONVER ENERGY
END ITERAT
END EXECUT
SOLVE PARDIS
BEGIN OUTPUT
TEXT "Output"
FXPLUS
BINARY
SELECT STEPS ALL /
END OUTPUT
*END
```

Figure F.13: Command for for non-linear analysis in Diana which was used

F.7. Results

Figure F.14 shows the relation between load and the displacement of the top node of the shell. All analyses are combined into one graph to show the impact of the imperfections on the displacement of the top. All contour plots are given in a separate section after the conclusion of this case study.

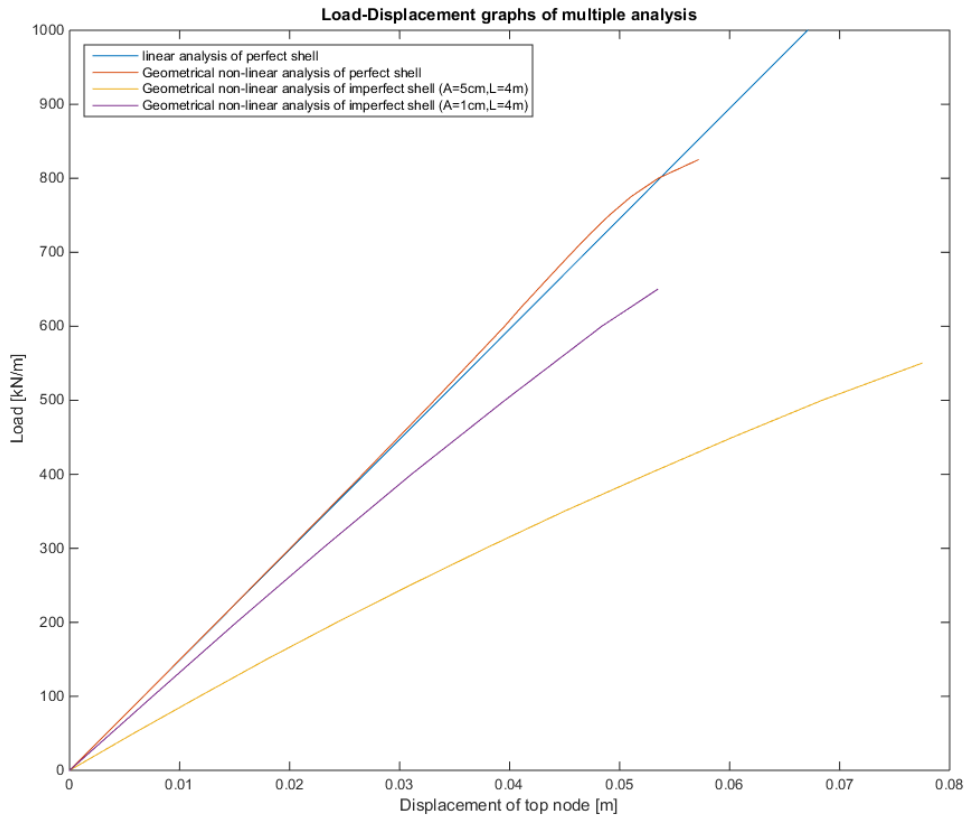


Figure F.14: Load displacement graph of top node of multiple analyses

The shell all buckles approximately 2 meter from the edge. So a load-displacement curve at this spot (figure F.15) was made to better view the behavior of the shell. Here the flattening of the ends of the graphs can be clearly seen. Because these were force controlled analyses, the downward phase where further buckling occurs can not be shown. This is not a problem because the goal of the case study was to compare the ultimate strength, which was reached for all analyses.

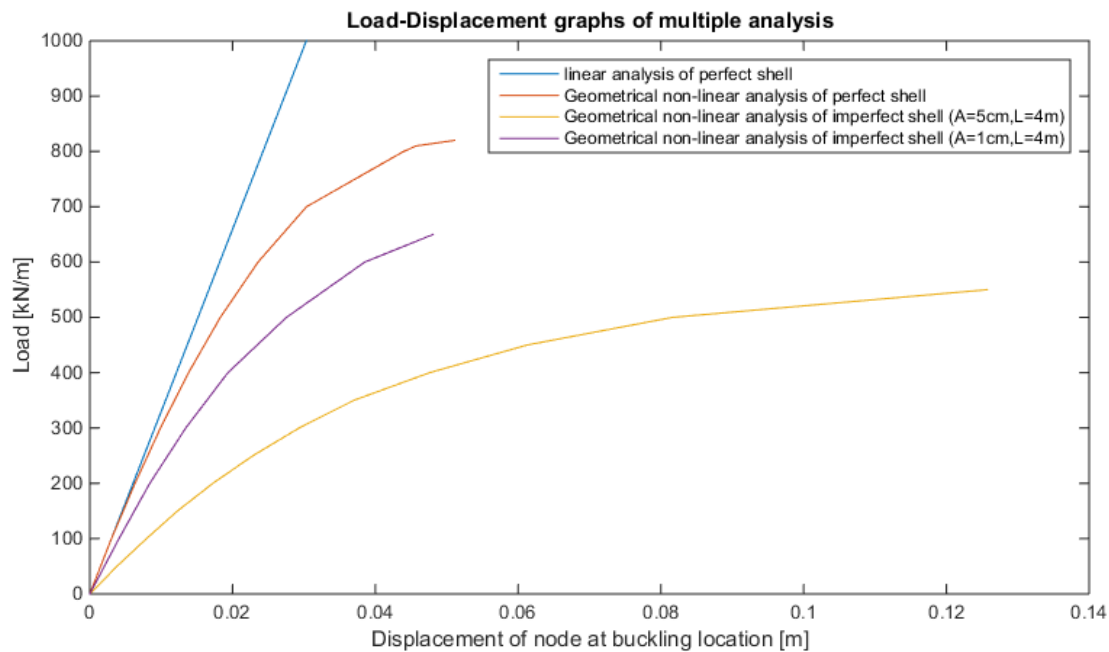


Figure F.15: Load displacement graph of node at buckling location of multiple analyses

F.8. Conclusion

The goal of this case study was to show the impact of imperfections in thin shells. Figure F.15 shows this impact clearly. It shows a knock down factor of 0.66 for 5 centimeters of amplitude of imperfection, which means that 33% of the total strength of the shell is lost due to the imperfection. The smaller imperfection with an amplitude of 1 cm clearly has less of an impact on the strength of the shell (knock down factor of 0.8).

This case study reached its goal in showing the impact of imperfections and that the size of the imperfection clearly influences the strength of a thin concrete shell. Although this is just one shell with one type of imperfection, the effect it has is clearly visible. For a precise quantification of the knock down factor, more research needs to be done. This was not included in this research, because it was not within the goal (and time) of this case study. More research on this topic has been done in other thesis's of structural engineering. For more information see the thesis report of Tien Chen ¹, which can be found on the TU Delft repository.

¹On Introducing Imperfection in the Non-Linear Analysis of Buckling of Thin Shell Structures, T. Chen.

F.9. Displacement and mean stress plots of all analyses

In this section the displacement and stress plots of all analyses are shown for the last 4 load steps to give an indication of the behavior of the shells. For readability not all produced contour plots are shown.

F.9.1. linear analysis of imperfect shell results

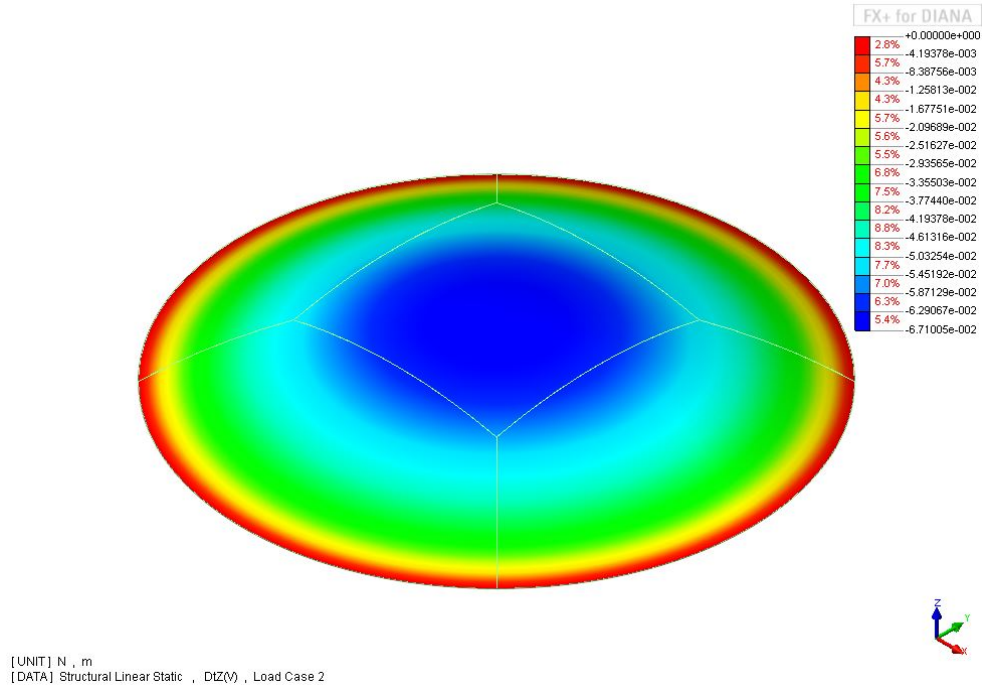


Figure F.16: Displacement in meter of z-coordinate of perfect shell, using linear analysis. Load is 1000 kN/m^2

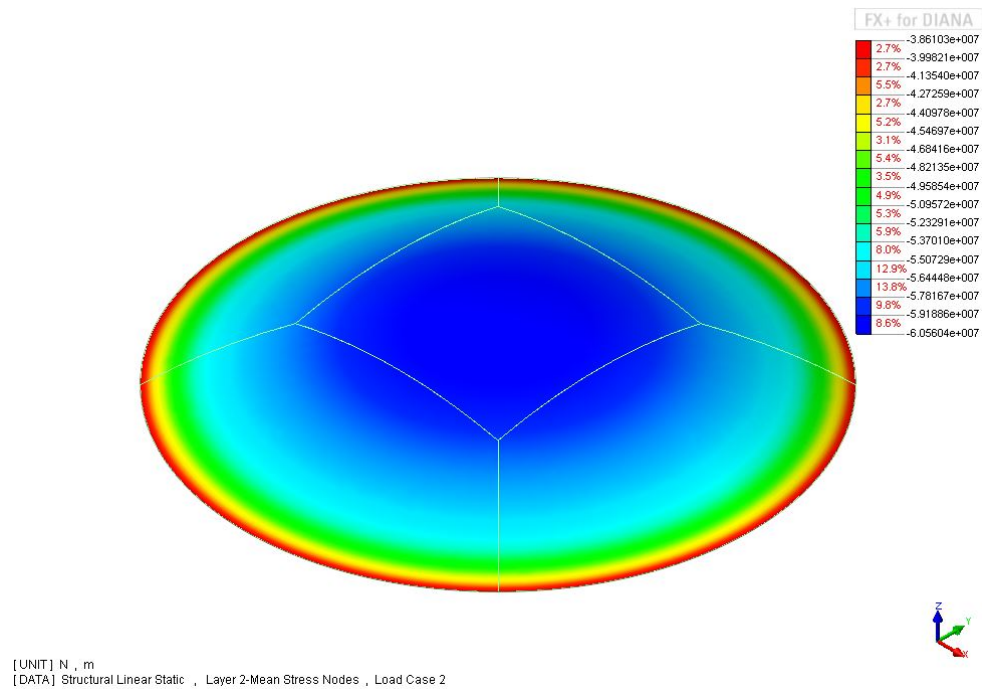


Figure F.17: Mean stress in N/m^2 of z-coordinate of perfect shell, using linear analysis. Load is 1000 kN/m^2

F.9.2. Non-linear analysis of perfect shell results

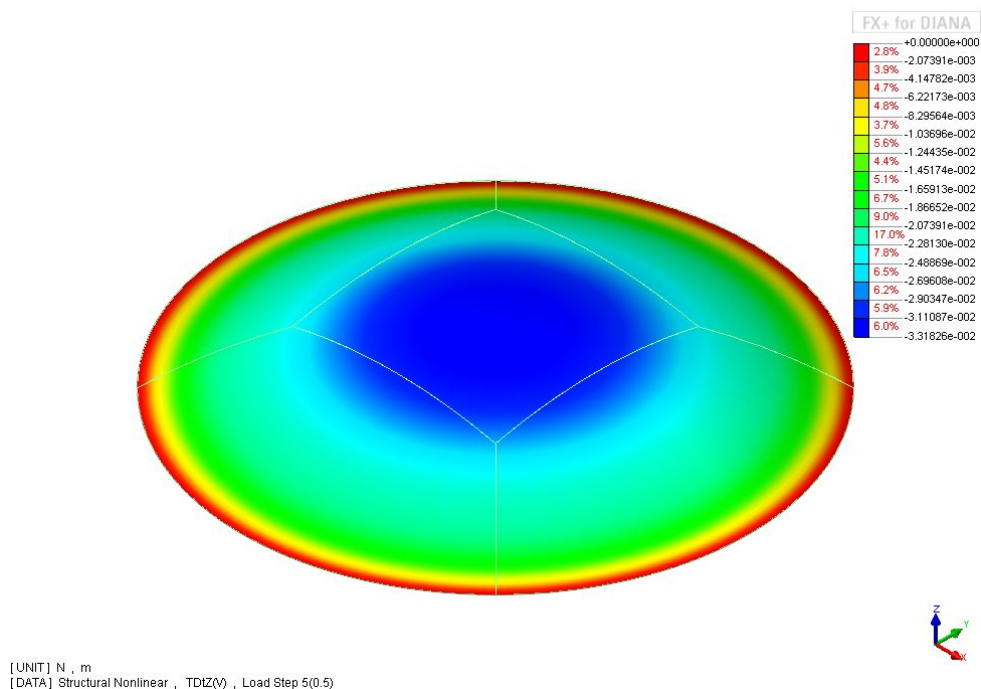


Figure F.18: Displacement in meter of z-coordinate of perfect shell, using non-linear analysis. Load step 500 kN/m^2

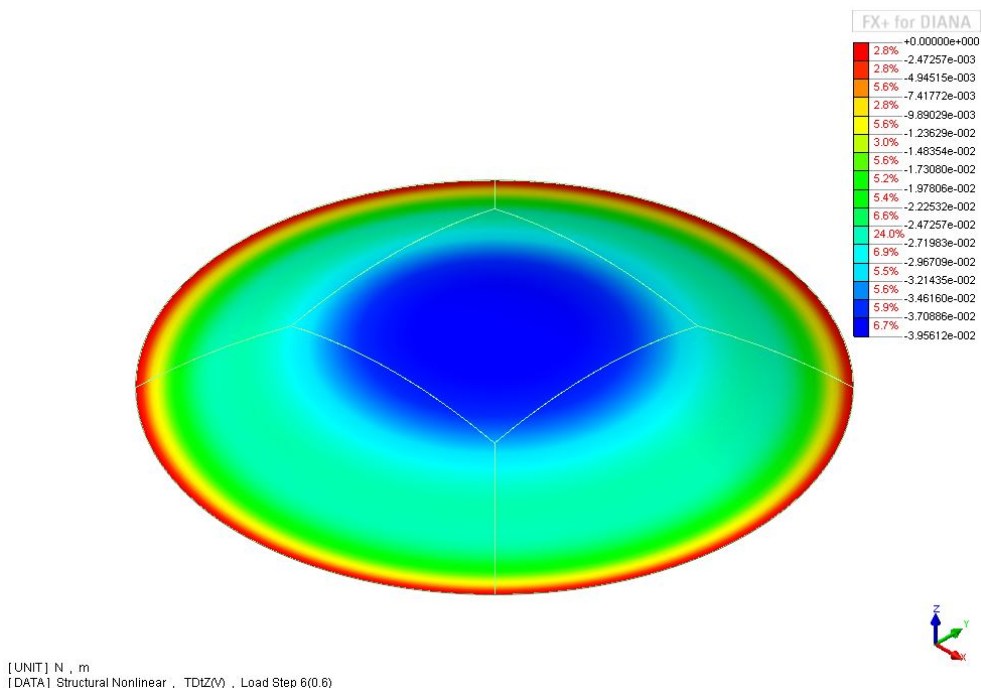
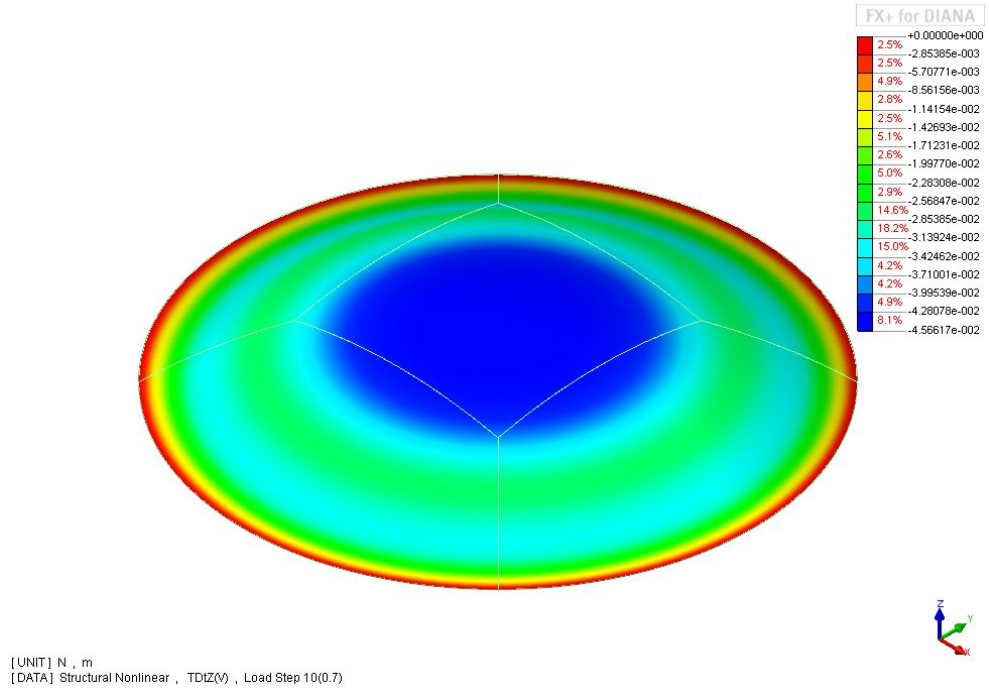
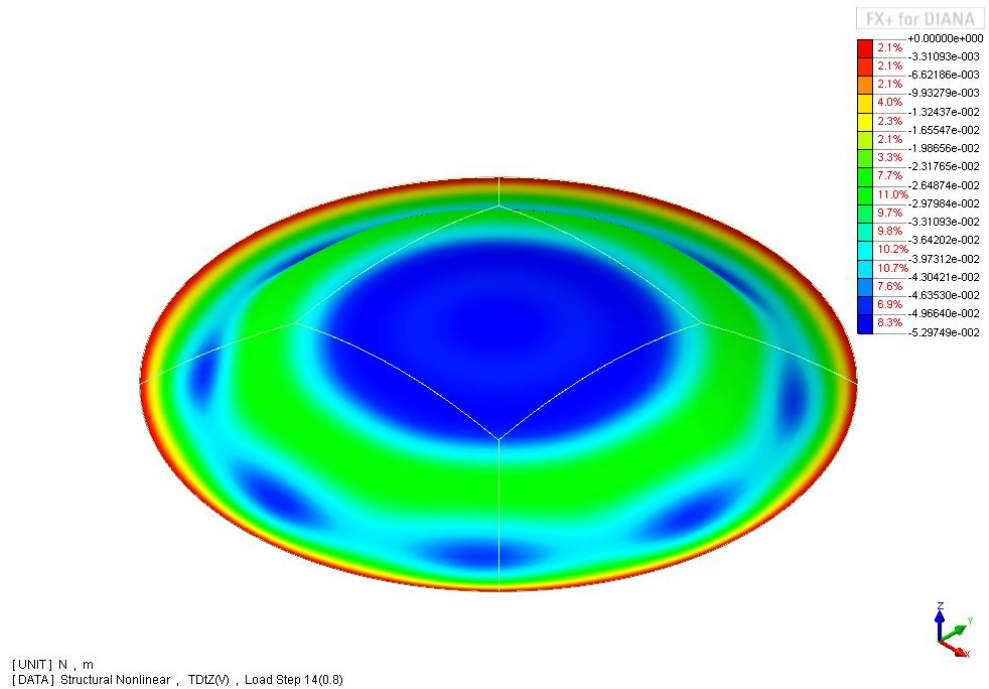


Figure F.19: Displacement in meter of z-coordinate of perfect shell, using non-linear analysis. Load step 600 kN/m^2

Figure F.20: Displacement in meter of z-coordinate of perfect shell, using non-linear analysis. Load step 700 kN/m^2 Figure F.21: Displacement in meter of z-coordinate of perfect shell, using non-linear analysis. Load step 800 kN/m^2

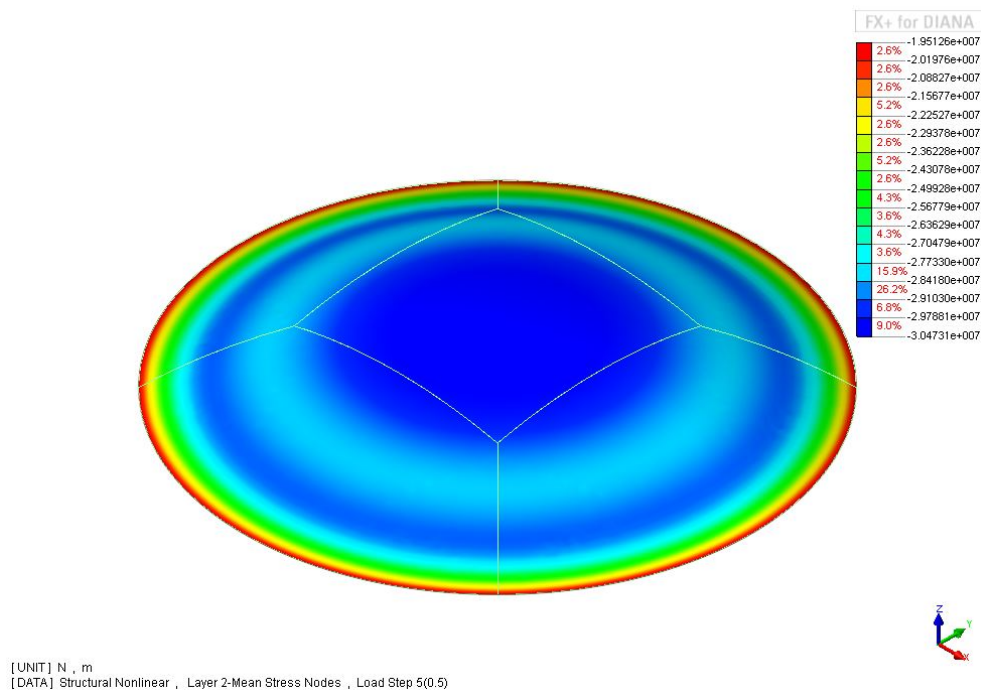


Figure F.22: Mean stress in N/m^2 of z-coordinate of perfect shell, using non-linear analysis. Load step 500 kN/m^2

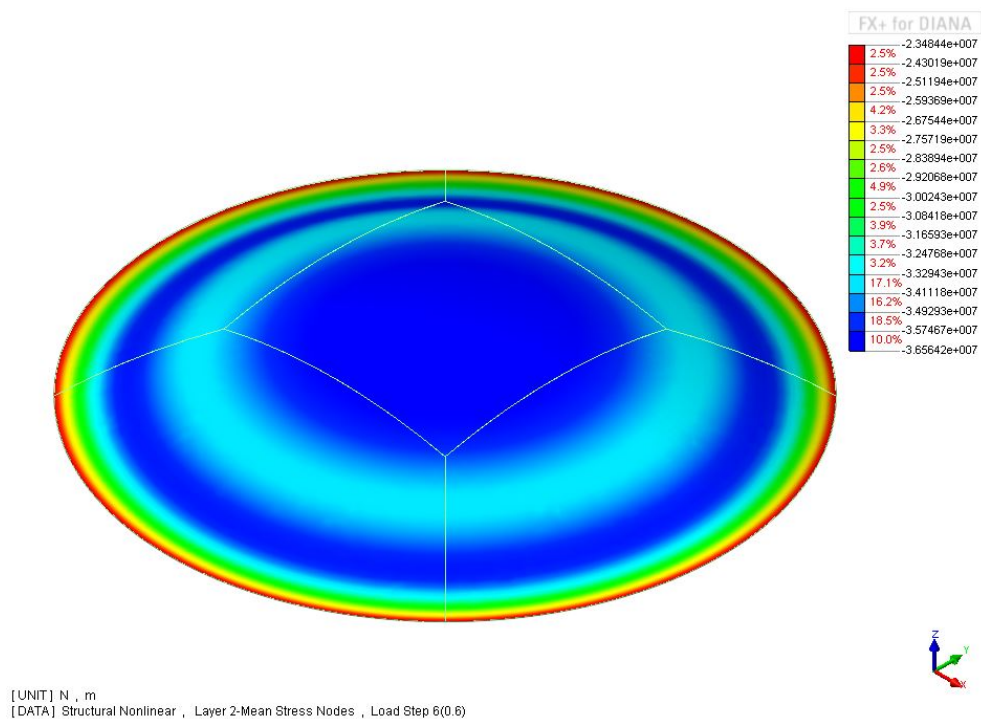


Figure F.23: Mean stress in N/m^2 of z-coordinate of perfect shell, using non-linear analysis. Load step 600 kN/m^2

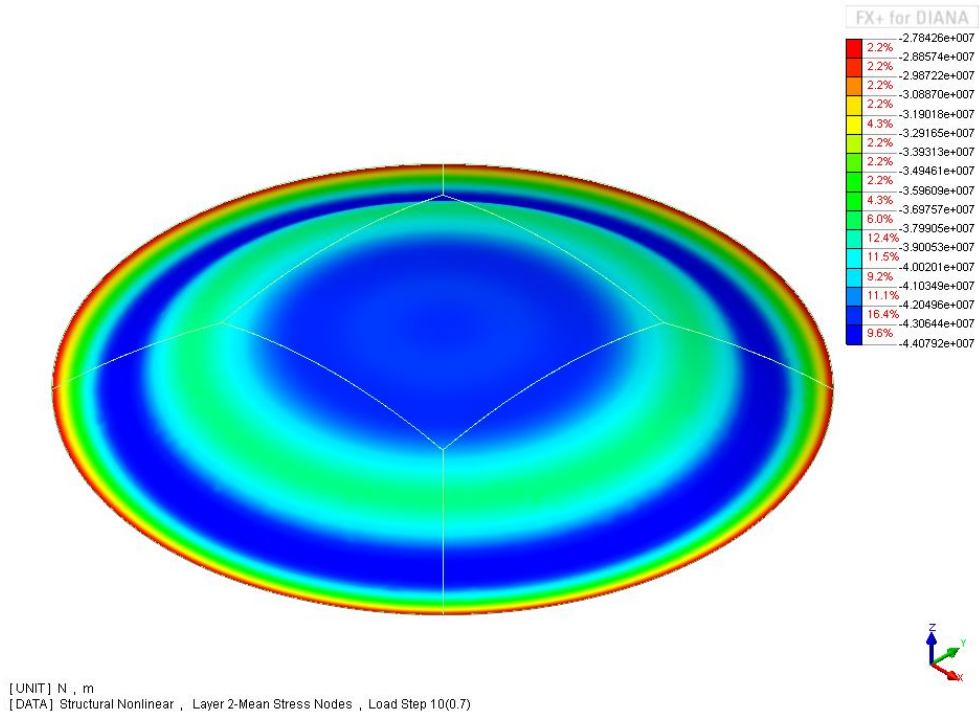


Figure F.24: Mean stress in N/m^2 of z-coordinate of perfect shell, using non-linear analysis. Load step $700\text{ kN}/m^2$

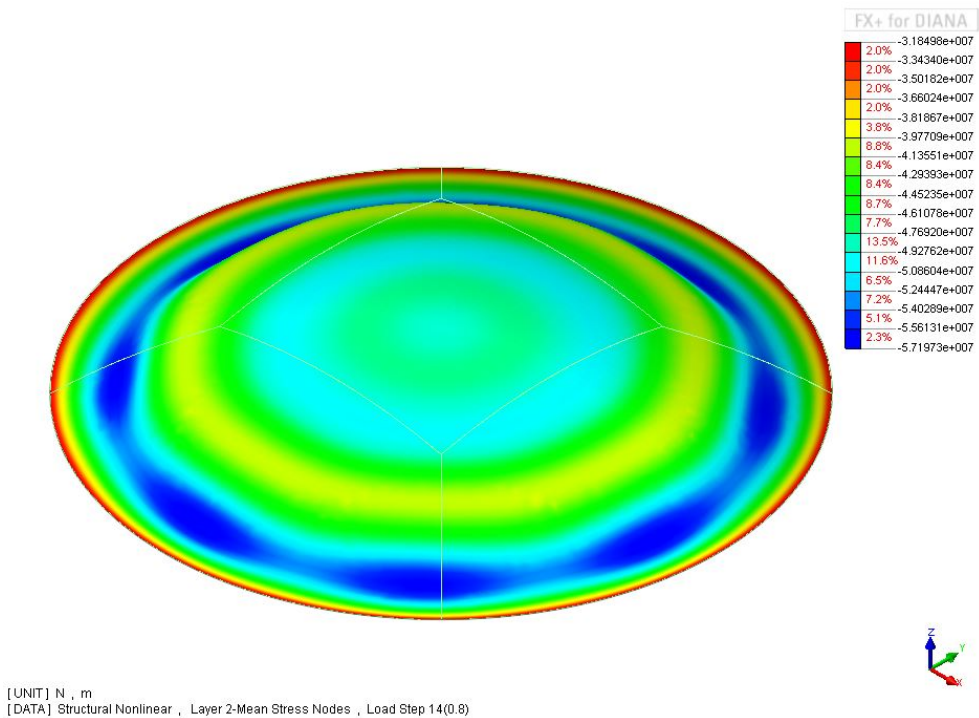


Figure F.25: Mean stress in N/m^2 of z-coordinate of perfect shell, using non-linear analysis. Load step $800\text{ kN}/m^2$

F.9.3. Non-linear analysis of imperfect shell (amplitude 5 cm) results

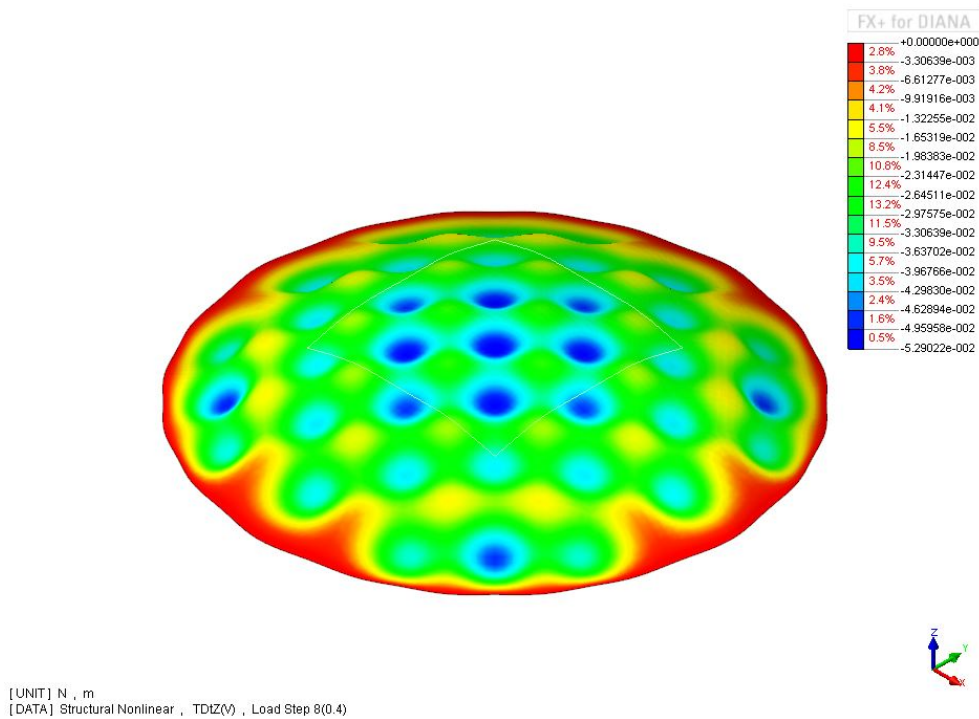


Figure F.26: Displacement in meter of z-coordinate of imperfect shell (amplitude 5 cm), using non-linear analysis. Load step 400 kN/m^2

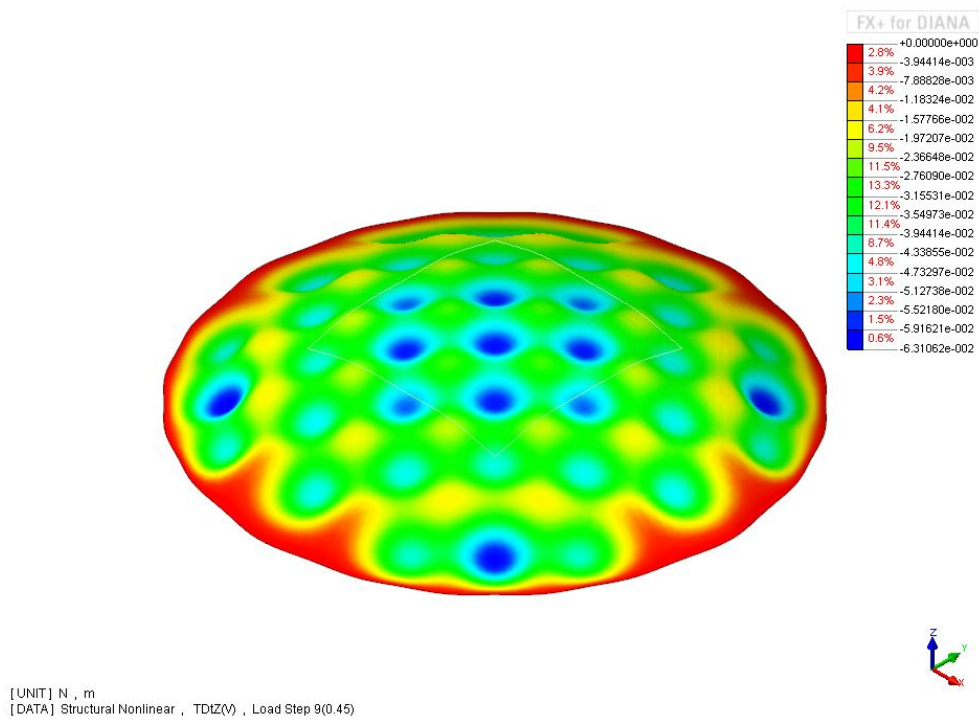


Figure F.27: Displacement in meter of z-coordinate of imperfect shell (amplitude 5 cm), using non-linear analysis. Load step 450 kN/m^2

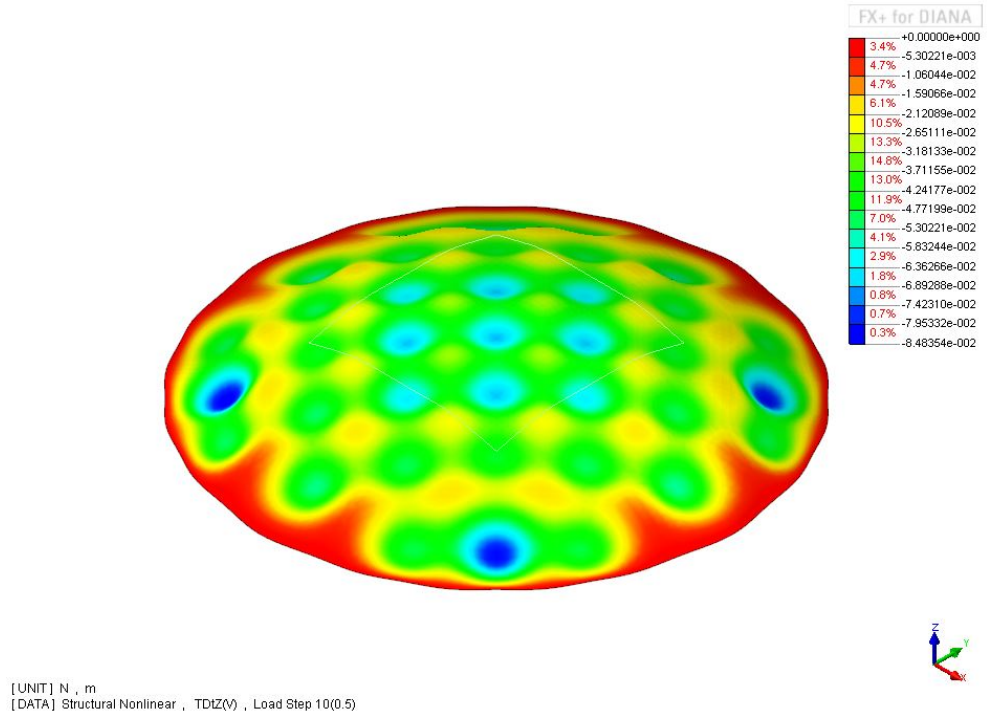


Figure F.28: Displacement in meter of z-coordinate of imperfect shell (amplitude 5 cm), using non-linear analysis. Load step 500 kN/m^2

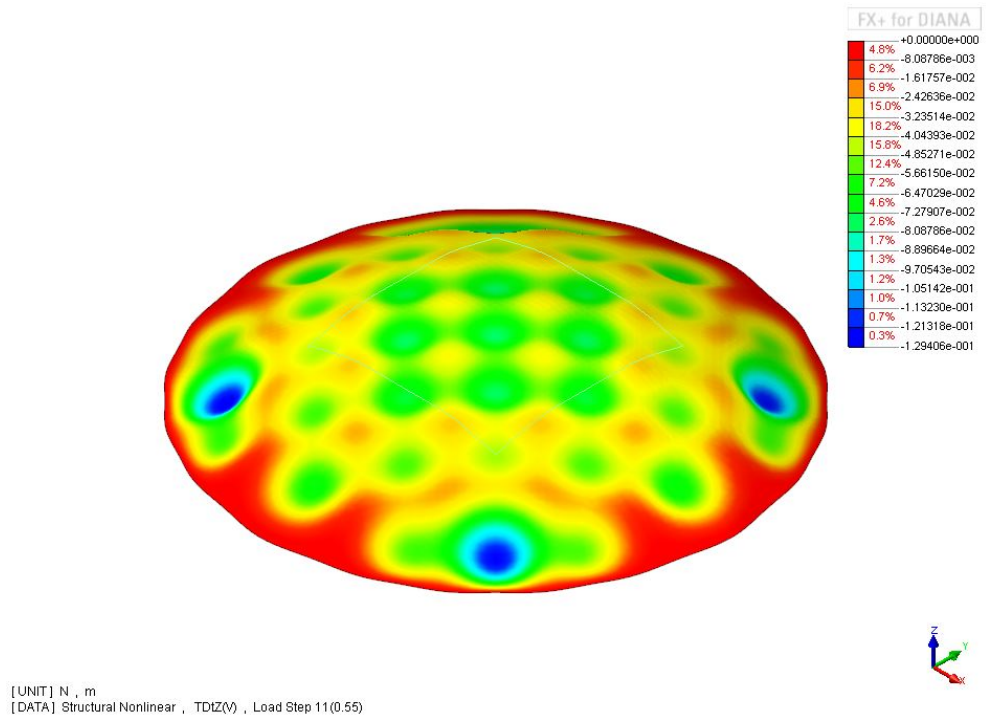


Figure F.29: Displacement in meter of z-coordinate of imperfect shell (amplitude 5 cm), using non-linear analysis. Load step 550 kN/m^2

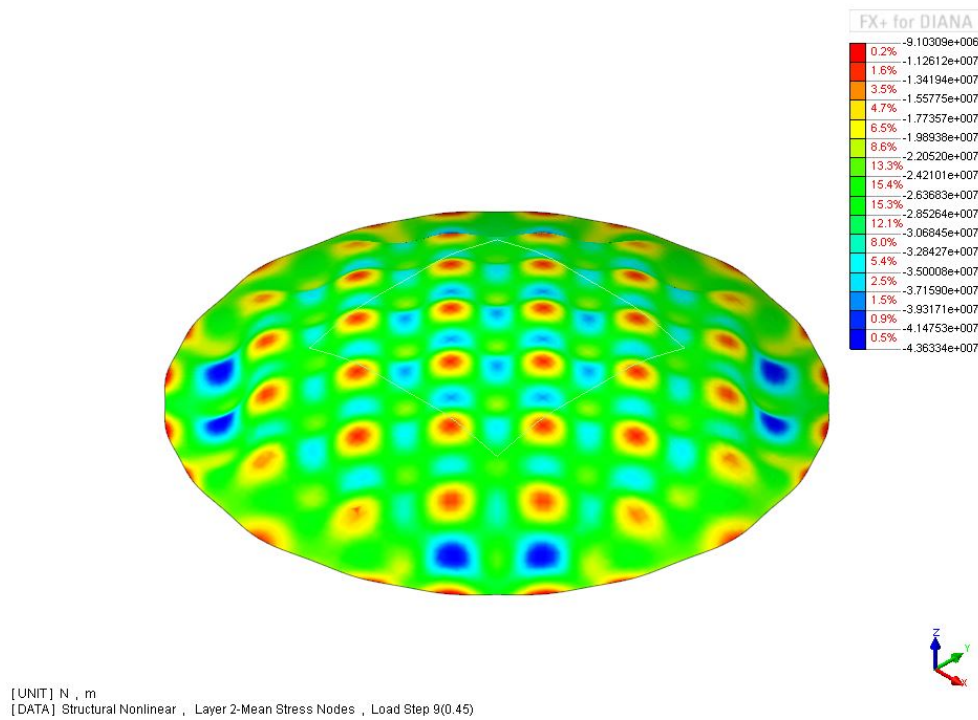


Figure F.30: Mean stress in N/m^2 of z-coordinate of imperfect shell (amplitude 5 cm), using non-linear analysis. Load step 400 kN/m^2

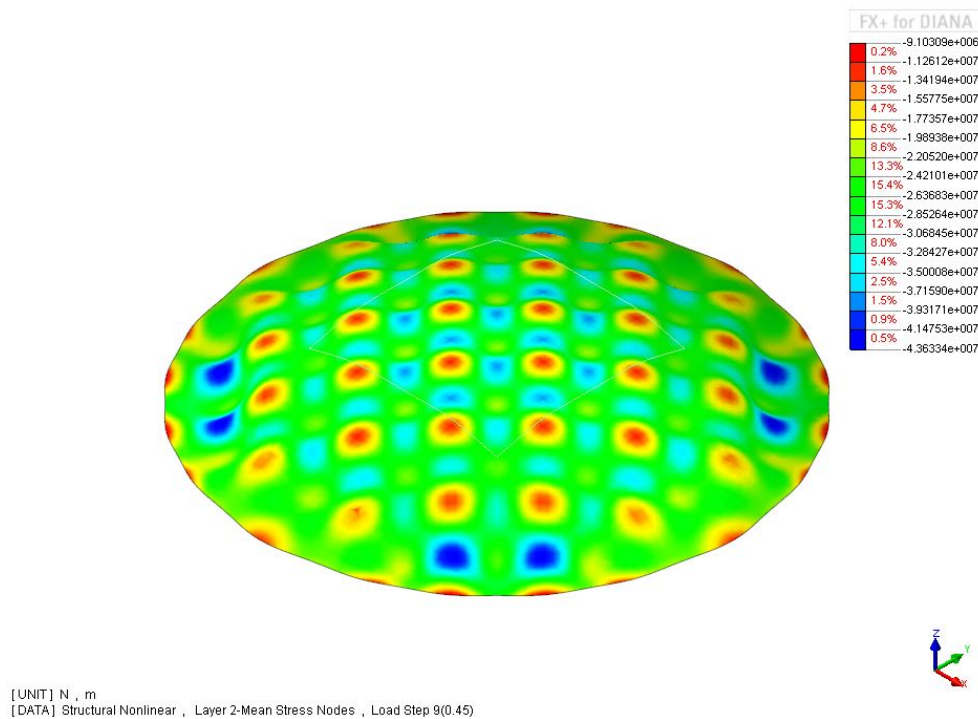


Figure F.31: Mean stress in N/m^2 of z-coordinate of imperfect shell (amplitude 5 cm), using non-linear analysis. Load step 450 kN/m^2

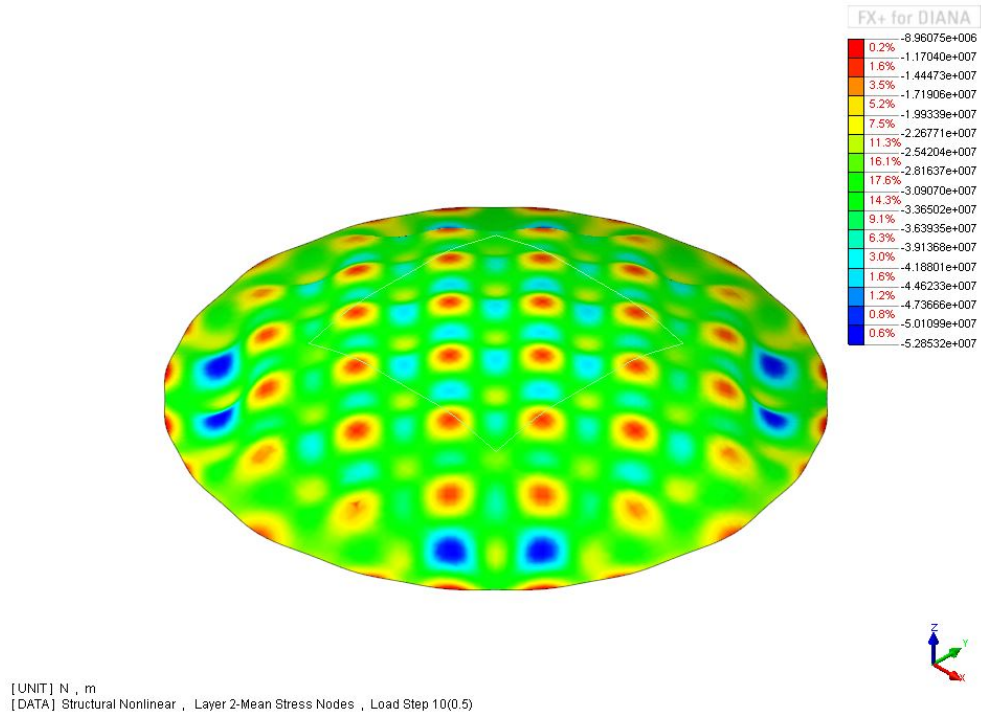


Figure F.32: Mean stress in N/m^2 of z-coordinate of imperfect shell (amplitude 5 cm), using non-linear analysis. Load step 500 kN/m^2

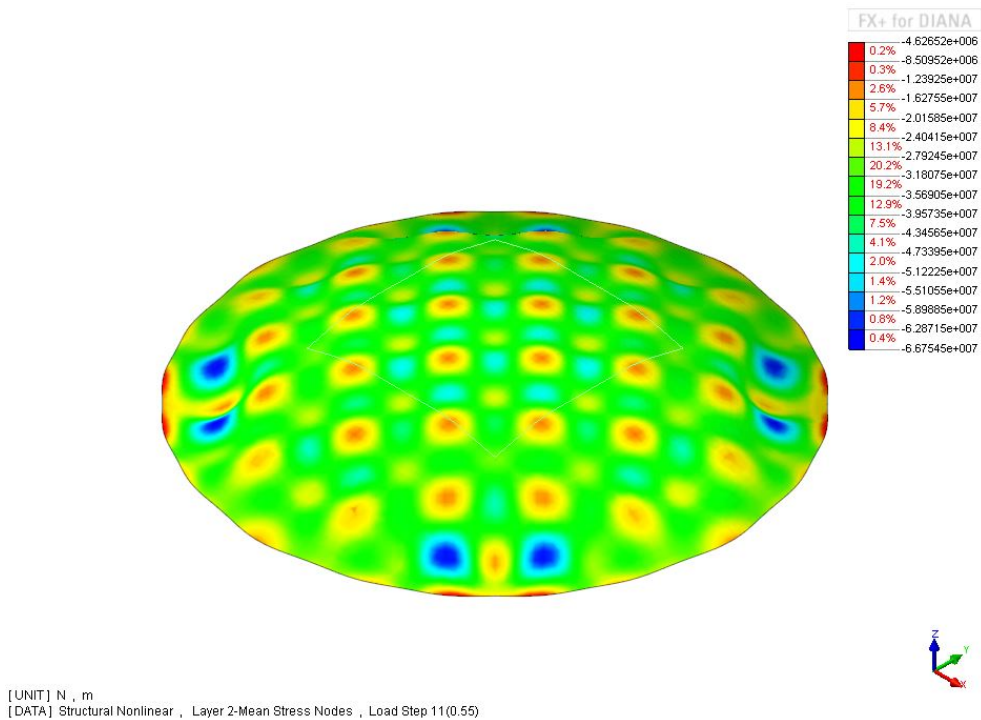


Figure F.33: Mean stress in N/m^2 of z-coordinate of perfect shell (amplitude 5 cm), using non-linear analysis. Load step 550 kN/m^2

F.9.4. Non-linear analysis of imperfect shell (amplitude 1 cm) results

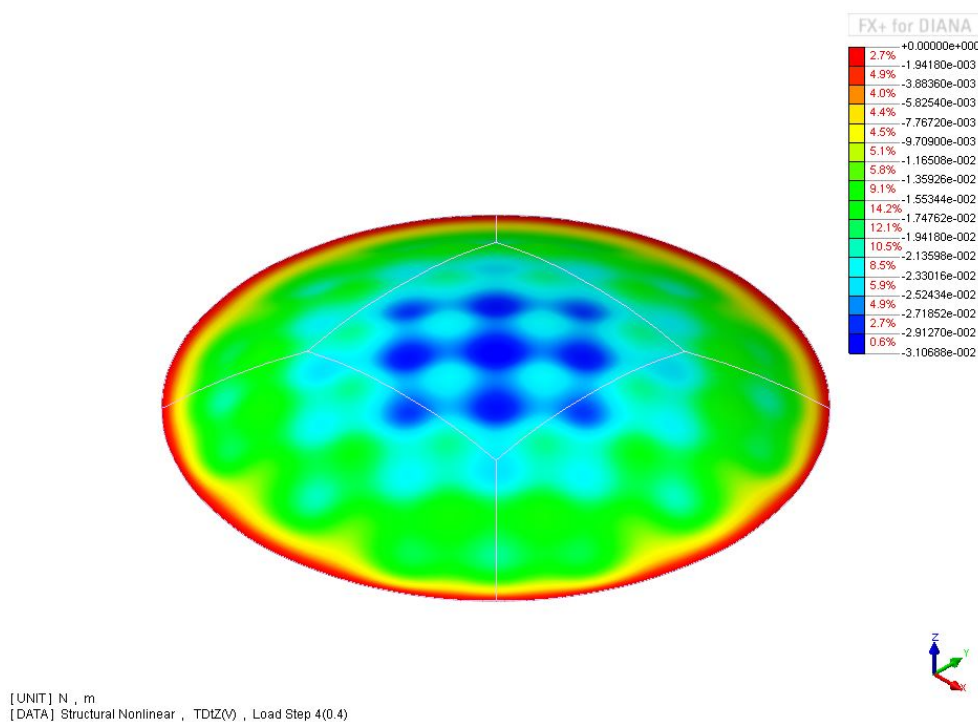


Figure F.34: Displacement in meter of z-coordinate of imperfect shell (amplitude 1 cm), using non-linear analysis. Load step 400 kN/m^2

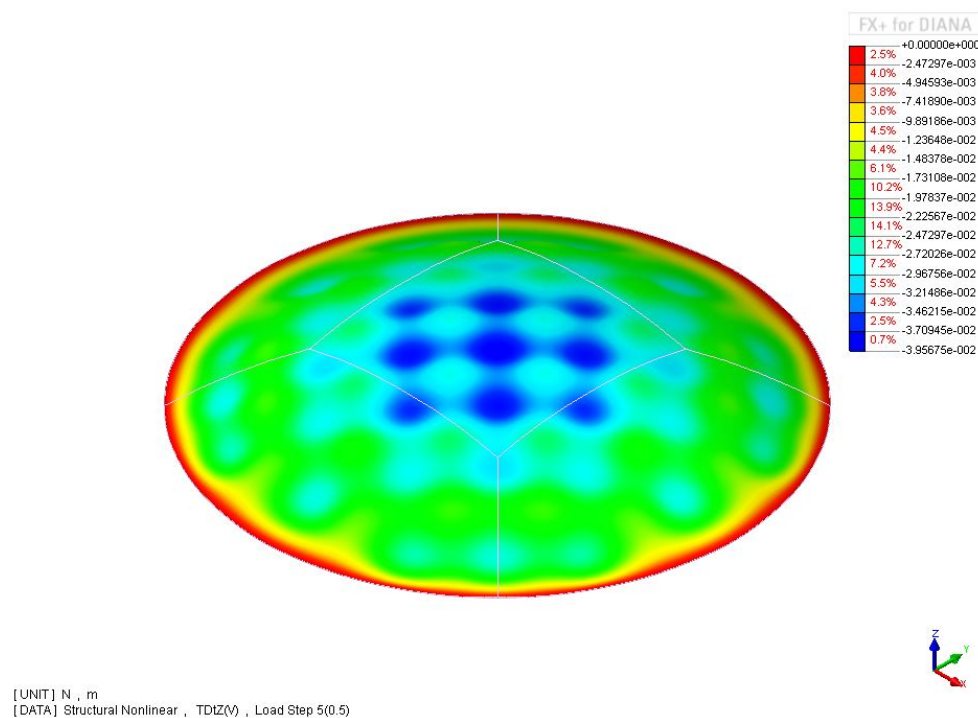


Figure F.35: Displacement in meter of z-coordinate of imperfect shell (amplitude 1 cm), using non-linear analysis. Load step 500 kN/m^2

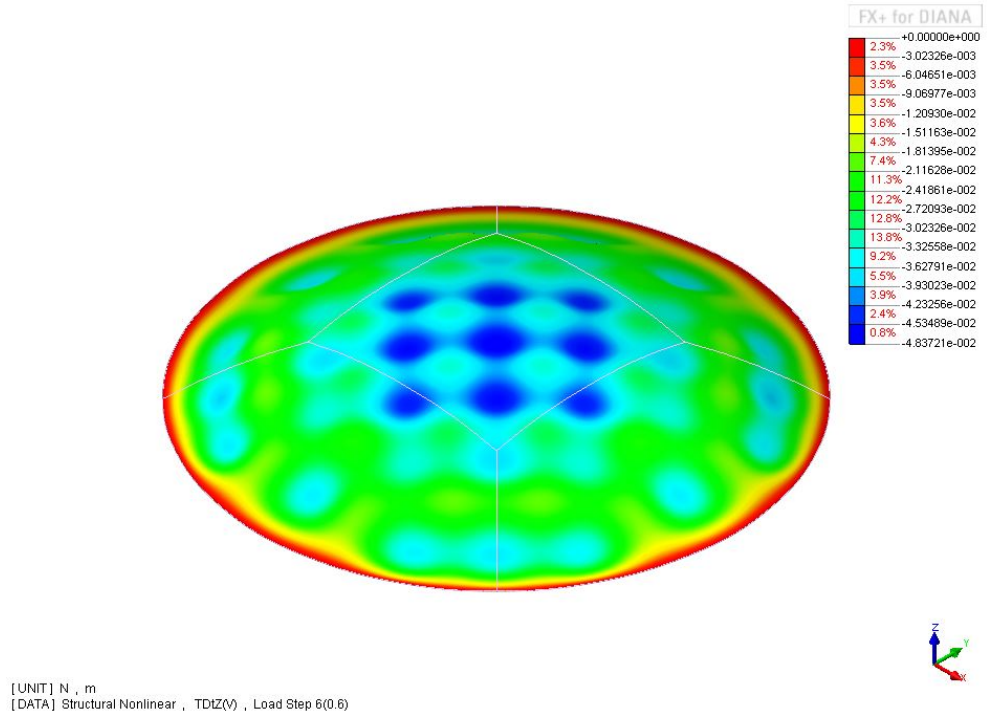


Figure F.36: Displacement in meter of z-coordinate of imperfect shell (amplitude 1 cm), using non-linear analysis. Load step 600 kN/m^2

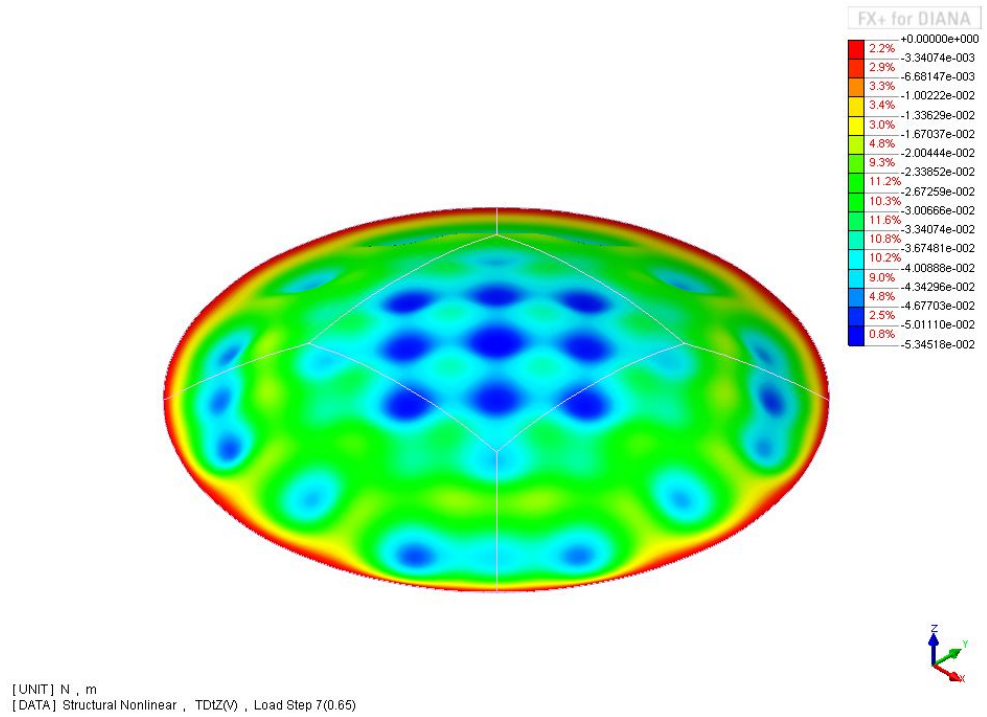


Figure F.37: Displacement in meter of z-coordinate of imperfect shell (amplitude 1 cm), using non-linear analysis. Load step 650 kN/m^2

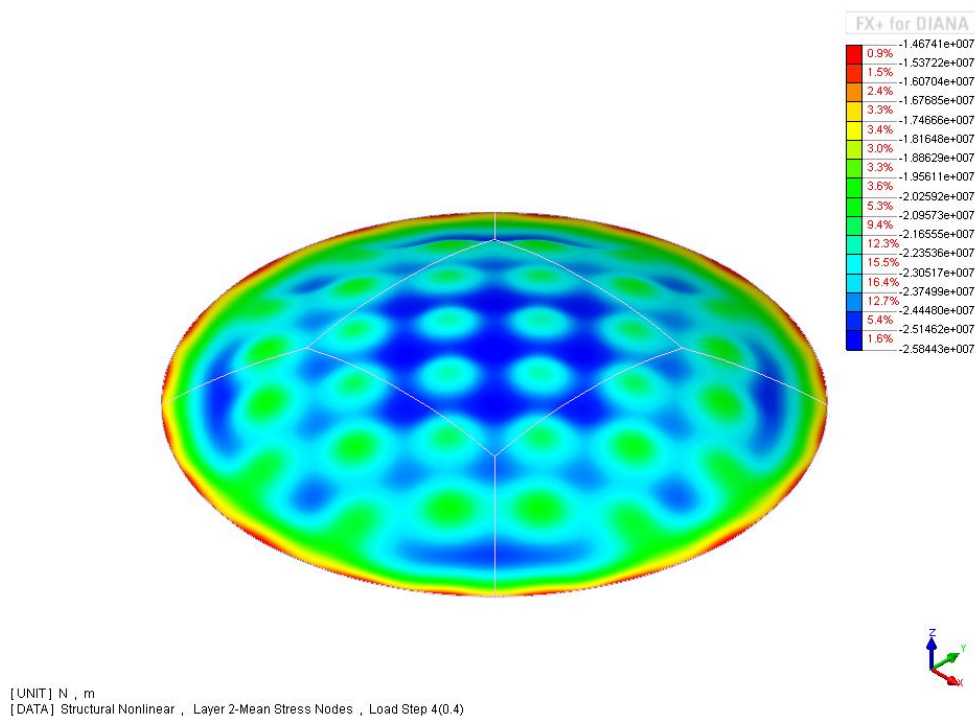


Figure F.38: Mean stress in N/m^2 of z-coordinate of imperfect shell (amplitude 1 cm), using non-linear analysis. Load step 400 kN/m^2

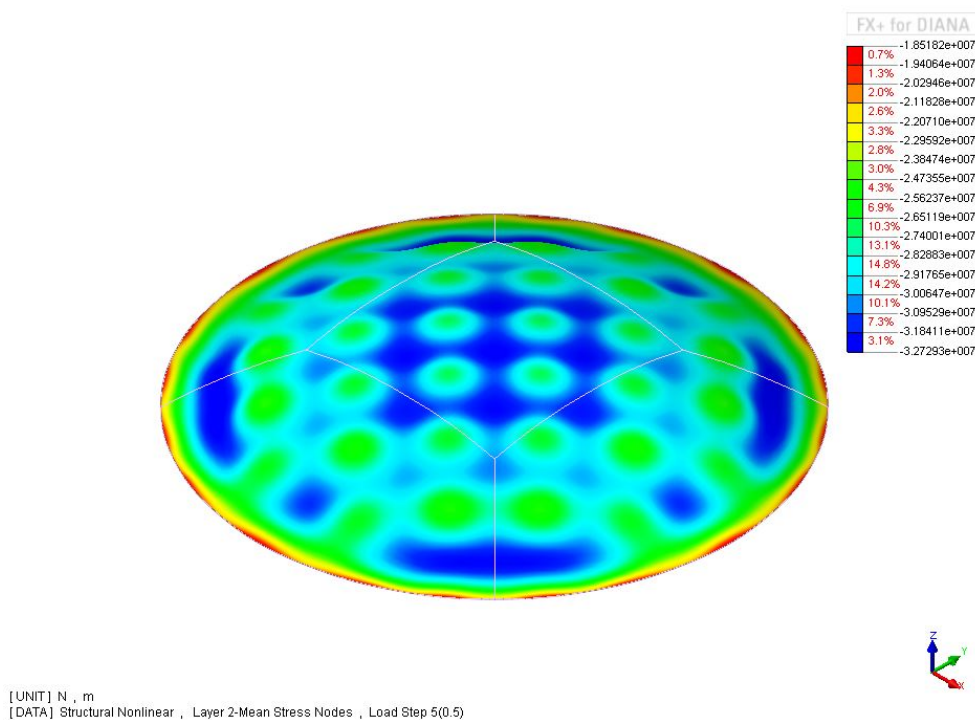


Figure F.39: Mean stress in N/m^2 of z-coordinate of imperfect shell (amplitude 1 cm), using non-linear analysis. Load step 500 kN/m^2

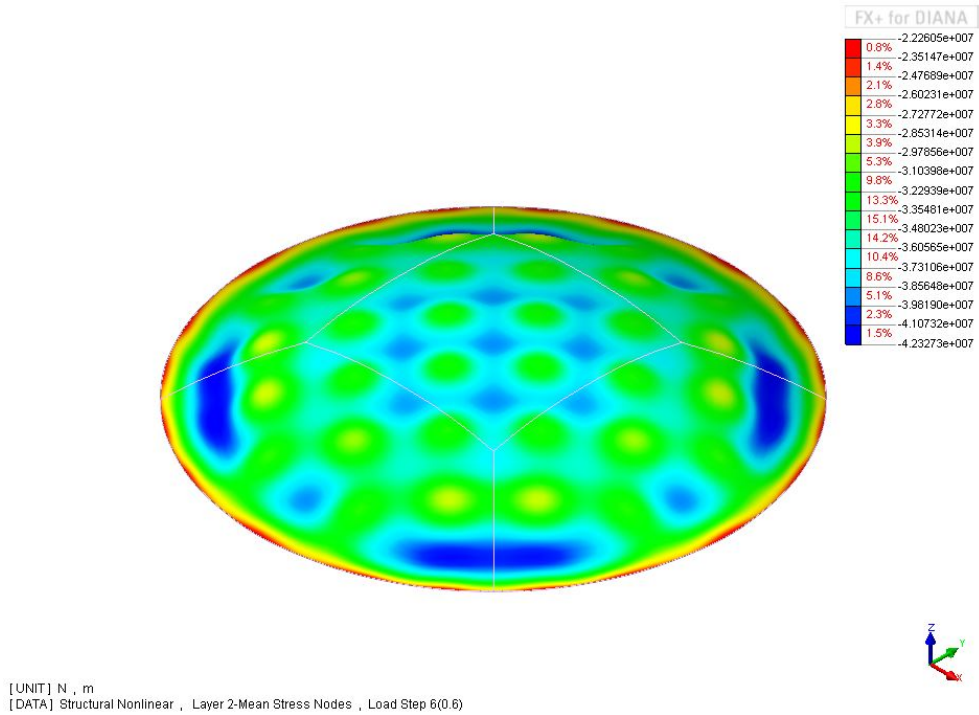


Figure F.40: Mean stress in N/m^2 of z-coordinate of imperfect shell (amplitude 1 cm), using non-linear analysis. Load step 600 kN/m^2

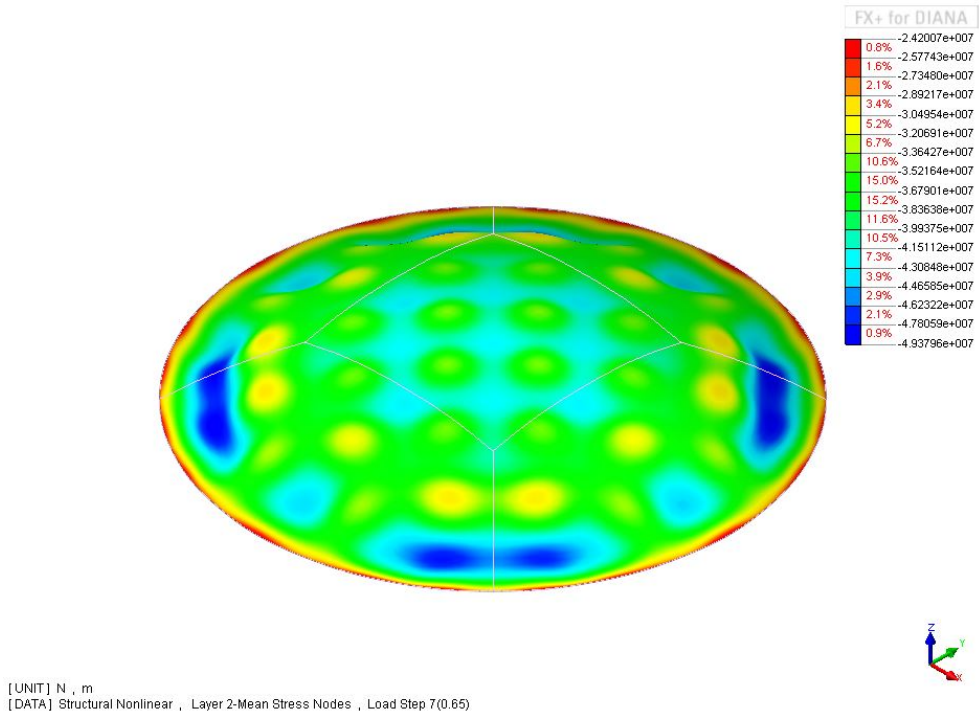
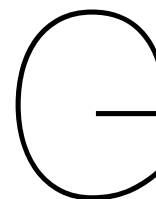


Figure F.41: Mean stress in N/m^2 of z-coordinate of perfect shell (amplitude 1 cm), using non-linear analysis. Load step 650 kN/m^2



ANWB head office results and method

The ANWB head office was not suitable for producing reliable results using the DGCN-method, because not a large enough rectangular and continuous piece could be cut out of the data. For the ANWB head office a different method was tried, but due to the small imperfections found (max of 1.5 cm) and the fact that the finish of the dome was not homogeneous in thickness, results were not useable for this research. Below a description of the method is given. It may contain elements which could be useful for future research.

G.1. Method

G.1.1. Input

All the data was collected by the Faro Focus 3d x130 laser scanner and was turned in to a point cloud by using Scene (software from Faro). In this file every point has a x, y and z-coordinate, which can be loaded into several drawing programs. In this research Rhinoceros 5.0 in combination with the plug-in Grasshopper will be used.

G.1.2. How to compare surfaces

In Rhinoceros it is not possible to compare the geometry of 2 surfaces to each other. Using Grasshopper it is possible to subtract the coordinates of points from one another. So the method that was used for comparison of the surfaces, was based on point comparison instead of surface comparison. Points can only be compared to each other if they are exactly on the same place in every segment, that is why points need to be projected on a surface fitted through points. The measured points of the scanner do not have the same point density for the entire field of view. Therefore a rectangular array of points will be projected on the NURBS surface so that every point has the same x and y-coordinate. Then the z-coordinates can be subtracted and averaged for comparison, if the shell segments are close to horizontal.

G.1.3. ANWB: From measured points to rectangular point cloud

In the following sections the partitioning of the shell and the averaging of the segments will be discussed. This is only applicable for the ANWB results, not for the other shells. Their process is just comparing the detailed and smooth NURBS patches representing the intended shape. After partitions are created all segments must be placed at a precise distance from each other. In this example the shell of the ANWB head office will be used. This is a half circle with an oculus in the middle. It can be partitioned in 4 segments, because it is symmetric in every horizontal axis. When the 4 segments are made they are placed in a row and rotated in the same direction (see figure G.1).

After this step a patch can be made through each segment. Patch is the function in Rhino for creating a NURBS surface through a point cloud. The patches will be cut by using the trim function with a projected trapezoid on the created surface. Two patches will be created per segment, one in high detail and a smooth one (first for comparing, second for the average geometry). In figure G.2 the fine patch is shown and in figure G.3 the smooth patch is shown. The difference in color is due to the different layers the patches were made in.

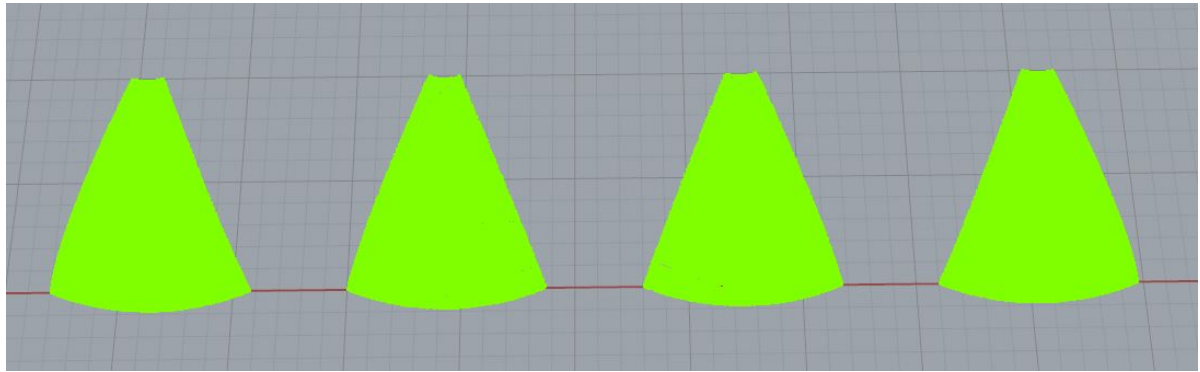


Figure G.1: 4 segments of the ANWB shell aligned

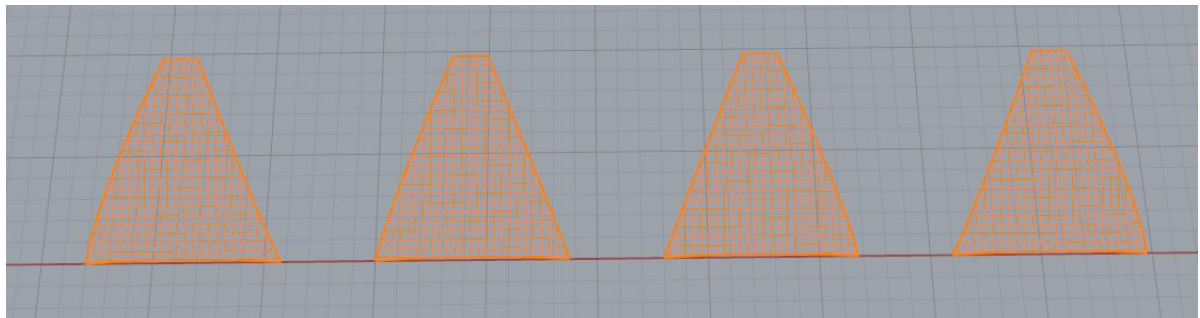


Figure G.2: Created NURBS surfaces with 30 by 30 nodes and stiffness equal to 1

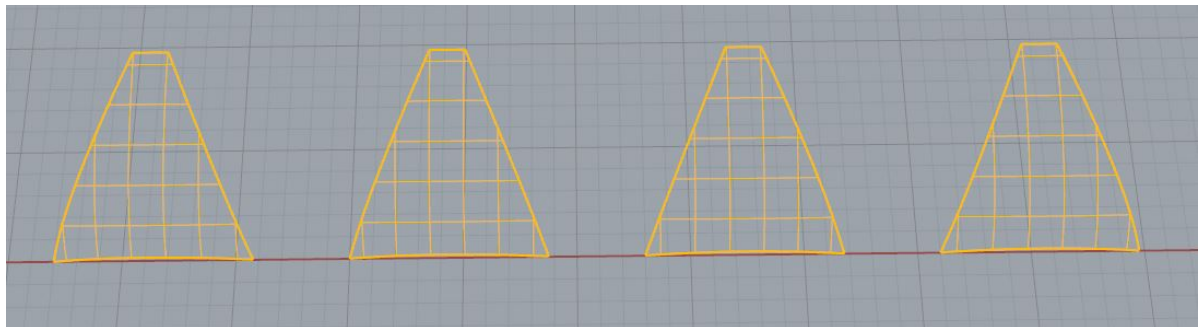


Figure G.3: Created NURBS surfaces with 7 by 7 nodes and stiffness equal to 15

G.1.4. Projecting the rectangular grid

A rectangular grid is created in Grasshopper, because it is easier to adjust in this way. The grid starts at the lower left corner and has a constant distance between point of 10 centimeter. The grid on the x-y plane (or ground grid) from now on can be seen in figure G.4. This grid of points can be projected on the surface of the NURBS by using the project function. The projected points can be seen in figure G.5. All segments now have an equal number of points on their surface with the same x and y coordinates. The cutout segments are trapezoidal instead of following the exact shape to make sure that all segments have the same amount of points. When precisely following the segment shape this is not always the case and this is very important because; one extra point will disturb the next steps.

G.1.5. Averaging and comparing

The projected points will now be loaded into grasshopper. The scheme in figure G.6 is a Grasshopper script to average three projected point clouds with one and give the results a color. This picture is gives a representation of the workings of Grasshopper, but this chapter does not go into detail, for more information on the script see appendix B.

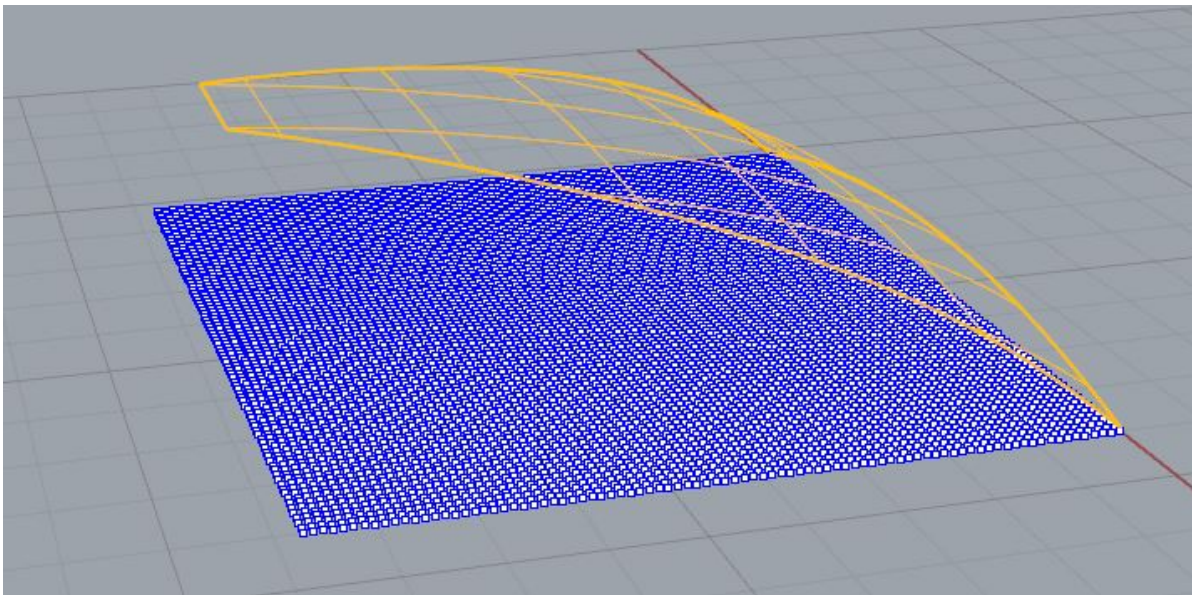


Figure G.4: Rectangular ground grid under segment patch

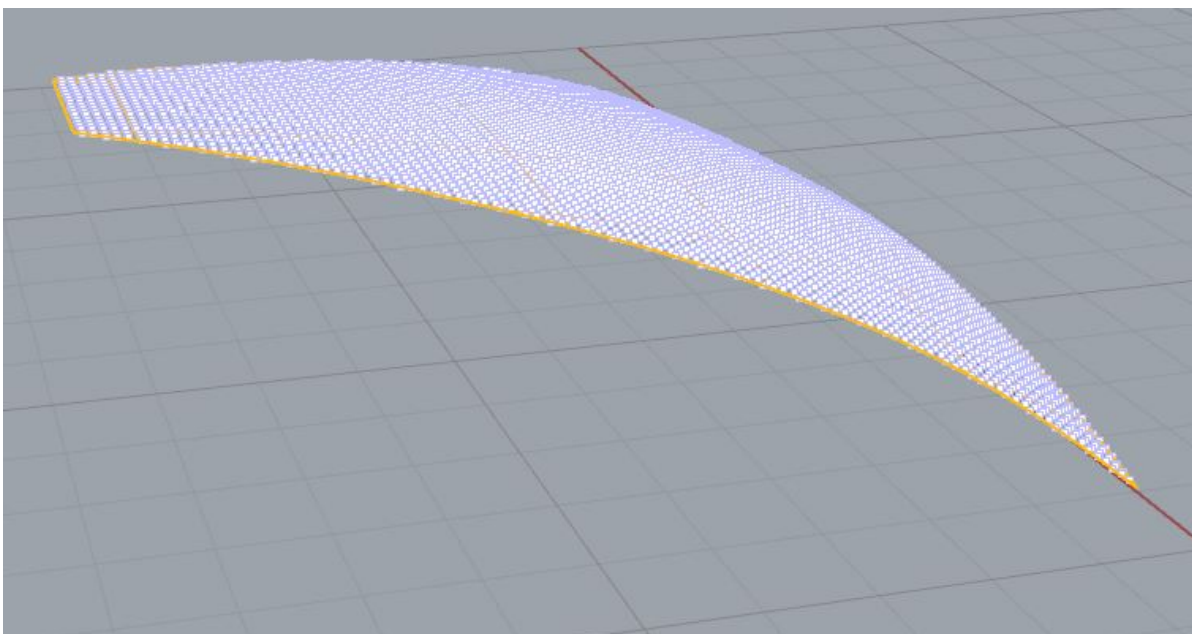


Figure G.5: Projected grid on patch

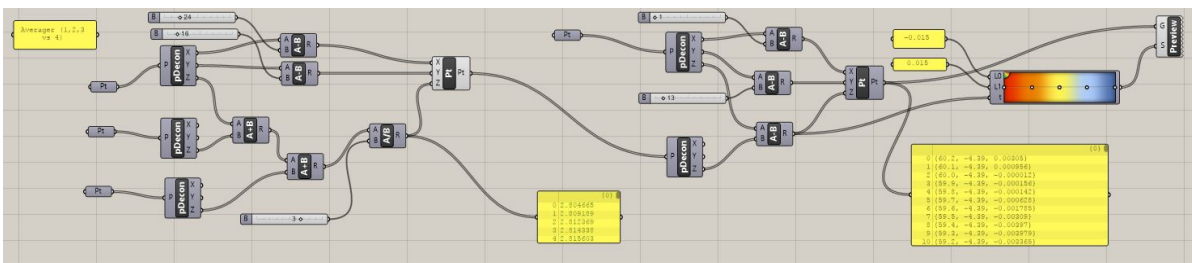


Figure G.6: Grasshopper scheme for creating an average and comparing it to 1 segment

G.2. Results

G.2.1. Point deviation

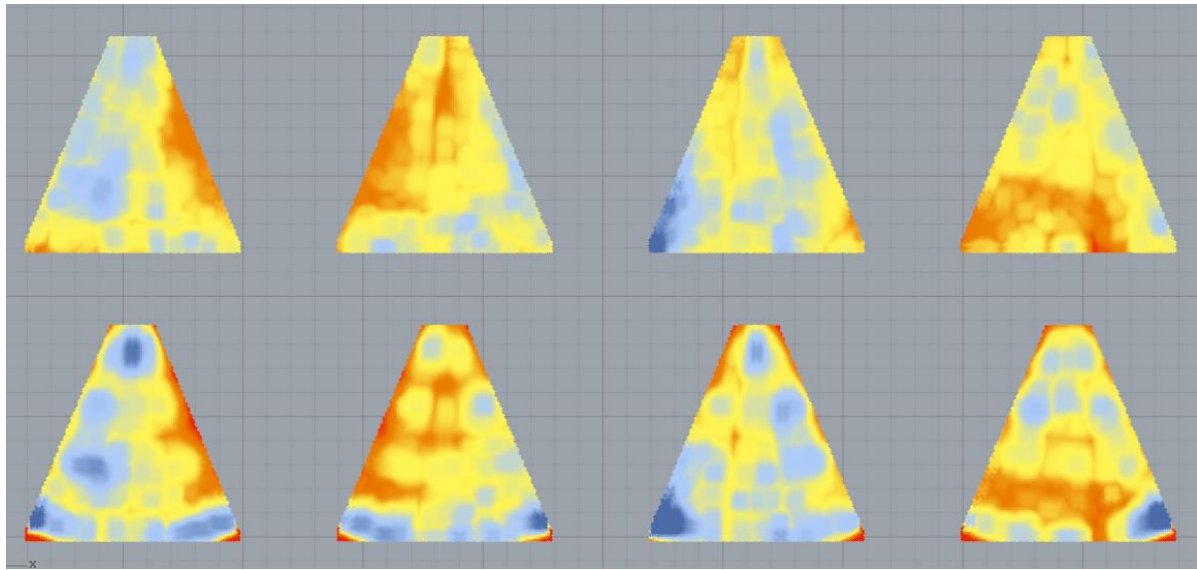


Figure G.7: Results. First row is compared to an average of detailed patches and second row is a detailed patch compared to the average of rough patches. Red is -1.5 cm to blue is +1.5 cm of difference

G.2.2. Histogram

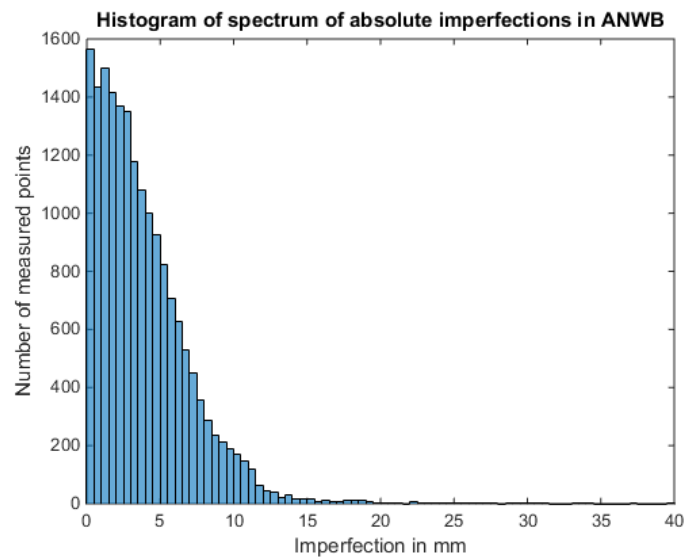
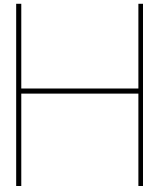


Figure G.8: ANWB absolute histogram



Bibliography

- P.C.J. Hoogenboom, CIE4143 Shell analysis, theory and application handouts.
- Journal of international association for shell and spatial structures (IASS) vol 52 NO. 3, page 161-169, Heinz Bösigler
- FARO laser scanner Focus3D x130 techsheet, www.faro.com/nl-nl/
- A. Borgart, P. Eigenraam, Scanning in 3D and analysing the models of Heinz Isler, the preliminary results, 2012
- B. Elferink, P.C.J. Hoogenboom, J.G. Rots, P. Eigenraam, Shell imperfections, HERON vol 61 (2016) No. 3
- P.J. Schneider, NURB Curves: A Guide for the Uninitiated, http://www.mactech.com/articles/develop/issue_25/schneider.html
- A. Nambiar, Non-uniform rational B-spline (NURBS), 2011, <http://whatis.techtarget.com/definition/nonuniform-rational-B-spline-NURBS>
- TNO Diana bv, Diana Finite Element Analysis Users Manual 9.6 : Getting started, 2011
- TNO Diana bv, Diana Finite Element Analysis Users Manual 9.6 : Theory, 2011
- TNO Diana bv, Diana Finite Element Analysis Users Manual 9.6 : FX+ for Diana, 2011
- Weisstein, Eric W. "Fast Fourier Transform." From MathWorld-A Wolfram Web Resource, <http://mathworld.wolfram.com/FastFourierTransform.html>
- J. Chilton, The Engineer's Contribution to Contemporary Architecture: Heinz Isler, 2000
- T. Chen, On Introducing Imperfection in the Non-Linear Analysis of Buckling of Thin Shell Structures